



**HAL**  
open science

## CLIMATE VARIABILITY AS RECORDED IN LAKE TANGANYIKA (CLIMLAKE)

J.-P. Descy, P.-D. Plisnier, B. Leporcq, S. Sténuite, J. Stimart, L. André, L. Alleman, D. Langlet, W. Vyverman, C. Cocquyt, et al.

► **To cite this version:**

J.-P. Descy, P.-D. Plisnier, B. Leporcq, S. Sténuite, J. Stimart, et al.. CLIMATE VARIABILITY AS RECORDED IN LAKE TANGANYIKA (CLIMLAKE): Final report. Belgian Science Policy. 2006. hal-04278418

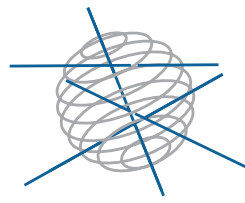
**HAL Id: hal-04278418**

**<https://hal.science/hal-04278418>**

Submitted on 10 Nov 2023

**HAL** is a multi-disciplinary open access archive for the deposit and dissemination of scientific research documents, whether they are published or not. The documents may come from teaching and research institutions in France or abroad, or from public or private research centers.

L'archive ouverte pluridisciplinaire **HAL**, est destinée au dépôt et à la diffusion de documents scientifiques de niveau recherche, publiés ou non, émanant des établissements d'enseignement et de recherche français ou étrangers, des laboratoires publics ou privés.



# SPSD II

## CLIMATE VARIABILITY AS RECORDED IN LAKE TANGANYIKA (CLIMLAKE)

J.-P. DESCY, L. ANDRÉ, W. VYVERMAN, E. DELEERSNIJDER



### PART 2

GLOBAL CHANGE, ECOSYSTEMS AND BIODIVERSITY



ATMOSPHERE AND CLIMATE



MARINE ECOSYSTEMS AND  
BIODIVERSITY



TERRESTRIAL ECOSYSTEMS  
AND BIODIVERSITY



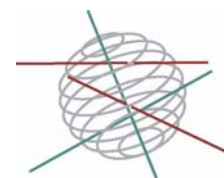
NORTH SEA



ANTARCTICA



BIODIVERSITY



**Part 2:**  
**Global change, Ecosystems and Biodiversity**

FINAL REPORT



**CLIMATE VARIABILITY AS RECORDED IN LAKE TANGANYIKA  
(CLIMLAKE)**

**EV/02**

J.-P. Descy<sup>1</sup>, P.-D. Plisnier<sup>1-2</sup>, B. Leporcq<sup>1</sup>, S. Sténuite<sup>1</sup>, S. Pirlot<sup>1</sup>,  
J. Stimart<sup>1</sup>, V. Gosselain<sup>1</sup>, L. André<sup>2</sup>, L. Alleman<sup>2</sup>, D. Langlet<sup>2</sup>,  
W. Vyverman<sup>3</sup>, C. Cocquyt<sup>3</sup>, A. De Wever<sup>3</sup>, M.P. Stoyneva<sup>3,7</sup>,  
E. Deleersnijder<sup>4</sup>, J. Naithani<sup>4</sup>, D. Chitamwebwa<sup>5</sup>, A. Chande<sup>5</sup>,  
I. Kimirei<sup>5</sup>, B. Sekadende<sup>5</sup>, S. Mwaitega<sup>5</sup>, S. Muhoza<sup>5</sup>, D.  
Sinyenza<sup>6</sup>, L. Makasa<sup>6</sup>, C. Lukwessa<sup>6</sup>, I. Zulu<sup>6</sup> & H. Phiri<sup>6</sup>.

1. Facultés Universitaires Notre-Dame de la Paix / Laboratory of Freshwater Ecology, Research Unit in Biology of Organisms
2. Royal Museum for Central Africa / Section of Mineralogy and Geochemistry, Department of Geology
3. Ghent University / Protistology en Aquatic Ecology, Department of Biology
4. Catholic University of Louvain / Institute of Astronomy and Geophysics G. Lemaître
5. Tanzanian Fisheries Research Institute, BP 90 Kigoma, Tanzania
6. Department of Fisheries, BP 55 Mpulungu, Zambia
7. University of Sofia "St Kliment Ohridski", Faculty of Biology, Department of Botany



BELGIAN SCIENCE POLICY



D/2006/1191/21  
Published in 2006 by the Belgian Science Policy  
Rue de la Science 8  
Wetenschapsstraat 8  
B-1000 Brussels  
Belgium  
Tel: +32 (0)2 238 34 11 – Fax: +32 (0)2 230 59 12  
<http://www.belspo.be>

Contact person:  
*Mrs Martine Vanderstraeten*  
Secretariat: +32 (0)2 238 36 13

Neither the Belgian Science Policy nor any person acting on behalf of the Belgian Science Policy is responsible for the use which might be made of the following information. The authors are responsible for the content.

No part of this publication may be reproduced, stored in a retrieval system, or transmitted in any form or by any means, electronic, mechanical, photocopying, recording, or otherwise, without indicating the reference.

## Table of contents

<b>ABSTRACT</b> .....	<b>5</b>
<b>1. INTRODUCTION</b> .....	<b>13</b>
<b>2. MATERIAL AND METHODS</b> .....	<b>17</b>
2.1 Study sites.....	17
2.2 Meteorology.....	18
2.3 Water column sampling and measurements .....	18
2.4 Remote sensing .....	18
2.5 Elemental analysis.....	19
2.6 Phytoplankton pigment analysis and processing of data .....	19
2.7 Mesozooplankton abundance and biomass .....	20
2.8 Primary production .....	21
2.9 Bacterial production.....	22
2.10 Phytoplankton (microscopic observations) and heterotrophic organisms: .....	22
2.11 Geochemistry of the water column: major, minor and trace elements .	23
2.12 The bivalves monitoring.....	24
2.13 Silicon isotopic fractionations .....	25
2.14 Time series.....	26
<b>3. RESULTS</b> .....	<b>27</b>
3.1 Environmental monitoring.....	27
3.1.1 Meteorology .....	27
3.1.2 Limnology.....	29
3.1.3 Remote sensing .....	39
3.1.4 Present plankton in the pelagic waters .....	42
3.1.5 Ecological processes .....	58
3.1.6 Geochemistry of the water column: Major, minor and trace elements .....	61
3.1.7 The Bivalves Monitoring – Hydrological changes in Lake Tanganyika recorded in bivalve shells .....	64
3.1.8 Silicon isotopic fractionations .....	67
3.1.9 Data base.....	72
3.2 Proxies studies: plankton in the sediments.....	72
3.3 Eco-hydrodynamic modelling of Lake Tanganyika .....	74
3.3.1 Introduction .....	74
3.3.2 Amplitude and frequency of free oscillations .....	74
3.3.3 Origin of thermocline oscillations.....	75
3.3.4 Internal Kelvin waves .....	76
3.3.5 Eco-Hydro Model .....	77
3.3.6 Model Climatological Run .....	82

<b>4.</b>	<b>DISCUSSION AND CONCLUSIONS</b> .....	<b>87</b>
4.1	Meteorological and limnological variables .....	87
4.2	Phytoplankton composition and biomass .....	88
4.3	Chlorophyll a .....	90
4.4	Primary production .....	92
4.5	Importance of heterotrophic plankton .....	92
4.6	Geochemistry of the water column .....	93
4.7	Mollusk shells as geochemical archives of hydrological changes .....	93
4.8	Si concentration and Si isotopes .....	94
4.9	Modelling .....	95
4.10	Perspectives .....	96
4.11	The microbial food web .....	97
4.12	Biogeochemical cycles of nutrients .....	97
4.13	Model development and forcing .....	98
<b>5.</b>	<b>ACKNOWLEDGMENTS</b> .....	<b>99</b>
<b>6.</b>	<b>LIST OF PUBLICATIONS RELATED TO THE PROJECT</b> .....	<b>101</b>
<b>7.</b>	<b>REFERENCES</b> .....	<b>105</b>
<b>8.</b>	<b>APPENDIX</b> .....	<b>111</b>
	Appendix 1: Eco-hydrodynamic model of Lake Tanganyika .....	111
	Appendix 2: Phytoplankton and diatoms taxa list (CLIMLAKE 2002-2004) .....	116

## ABSTRACT

The CLIMLAKE project involved an integrated approach combining hydrodynamics, nutrient distribution, plankton dynamics, geochemical signals and paleoecology for improving the understanding of Lake Tanganyika variability and sensitivity to climate change. The project started in 2001 and included a 3-year survey of the lake over the period 2002-2004, with the participation of Tanzanian (TAFIRI, Kigoma) and Zambian (DOF, Mpulungu) teams. Sampling and analyses were carried out at two stations, Kigoma (north basin) and Mpulungu (south basin), and three cruises between the two sites were organised, two in the dry season (July 2002 – 2003), one in the rainy season (February 2004).

The project comprised several components:

- (1) environmental monitoring, consisting of meteorological measurements and limnological sampling at the two stations; in addition to this field data acquisition, satellites images have been used for getting whole-lake surface temperature data;
- (2) a study of the present plankton, particularly phytoplankton, based on the fact that phytoplankton composition and biomass directly respond to fluctuations of various environmental factors (light, temperature, mixing regime, nutrient inputs to surface layers); variations of algal composition can indicate changes that occurred in the lake for the past decades, and can provide clues for interpreting changes in the sediment diatom record; other plankton components and processes have been studied: bacterioplankton, protozooplankton (ciliates and heterotrophic nanoflagellates), mesozooplankton (copepods), primary production, bacterial production; parallel research on specific ecological processes or on microbial diversity, has been conducted.
- (3) geochemical studies, including several aspects: measurements of major and trace elements in the water column in order to identify the controlling factors of water and particles geochemistry, and to record and quantify the deep water upwelling; measurements of trace elements in a bivalve mollusk shell (*Pleiodon spekii*) as a proxy for environmental change; use of silicon isotopes fractionation by diatoms ( $\delta^{29}\text{Si}$ ) to track changes of diatom production in the surface waters, with the objective of applying this technique to quaternary diatom-rich sediments, in an attempt to quantify paleo-productivity.
- (4) diatom analysis in sediment cores collected in a previous project: interpretation of the variation of abundance of diatom frustules in the sediment, based on improved knowledge on ecological requirements of the species, to help to track environmental changes in Lake Tanganyika during the past 1500 years.
- (5) development of an eco-hydrodynamic model, for simulating the major hydrodynamics events in the lake as driven by wind forcing and how these events affect ecological processes and the main ecosystem components.

Two main seasons are observed in Lake Tanganyika area. The dry season from April-May to September-October is characterised mainly by monsoonal SE winds while the rainy season is characterised by NE monsoonal NE winds. This was well observed during all the monitoring period from 2002 to 2005.

There are pulses in the strength of the SE winds. The periodicity of those pulses is close from the internal lake periodicity and there appear to be resonance between the winds oscillations and the lake oscillation of the thermocline (Naithani et al, 2002). There could be pulses in the NE winds also but this was not verified yet.

During the dry season, an upwelling is well observed at the southern end of the lake as it was shown previously (Coulter 1990, Plisnier et al, 1999, Langenberg 2003). The project has detailed the limnological change during the southern upwelling as main nutrients (N, P and Si) are increasing 2 to 3 times depending of the strength of the upwelling. This event was more important in 2003 than in 2002. The thermal stability was decreased during part of the 2003 dry season. The water was then colder and nutrient concentration was more important near the surface. There was however unfortunately not well other marked interannual variability during the sampling period.

Beside the seasonality and inter-annual variability, a third source of environmental variability arises from the presence of internal waves of period of around 3 weeks. Pulses of deeper water are regularly observed with the periodic increase and decrease of nutrients in the epilimnion. The observation of inversed correlation between the temperature fluctuation from the depth of 100 m at Kigoma and Mpulungu indicates that the wave type is most probably uninodal.

Dissolved N and P concentrations were lower during the rainy seasons than in the dry seasons. The availability of these potentially limiting nutrients for primary producers is also dependent on internal waves that may favour pulsed transport through the thermocline

The chlorophyll *a* temporal profiles show a higher variability in Mpulungu than in Kigoma. This can be explained by a strong seasonality and yearly upwelling occurrence added to the fact that Mpulungu station is at one end of the lake where the amplitude of internal waves is stronger than in Kigoma.

It was found that several types of variability have added impact for explaining the water quality changes: strong winds generate not only a strong seasonal upwelling but also strong waves later on. It can be hypothesised that two windy seasons in a row are most favourable for a combination of mixing during seasonal epilimnion turnover and high wave amplitude resulting from the previous wind season. Since strong wind is generally associated with decreased air temperature, a strong hydrodynamic activity impact on the nutrient level in the upper water and induces phytoplankton development in a way that the abundance of phytoplankton in the



sediments may be indirectly related to the air temperature at the time of the planktonic development.

A total of about 200 images of the lake surface temperature were obtained from the processing of the AVHRR satellite images, which allowed analysing contrasted seasonal situations at the scale of the whole lake. From all images available, temperature data were extracted and arranged in arrays according to their position (geographical coordinates).

The 3-year survey of chlorophyll and carotenoid pigments allowed following the variation of phytoplankton biomass and composition at the two study sites and during the cruises. Chlorophyll *a* concentrations were low ( $0.3 - 4 \text{ mg m}^{-3}$ ) and average chlorophyll *a* integrated through the 100 m water column were similar for both stations and years ( $36.4 - 41.3 \text{ mg m}^{-2}$ ). Most pigments were located in the 0-60 m layer and decreased sharply downward. Chlorophyll *a* degradation products (phaeophytins and phaeophorbides) were detected at 100 m depth, whereas carotenoids became undetectable. Temporal and seasonal variation of the vertical distribution of pigments was high. The biomass of phytoplankton groups was calculated from marker pigment concentrations over the 0-100 m water column using the CHEMTAX software. On average for the study period, chlorophytes dominated in the northern station, followed by cyanobacteria T1 (type 1, or *Synechococcus* pigment type), whereas cyanobacteria T1 dominated in the south. Cyanobacteria T2 (type 2, containing echinenone), presumably corresponding to filamentous taxa, were detected in the rainy season. Diatoms (and chrysophytes) developed better in the dry season conditions, with a deep mixed layer and increased nutrient availability. Very large variation in the vertical distribution of algal groups was observed. The survey of phytoplankton pigments in the littoral zone at the two sites showed similar variations of algal composition and biomass than in the pelagic zone, with greater contrasts. Our observations on phytoplankton composition at the class level are broadly consistent with those from previous studies. Our pigment data provide evidence for the lake-wide importance of picocyanobacteria, and high interannual variation and spatial heterogeneity of phytoplankton in Lake Tanganyika. This large temporal and spatial variation may render difficult assessment of long-term changes in phytoplankton based solely on algal biomass and composition (at the class level) from a few samples.

The phytoplankton composition as determined by inverted and epifluorescence microscopy largely confirms the observations from the pigment analysis and provides additional information on the phytoplankton species composition. The picophytoplankton counts revealed an overall high contribution of this small size class (26-53% in Kigoma and 65-92% in Mpulungu). Detailed species data showed seasonal differences in the occurrence of particular species. The long diatom

*Nitzschia asterionelloides* was the dominant species during the dry season in Kigoma, while a small *Nitzschia* (*N. aff. fonticola*) occurred at the end of the rainy season. Chlorophyte species belonging to the *Dictyosphaerium/Lobocystis* complex and *Kirchneriella obesa* have an important contribution to the phytoplankton biomass respectively during the dry season in Kigoma and during the rainy season in Mpulungu. Filamentous cyanobacteria, which were also observed by HPLC-analysis (echinenone containing) after the dry season, were identified as *Anabaena flos-aquae* and *Anabaenopsis tanganyikae*, while Chroococcales were important during the rainy season in Mpulungu.

Total plankton biomass, as estimated by particulate organic carbon concentration, tends to be maximal during the dry seasons, except in 2002 when, as for chlorophyll a, maxima were reached after the end of the dry season. POC concentration was higher in Mpulungu than in Kigoma, in agreement with the expected higher production at the southern station. This difference is observed for both seasons: the dry season averages were 122 mg C m<sup>-3</sup> at Kigoma vs. 199 mg C m<sup>-3</sup> at Mpulungu, and the rainy seasons averages were, respectively, 108 mg C m<sup>-3</sup> vs. 163 mg C m<sup>-3</sup>. Autotrophic plankton biomass was only a part of this total plankton carbon, and was often lower than the biomass of heterotrophic plankton, indicating the importance of bacteria and microzooplankton in the food web.

The analysis of elemental ratios suggests that macronutrient limitation of phytoplankton may occur in Lake Tanganyika, but also that P limitation may have been more frequent than N limitation. The variation of the C: P ratio was clearly seasonal and related to the mixing pattern of the water column.

In both stations, copepod biomass was low in the beginning of each year, and increased in the dry season or in the following months. Overall, mesozooplankton biomass follows closely, or with some delay, phytoplankton biomass and production. Annual averages were comprised between 0.56 and 1.0 g C m<sup>-2</sup>, which is in the same range as in the years 1994-1995. Calanoids copepods were, overall, more abundant in Mpulungu, whereas cyclopoids usually dominated at Kigoma.

Enumeration of bacteria and heterotrophic protists revealed high densities of those groups and supports, together with high picophytoplankton densities, the hypothesis of a high importance of the microbial food web. Bacterial densities range between 1 and 6 × 10<sup>6</sup> cells ml<sup>-1</sup>, heterotrophic nanoflagellates (HNF) are present at densities of 0.4-3.9 × 10<sup>3</sup> cells ml<sup>-1</sup> and ciliate densities range up to 7.0 × 10<sup>3</sup> cells l<sup>-1</sup>. Highest protist grazer densities are observed during the dry season. The overall biomass of bacteria and heterotrophic protists is of the same order of magnitude as that of autotrophs, which underscores their ecological significance in the lake.

Measurements of phytoplankton photosynthesis allowed estimation of the photosynthetic parameters of the algal assemblages and assessment of daily and annual primary production. Daily phytoplankton production in 2002-2003 showed a clear contrast between seasons in Kigoma, with higher production in August – September. This contrasted pattern was also visible in Mpulungu in 2003, but not in 2002. Isolated peaks of primary production occurred in the rainy season, particularly in Mpulungu. Average annual production was 130 (2002) and 138 g C m<sup>-2</sup> y<sup>-1</sup> (2003) at Kigoma, and 167 g C m<sup>-2</sup> y<sup>-1</sup> (2002) and 224 g C m<sup>-2</sup> y<sup>-1</sup> (2003) at Mpulungu. Data from the two dry season cruises confirm a difference of primary production between north and south of the lake. Bacterial production was measured on several instances during the dry and rainy season 2002 and 2003. The range of bacterial production calculated for the 100 m water column was comprised between 49 to 276 mg C m<sup>2</sup> d<sup>-1</sup>. Highest values were obtained at Mpulungu during the dry season 2002 and at Kigoma during the rainy season 2004: they reached the lower range of phytoplankton production, showing the importance of heterotrophic vs. autotrophic production in Lake Tanganyika.

The geochemical signature of Lake Tanganyika has been assessed through a deep water samplings and surface water monitoring in the southern and northern basin for both the dissolved and particulate fraction. Such an exhaustive approach was completed by a large spectrum of major, minor and trace elements analyses obtained by various ICP techniques depending on the detection limits required. Confirmation from past values for mostly major elements indicates a rather stable geochemical signature on a decadal time scale. First observed anomalies for redox sensitive elements on deep water profiles suggest unexpected sources at depth from riverine inputs or interstitial water diffusion. A statistical treatment of the dataset indicates a strong influence on both dissolved and particulate phases from upwelling sources in the southern basin while the northern basin geochemical signature reflects mainly the detrital and biogenic influences.

Detailed analysis of the bivalve *Pleiodon spekii* shells have shown that high-resolution profiles of Mn, Sr and δ<sup>18</sup>O exhibit cyclic variations, similar in all shells analysed. Both environmental and biological factors may have an influence on chemical record contained in the shell.

High-resolution profiles of Mn could provide a detailed record of short-term environmental changes linked with recent or past mixing events in Lake Tanganyika but also in other deep stratified African lakes where an upwelling tuned by monsoon regime occurs. Our results support the idea that paleo-environment researches could benefit from geochemical analysis of recent and well preserved fossils of *P. spekii*.

By contrast, the Sr and  $\delta^{18}\text{O}$  profiles in shells show cyclic variations that are not correlated with the composition or the temperature variations in lake surface waters.  $\delta^{18}\text{O}$  and Sr are mostly controlled by biological activity, which hampers their direct use as temperature proxies. However, they might provide data critical for the description of the thermal amplitude

As part of the CLIMLAKE program, silicon isotopic compositions in Lake Tanganyika have been analyzed by MC-ICP-MS on dissolved samples and biogenic particles collected during the surface water survey (bi-weekly monitoring in 2002-2003) in the southern basin. A new methodology for measuring Si isotopes has been developed to better constrain the recent climate changes in the Si cycle. Deep-water Si isotopic profiles from a north-south transect cruise performed in July 2002 were also measured along with some of its major tributaries. The biological isotopic discrimination induced by diatoms biomineralisation in a fresh water system is demonstrated by the nutrient-like shape of dissolved Si profiles and the isotopic disequilibrium between surface ( $\delta^{29}\text{Si} = 0.87 \pm 0.08 \text{‰}$ ) and deep waters ( $0.61 \pm 0.05 \text{‰}$ ). Short-term surface water Si isotopic and diatom biomass variations obtained during the one-year monitoring in the south have confirmed such a biological effect. Five epilimnion biogenic opal samples signatures ( $\delta^{29}\text{Si}$  of  $0.28 \pm 0.12 \text{‰}$ ) compared to those of surrounding waters are consistent with the diatom isotopic fractionation effect measured on marine tropical diatoms. This supports the non-species, non-temperature dependent character of the silicon isotope fractionation by diatoms. River signatures present variable  $[\text{Si}(\text{OH})_4]$  positively correlated to  $\delta^{29}\text{Si}$  values in the range of previously published world river data. Because of its fast response to climate variability, nutrient dynamics and limnological changes,  $\delta^{29}\text{Si}$  in siliceous organisms should be very useful to study environmental changes and particularly the recent decline of diatom Si utilization in Lake Tanganyika.

Two out of three key diatom species found in the sediment core are observed in the modern plankton. These two species, *N. asterionelloides* and *N. aff. fonticola*, show a similar pattern in core sections analysed at high resolution (100  $\mu\text{m}$ ). In contrast, *Cyclostephanos* is negatively correlated with variation in abundance of these above-mentioned species in the core. The conspicuous absence of this species in the modern plankton can be related to recent increases in Si: P ratio, which may be related to the decreased diatom productivity in recent decades. The alternating patterns of occurrence of long *Nitzschia* species and *Cyclostephanos* sp. in core sections analysed at high resolution indicate that it is possible to use diatom analyses at a nearly seasonal scale. Difficulties in core dating however prevent the detailed interpretation of the analyses performed on this core.

We developed a finite-difference, reduced-gravity model for the numerical simulation of the horizontal velocity components in the epilimnion and the thermocline depth of Lake Tanganyika. We first studied the thermocline oscillations due to the seasonal cycle of the wind stress over the lake. In accordance with all available data, the amplitude of the thermocline displacements was shown to be equivalent to the typical depth of the epilimnion, *i.e.* about 50 metres. The model results suggest that it is essentially the first mode of oscillation that is excited. A wavelet study revealed that the wind stress presents significant variability at timescales ranging from 3 to 4 weeks, which is also the order of magnitude of the period of first-mode, free oscillations of the thermocline. Not surprisingly, the lake was seen to be resonating with the fraction of the wind forcing exhibiting variability at 3-4 weeks. These forced thermocline oscillations account for a larger fraction of the epilimnion depth variability than the free oscillations due to the seasonal cycle of the wind stress. Model simulations suggested that there exist internal Kelvin waves in Lake Tanganyika whose amplitude is sufficiently large that they may have an impact on the surface temperature and, perhaps, the ecology. For the abovementioned numerical studies, the thermocline was assumed to be an impermeable surface. We then included entrainment and detrainment terms in the hydrodynamic sub-model of the coupled ecological-hydrological model. Hypolimnion water is entrained into the upper layer in the upwelling regions during strong winds, and is detrained in the downwelling regions. The ecological sub-model for the epilimnion simulates nutrients, phytoplankton biomass and zooplankton biomass. Ecological model simulations showed a reasonably good agreement with the measurements or biomass estimates. The interesting result from the model studies is that the primary production, which strongly depends upon the light in the water column and entrainment of nutrients, is bottom-up controlled. While, it seems that predator abundance strongly controls zooplankton biomass (top-down control). By contrast, fish predation influence seems quite reduced on the phytoplankton level.

The project could reach a better understanding of the ecological variability in several components of the ecosystems. The seasonality, interannual variability and presence of internal waves were found to be three important source of variability to take into account. The interpretation of past climate was not possible due to the lack of well chronologically laminated sediments. The impact of the climate on the lake ecology could probably be simulated by the use of an improved model in the future.

**Keywords:** Lake Tanganyika, climate change, limnology, phytoplankton, plankton production, geochemistry, modelling



## 1. INTRODUCTION

CLIMLAKE is a multidisciplinary project on Lake Tanganyika, involving Belgian teams and African partners, funded by the Science Policy Office of Belgium (SPO). The project started in 2001 and extended until June 2005. The field work at Lake Tanganyika lasted from February 2002 until January 2005.

CLIMLAKE addresses the recent concerns about climate variability, a major issue to be tackled by decision makers, and its effect on ecological processes in Lake Tanganyika.

Recent publications have indeed provided evidence of the influence of climate change on large African lakes, particularly in Lake Tanganyika (Plisnier 2000; Livingstone, 2003; O'Reilly *et.al*, 2003; Verschuren, 2003; Verburg *et.al*, 2003).

When analysing climate, limnology and fisheries data, variability may be detected at least at four time-scales in Lake Tanganyika: monthly, seasonal, ENSO and a trend over the last 20 years. A previous project funded by the Belgian Government (PPS Science Policy 1996-2000) has confirmed the ENSO impact in East African climate and on terrestrial vegetation from remote sensing and climate data. Climatic teleconnections with Lake Tanganyika, climate and fish catches have also been shown (Plisnier, 1997; Plisnier *et.al*, 2000). Within the same project, sediment cores of Lake Tanganyika were collected in Zambian and Tanzanian waters in 1998. Studies of these sediments have confirmed the occurrence of laminations but also various shifts in fossil diatom assemblages that could be linked to local and global environmental variability. Besides, the FAO/FINNIDA project (1992-2000) gathered recent important information about several ecological processes. Among these, new data on planktonic primary production have been acquired (Sarvala *et.al*, 1999), and relationships have been shown between internal waves subsequent to wind-driven processes and nutrient availability (Chitamwebwa, 1999; Plisnier *et.al*, 1999, 2001; Langenberg *et.al*, 2003). However, the limnological record of Lake Tanganyika is still too incomplete to describe the complex ecosystem interactions which lie behind those processes.

The CLIMLAKE project involves an integrated approach combining hydrodynamics, nutrient distribution, plankton dynamics, geochemical signals and paleoecology for improving the understanding of Lake Tanganyika variability and sensitivity to climate change.

The main components of the projects are:

1. Environmental monitoring, consisting of meteorological measurements (continuous) and limnological sampling (bimonthly) at two stations of Lake Tanganyika (Mpulungu, Zambia and Kigoma, Tanzania) during 3 years (2002 – 2004). Data acquisition and sampling have been carried out by Zambian and Tanzanian researchers supported by the project and Belgian researchers. An adequate equipment has been provided to both stations, which had already good facilities and personnel trained in limnological studies. In addition to this local data acquisition, satellites images have been used for getting whole-lake surface temperature data.

2. Study of present plankton, particularly phytoplankton, based on the fact that phytoplankton composition and biomass directly respond to fluctuations of various environmental factors (light, temperature, mixing regime, nutrient inputs to surface layers) and can provide information on changes that occurred in the lake for the past decades. Moreover, the study of present communities can provide clues for interpreting changes in the sediment diatom record. In addition, other plankton components and processes have been studied, in order to improve the knowledge of the ecosystem function and to provide the data needed for developing an ecological model: bacterioplankton, protozooplankton (ciliates and heterotrophic nanoflagellates), mesozooplankton (copepods), primary production, bacterial production. Parallel research on specific ecological processes, like grazing by heterotrophic protists, has been conducted.

### 3. Geochemical studies

Measurements of trace elements in the water column (Sr, B, Ba, Mn, Rare Earth Elements, Cd, Zn, Pb, Cu) in order to: (a) identify the controlling factors of water and particles geochemistry; (b) determine the oxycline dynamics; (c) record and quantify the deep water upwelling.

Measurements of trace elements in a bivalve mollusk shell (*Pleiodon spekii*) as a proxy for environmental change using microdrill and laser ablation with ICP-MS to perform reliable trace element distributions in chemically marked shells. The time-gauged geochemical (Mg, Sr, B, Ba, Mn, rare earth elements, Cd, Zn, Pb, Cu) patterns can be used to discriminate the respective role of environmental and physiological factors on the incorporation of trace elements.

Use of silicon isotopes fractionation by diatoms ( $\delta^{29}\text{Si}$ ) to track changes of diatom production in the surface waters by calibration against primary production



measurements. The final objective was to apply this silicon isotopes technique to quaternary diatom-rich sediments to quantify the paleo-productivities.

4. Diatom analysis in sediment cores collected in a previous project: interpretation of the variation of abundance of diatom frustules in the sediment, based on improved knowledge on ecological requirements of the species, to help to track environmental changes in Lake Tanganyika during the past 1500 years.

5. Development of an eco-hydrodynamic model, for simulating the major hydrodynamics events in the lake mainly driven by wind pattern and how these events affect ecological processes and the main ecosystem components. In a first step, the model has been developed using and reprocessing existing data from previous studies; subsequent steps involved validation of the hydrodynamic model with the new data acquired in the CLIMLAKE project and development of an ecological submodel including nutrients, phytoplankton biomass and production, as well as other components and processes.

Once calibrated and validated, it was hoped that the eco-hydrodynamic model could be used for interpreting observed changes in nutrient availability, plankton community structure and geochemical proxies, as driven by meteorological and seasonal changes. The final objective was to use the model for simulating the conditions which induced past changes and for predicting future ecological changes which could be driven by climate change.

The main objective of CLIMLAKE was scientific: hopefully, the project has helped to further understand the lake hydrodynamics, its geochemistry and its ecological functioning, and the influence of climate variability on these processes.

Here we report the main results of the different components of the CLIMLAKE project during the three-year period of the study. All data have been gathered in a data base, available on CD-Rom, joined to this report. Several publications were produced over the course of the study, and some are still submitted or in preparation. A list of these scientific papers appears in the bibliography.



## 2. MATERIAL AND METHODS

### 2.1 Study sites

From February 2002 to January 2005, water column samples were taken fortnightly from two offshore stations of Lake Tanganyika (Fig.1): Kigoma (Tanzania) in the north ( $04^{\circ}51.26'$  S,  $29^{\circ}35.54'$  E) and Mpulungu (Zambia), in the south ( $08^{\circ}43.98'$  S,  $31^{\circ}02.43'$  E). These two sampling sites were identical to those used in the FAO/FINNIDA LTR (Lake Tanganyika Research) project (Plisnier *et.al*, 1999). In addition, three cruises were organised from Kigoma to Mpulungu, two in the dry season (July 10-17, 2002; July 7-13, 2003) and one in the rainy season (Jan 30 – Feb 7, 2004), with several sampling sites (Fig. 1).

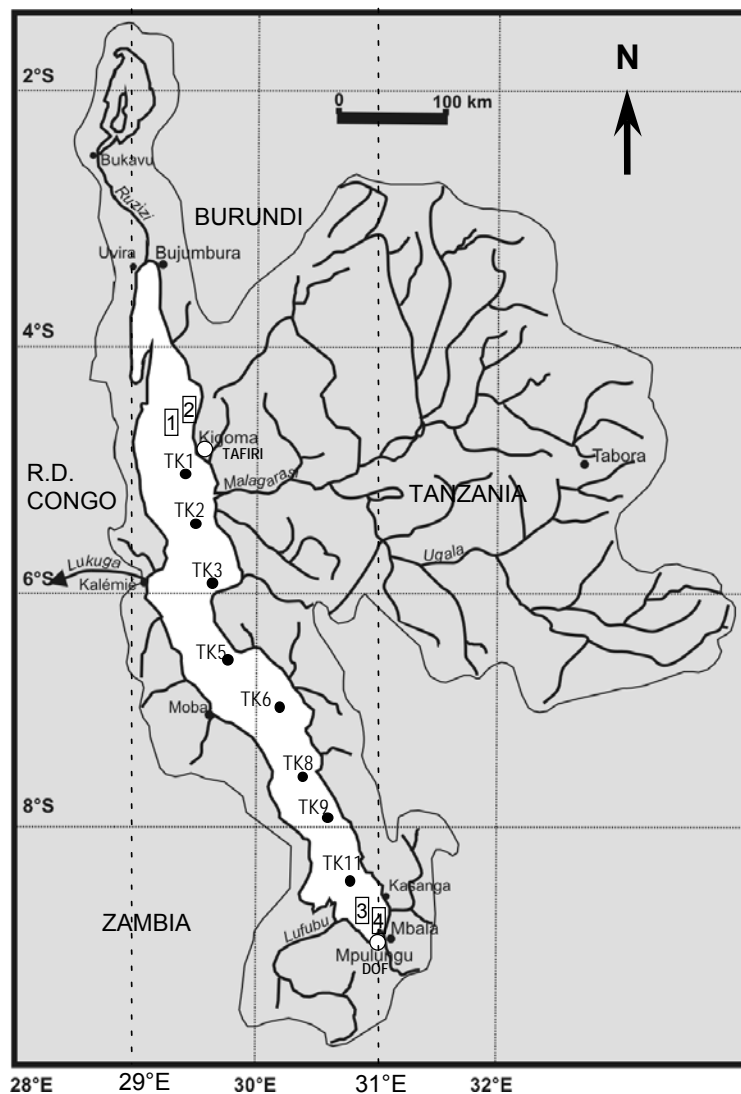


Figure 1 - Sampling sites for the CLIMLAKE regular survey [square boxes: (1) CLIMP-K, (2) CLIMC-K, (3) CLIMP-M and (4) CLIMC-M] and study sites of the research cruises (black dots). The research stations of TAFIRI and DOF are also indicated (circles).

## 2.2 Meteorology

Meteorological data of wind speed and air temperature are from Kigoma airport and DOF (Mpulungu) local monitoring (corrected with DAVIS automatic station data). Data on rainfall is from TAFIRI (Kigoma) and DOF observation near the lake. For the meteorological time series, an average of the preceding 15 days of meteorological observations before the limnological sampling is presented. The results are centred on the date of the sampling.

## 2.3 Water column sampling and measurements

Water column samples were collected with Hydrobios (5 L) or Go-Flo (up to 12 L) sampling bottles, every 20 m from the surface down to 100 m. Occasional additional sampling was done at 10 and 30 m, notably during the cruises. Limnological profiles using CTDs (Seabird 19 in Kigoma, Hydrolab in Mpulungu), transparency measurements (Secchi disk depth) and analyses of nutrients were carried out during regular sampling at the two stations and at all sites during the cruises. During the cruises, the Seabird CTD was used down to depth of max 1300m. DO, pH and turbidity were also occasionally measured with the Seabird and Hydrolab CTDs although the instruments suffered from occasional breakdowns.

Nutrient analyses were done using standard spectrophotometric techniques (A.P.H.A, 1992) or Macherey-Nägel® analytical kits; for inorganic N and P forms, absorbance of coloured samples was measured in 40 or 50 mm cells. Euphotic depth (depth at which light is 1% of subsurface light) was derived from Secchi depth (SD) by calculating the vertical light attenuation coefficient ( $k = 1.57/SD$ ). The conversion coefficient was obtained by calibration with measurement of PAR downward attenuation with LICOR quantum sensors. Depth of the mixed layer was estimated from the depth of the top of the thermocline, as shown by the temperature and oxygen vertical profiles obtained with the CTDs (CLIMLAKE, 2002; Descy & Gosselain, 2004).

The thermic stability, defined as the amount of energy per unit volume required to change a water column from stratified to fully mixed, was calculated for the upper 100m using potential energy anomaly (PEA, Simpson, 1982).

## 2.4 Remote sensing

Satellite data for 2002 have been provided by the AVHRR sensor. Images have been downloaded from the NOAA website and, with the help of the SURFACES laboratory led by Dr. Y. Cornet (University of Liège, Belgium); numerous images of surface temperature were acquired for the year 2002. A calibration was performed using the measured temperature at the two survey sites, Kigoma and Mpulungu, and satellite images available for the days when the measurements were done. A significant

regression of temperature-image against field temperature was obtained, with an accuracy of 0.988 °C, estimated from data available. Indeed, it is to be stressed that only 24 field values were available for this calibration, which will be improved with more lake surface temperature data in future projects. Errors on the temperature-image possibly increased when there was a partial cloud cover. In this case, lake temperature was obtained from processing with an algorithm developed by Dr. J.-M. Beckers (University of Liège).

## 2.5 Elemental analysis

Elemental analysis of the seston was carried out using a Carlo Erba NA1500 elemental analyser for C (carbon) and N (nitrogen) determinations, after treatment of the dried filter with HCl to remove carbonates possibly present. P (phosphorus) was measured by spectrophotometry of orthophosphate after digestion for 30 min at 120°C with potassium persulphate. C, N and P content of the seston of the surface waters (0 - 40 m) was then calculated taking into account the volume of water filtered and expressed in  $\mu\text{moles l}^{-1}$  before calculating the elemental ratios.

Limitation of phytoplankton growth by N or P can be appreciated by reference to the elemental ratio in the seston: in optimal growth conditions, the C:N:P proportions (by atoms) are 106:16:1 (Redfield ratio). A significant P limitation takes place when seston C:P > 130 or when N:P exceeds 22; N-limitation is considered to occur when C:N > 8.3 or N:P < 22 (Healey & Hendzel, 1979; Guilford & Hecky, 2000). However, some phytoplankton taxa do not experience significant P limitation with cell C:P around 200.

## 2.6 Phytoplankton pigment analysis and processing of data

This approach of phytoplankton is based on the use of marker pigments (chlorophylls and carotenoids) to study variations of algal composition at the class level. Chlorophyll a concentration (Chla) measures phytoplankton biomass and marker pigments allow calculating the contribution of the various algal classes to total chlorophyll a. The main features are

- the measurement of pure chlorophyll a, without interference from degradation products, most of them occurring from *in situ* processes (algae lysis and grazing by micro- and mesozooplankton)
- the ability to measure numerous samples; in this case, all sampling depths were analysed, which allows to observe vertical distribution of the plankton,
- the detection of all algae, even the smallest (picocyanobacteria), using the same analytical technique

Samples for HPLC analysis were obtained from filtration of 3 to 4 L on Whatman GF/F or Macherey-Nägel GF5 filters, of 0.7  $\mu\text{m}$  nominal pore size. The subsequent

procedure for pigment extraction and analysis followed Pandolfini *et al.* (2000) and Descy *et al.* (2000). Extracts in 90% acetone were then stored in 2 mL amber vials in a freezer (at -25°C) for several months (under the regular sampling scheme) or for 2-3 weeks at most (for the cruise samples), and transported to Belgium on ice in cooler boxes. A total of more than 800 samples were analysed over the three years from the two stations. In the rainy season 2003 (February-April), pooled samples from the 0-30 m layer were filter-fractionated before collection of the particulate material on the 0.7 µm filters: two subsequent filtrations were carried out on Nylax plankton nets to retain the particles > 28 µm and > 10 µm, followed by a third filtration on a Millipore membrane of 2 µm pore size. The subsequent treatment was identical to that applied to the non-fractionated samples and allowed estimation of biomass and composition of the following size fractions: > 28 µm, 10-28 µm, 2 – 10 µm and < 2 µm. Pigment data processing used the CHEMTAX software (Mackey *et al.*, 1996). Details of the processing method are given in Descy *et al.* (2005). The following algal classes were quantified: chlorophytes, chrysophytes + diatoms, cryptophytes, cyanobacteria type 1 (T1), cyanobacteria type 2 (T2), and dinoflagellates. Euglenophytes, poorly represented in Lake Tanganyika, were not included in the analysis. The distinction between cyanobacteria T1 and cyanobacteria T2 was based on different zeaxanthin: chlorophyll a ratios and presence of echinenone in cyanobacteria T2.

The C: Chla ratio is usually determined from linear regression of POC (particulate organic carbon) against chlorophyll a concentration, and is used for converting chlorophyll a biomass into phytoplankton carbon. This ratio is expected to vary as a function of the light climate (algal cells contain less chlorophyll a in high light conditions, *i.e.* C: Chla is high), and can be influenced by nutrient, especially N, availability.

## 2.7 Mesozooplankton abundance and biomass

The water column was sampled with a 100 µm mesh plankton net in the 0-100 m layer. The samples were concentrated by settling in a 250 mL PVC cylinder for 48 h; after removal of the supernatant, the final volume was adjusted to 100 mL, with lake water added with formalin. Zooplankton counts were carried out with a Leica DIML inverted microscope, at a maximal enlargement of 400 X, most of the time on subsamples. Four species of copepods were identified:

*Microcyclops cunningtoni* (Sars)

*Tropocyclops tenellus* (Sars)

*Mesocyclops aequatorialis aequatorialis* (Kiefer)

*Tropodiptomus simplex* (Sars)

Data were expressed per unit area, taking into account net opening size and the sampling over a 100 m water column. For individual carbon content of copepods

used for converting numbers to biomass, we used the same values as those used by the LTR project (Kurki *et.al*, 1999): 2.25 µg C for adult calanoids, 2 µg C for adult cyclopoids, 1.3 µg C for calanoid copepodites, 0.75 µg C for cyclopoid copepodites, and 0.175 µg C for nauplii. Several samples from Kigoma were missing, particularly in 2004. Shrimps and medusae were counted only in the 2002 samples; these data are not reported here.

## 2.8 Primary production

Phytoplankton production was measured using the  $^{14}\text{C}$  method (Steeman Nielsen, 1952). Water samples collected at 0, 10, 20, 30 m were pooled, added with 25 µCi  $^{14}\text{C}$ -bicarbonate and incubated in 180-200 mL flasks shaded with neutral screens to obtain a gradient of light. All flasks were placed in a tray with lake water which was renewed frequently to keep the flasks at lake temperature. Incident solar radiation recorded during the incubations allowed to estimate average irradiance received by each flask during the incubation. At the end of the incubations, the water was added with neutralised formalin to stop biological activity and the content of each flask was filtered on GF 5 filters (porosity 0.7 µm). The filters were then dried and transferred to scintillation vials. Back to Belgium, the radioactivity of each vial was measured by liquid scintillation, and radioactivity counts were converted to carbon uptake, using initial radioactivity in the flasks, available inorganic carbon (calculated from pH and alkalinity) and incubation time. These data allowed to construct photosynthesis (carbon uptake as µg C l<sup>-1</sup> h<sup>-1</sup>) – light (µE m<sup>-2</sup> s<sup>-1</sup>) relationship; the photosynthesis parameters, P<sub>max</sub> and I<sub>k</sub>, were determined using non-linear regression for fitting to the Vollenweider's equation (Vollenweider, 1965). Daily carbon uptake by phytoplankton (primary production) was calculated using integration of photosynthesis over time and depth of the euphotic zone, with measured light attenuation coefficient (usually calculated from Secchi disk depth), and hourly irradiance. *In situ* measurements of irradiance were used when available, whereas irradiance calculated from date and latitude was used when *in situ* light measurements were missing. The method measures only particulate primary production, without accounting for “dissolved” production (*i.e.* extracellular release of photosynthetic products

Measurements were carried out weekly at Kigoma during the rainy season 2002 (February – April), at Mpulungu in the rainy season 2003 (February to May), in the dry season 2004 (August 2004) and during the three cruises, in a variable number of sites. In total, 42 measurements allowing estimates of daily particulate phytoplankton production and evaluation of the photosynthetic parameters are available for the study period. ). Finally, we calculated daily photosynthesis at each routine sampling date, using the photosynthetic parameters (see below), calculated incident light,

average chlorophyll a in the 0-40 m layer, and vertical extinction coefficient from Secchi depth. This “modelled” photosynthesis is used to follow variations of primary production with time at both sampling sites, and to infer annual rates.

## **2.9 Bacterial production**

Bacterial production was obtained by an incorporation of tritiated thymidine into bacterial cells, which is proportional to the incorporation of carbon by bacteria (Fuhrman & Azam, 1980, 1982). Measurements were carried out during the research cruises of July 2002, July 2003 and January 2004, from samples of the mixed layer (0 to 40 m). In addition, during two CLIMLAKE sampling missions at the two monitoring stations, bacterial production was measured on samples taken in the mixed layer, at 60 m, and at 100 m depth

## **2.10 Phytoplankton (microscopic observations) and heterotrophic organisms:**

Subsamples for enumeration of phytoplankton (both  $< 5 \mu\text{m}$  and  $\geq 5 \mu\text{m}$ ), bacteria, heterotrophic nanoflagellates (HNF) and ciliates were fixed according to the lugol-formalin-thiosulphate method (after Rassoulzadegan in Sherr and Sherr 1993).

Bacteria were stained with DAPI (4',6'-diamidino-2-phenylindole 37) and filtered onto a  $0.2 \mu\text{m}$  pore size membrane filter. For enumeration of phytoplankton  $< 5 \mu\text{m}$ , a subsample was filtered onto a  $0.8 \mu\text{m}$  pore size membrane filter after DAPI staining to allow HNF enumeration.

One-litre subsamples for phytoplankton counts were settled for sedimentation during 48 h in the laboratory of TAFIRI at Kigoma and DOF at Mpulungu. The supernatant was removed and the concentrated samples were transferred to 100 ml bottles for transportation. Before counting, the samples were reconcentrated in order to transfer the sample in a 10 ml sedimentation chamber. A drop of Rose Bengal (Aldrich Chem. Co) was added to enhance visibility of the cell content. Permanent diatom slides of net samples were prepared and embedded in Naphrax (PhycoTechn Inc., USA).

Bacteria, phytoplankton  $< 5 \mu\text{m}$  and HNF were enumerated using epifluorescence microscopy. For bacteria, pico- and nanophytoplankton counts, at least 400 cells were enumerated using UV, violet-blue (395-440 nm excitation filter and 470 nm emission filter) and green light illumination (510-560 nm excitation filter and 590 nm emission filter) using a Zeiss Axioplan microscope at 1000 $\times$  magnification (Maclsaac and Stockner 1993). A distinction was made between picophytoplankton ( $< 2 \mu\text{m}$ ) and phytoplankton of 2-5  $\mu\text{m}$  in size. Heterotrophic nanoflagellates were stained with DAPI and filtered onto  $0.8 \mu\text{m}$  pore size filters. A minimum of 100 cells was counted using UV-illumination (365 nm excitation filter and 397 nm emission filter). Phytoplankton cells larger or equal to  $5 \mu\text{m}$  were counted in 30 fields with a Zeiss Axiovert 135 inverted microscope at 400 $\times$  magnification according to the Utermöhl



method (Uthermöhl 1931). Standard floras (e.g. Geitler 1932, Komárek and Fott 1983, Starmach 1985) and more specific literature on Lake Tanganyika (e.g. Van Meel 1954, Hecky *et.al* 1978, Cocquyt 1998, Caljon pers. notes) were used for the identification of phytoplankton species. The permanent diatom slides were used for species determination where necessary. These slides were studied with an Olympic BX 50 light microscope, equipped with differential interference contrast. Ciliates were enumerated by means of inverted microscopy during phytoplankton counts. The quantitative protargol staining technique was used for identification of the dominant species (Montagnes and Lynn 1993). Phytoplankton and HNF biovolumes were calculated from mean linear cell dimensions of each species using appropriation formulas (Hillebrand *et.al* 1999). Fresh biomass estimations, expressed as  $\text{mg m}^{-3}$ , were calculated assuming a density of 1.

### **2.11 Geochemistry of the water column: major, minor and trace elements**

Dissolved and particulate samples ( $> 0.4\mu\text{m}$ ) for geochemical analyses were collected in Kigoma and Mpulungu just below the surface ( $\sim 0\text{m}$ ) at the coastal sites, at 20 and 100m depth at the pelagic sites. A similar dual approach was performed during a transect cruise in July 2002 and for the dissolved phase only in July 2003 and January-February 2004 for deep profiles at station 1 (northern basin) and 8 (southern basin). The sampling protocol is detailed in the Field Manual (CLIMLAKE, 2002). In a clean laboratory, filtered particles were digested in a concentrated mixture of Suprapur acid ( $\text{HCl}/\text{HNO}_3/\text{HF}$ ) at  $90^\circ\text{C}$  in Teflon beakers. After evaporation, the residue was dissolved in 0.5%  $\text{HNO}_3$  Suprapur solution. Acidified dissolved fractions were analysed directly for trace and major elements. Trace elements (Sc, Co, Cu, Zn, Ga, Ge, Rb, Sr, Y, Zr, Nb, Mo, Cs, Ba, REE, Hf, Ta, W, Pb, Th, U) were analyzed by inductively coupled plasma-mass spectrometry (ICP-MS - VG Elemental Plasmaquad PQ2 + for particulate material and by HR-ICP-MS – Finnigan Element II (cruise 2003, 2004 and monitoring) for the dissolved fraction. Matrix and instrumental drift effects were monitored and corrected for mass spectrometry by measuring the fluctuations of internal standards ( $^{99}\text{Ru}$ ,  $^{115}\text{In}$ ,  $^{185}\text{Re}$ ,  $^{209}\text{Bi}$ ) added to the samples. Major and minor elements in particulate matter (Al, Ba, Ca, Fe, K, Mg, Mn, Na, P, S, Si, Sr, and Ti) were measured by ICP-AES (Thermo Optek Iris Advantage) using Y and Au as internal standards to correct for the instrumental drift. External calibrations were performed using artificial standard solutions and diluted mineralised natural rock standard (e.g., BHVO-1, DWA, CCH-1 SGR-1, and JGB-1) or freshwater standard (SLRS-4). Experimental blank and blank filters were processed under the same conditions as the samples and blank signals were subtracted. Elements such as Ba and Sr have been analyzed using both ICP-MS and ICP-AES techniques, showing a good reproducibility within 15%. Only a few significant results for trace and

major elements will be reported here owing to the large amount of data produced in this study.

## 2.12 The bivalves monitoring

New analytical methodologies using in-situ Laser Ablation (LA-ICP-MS) and microdrilling methods coupled with High-Resolution ICP-MS (HR-ICP-MS) were developed to perform reliable chemical profiles with a monthly to weekly definition in the aragonitic shell of the bivalve mollusc *Pleiodon spekii*. High-resolution chemical profiles (trace metal elements; isotopic composition of C and O) were compared to the results of a two years limnological monitoring of lake waters.

Every 6 months, living specimens were collected by diving in two sites: one near Kigoma, Tanzania, the other close to Mpulungu (Mbita Island), Zambia. Because all the results cannot be described in detail here, this report is focused on the Southern site of Mpulungu where a well-marked seasonal upwelling occurs and on two well studied specimens (MPU-V10 and MPU-V72) that illustrate our main results (Mn, Sr,  $\delta^{18}\text{O}$ ) and conclusions.

Periodic measurements and experimental chemical markings were done to create temporal marks in shells. From July 2002 to February 2005, specimens were measured for length (L) the width (W) and height (H) and labelled using "bee tags" before being replaced in the field site. At each mission, some of the retrieved and measured specimens were sacrificed and the shells brought back for analysis in the Royal Museum for Central Africa, Tervuren.

Chemical analyses were done on polished sections. Shells were cut with diamond saw along a growth axis (Fig. 2a), mounted on a petrographic slide and polished to identify growth structures (Fig. 2b). All analyses were performed in the middle nacreous layer (Fig. 2b). Trace/minor elements profiles were done by using (1) an in-situ analysis by LA-ICP-MS for trace elements (UV laser; MRAC-Tervuren; operating conditions in Lazareth *et.al* 2003), and (2) a solution nebulisation HR-ICP-MS (MRAC-Tervuren) on micro-milled samples (Merchantek MicroMillIT Sampler). Oxygen and carbon isotope analysis were done by using a ThermoFinnigan Kiel III coupled IRMS on micromilled samples (Vrije Univ. Brussels; see Gillikin et al, *in press*).

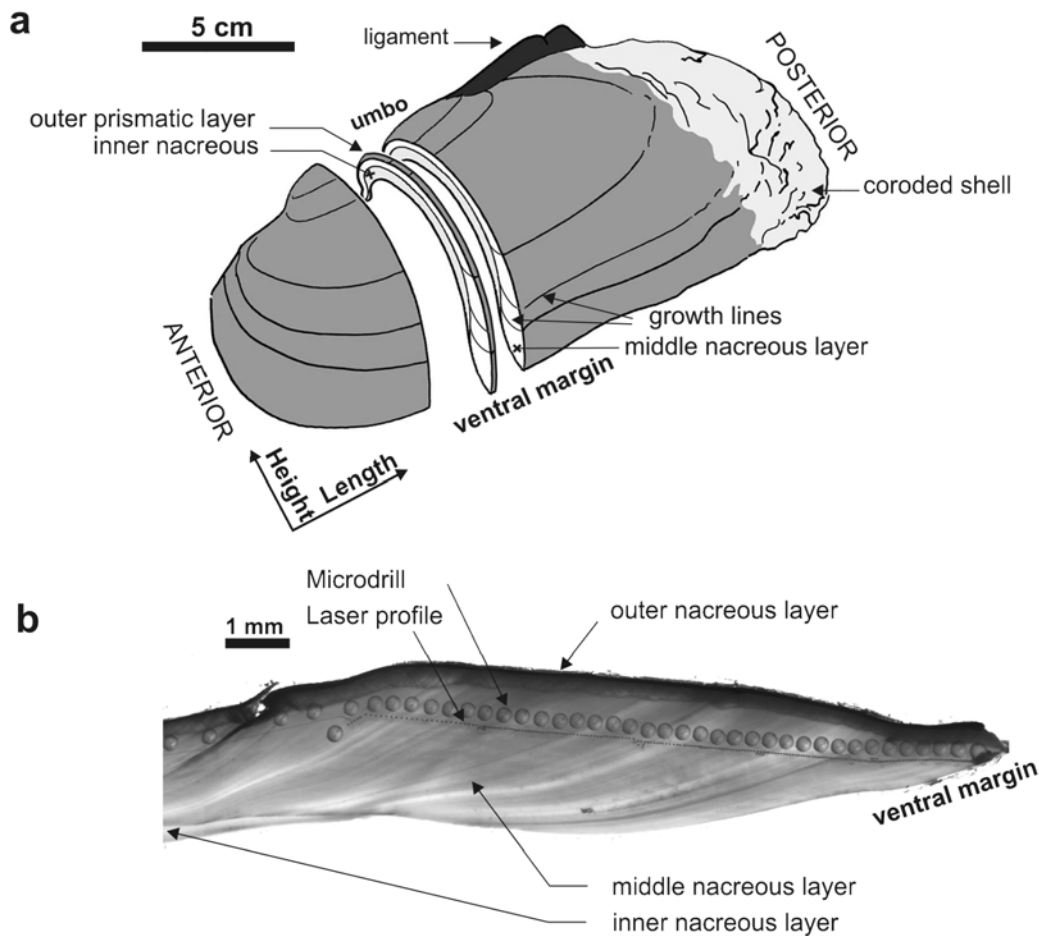


Figure 2: (a) Scheme of a shell valve of *P. spekii* cut in the anterior part from the umbo to the ventral margin (radial section). (b) Microphotograph of a radial section of *Pleiodon spekii* shell showing the growth structures and the sampling profiles in the middle nacreous layer, well preserved from biocorrosion. Microdrill and laser pits are 300 $\mu$ m and 50 $\mu$ m in diameter respectively.

### 2.13 Silicon isotopic fractionations

Water samples for Si isotopic compositions were collected for each monitoring sites in Kigoma and Mpulungu at 0 m for the coastal sites and 20 and 100 m for the pelagic sites. The sampling bottles (5 or 10 L Go-Flo or Hydrobios) were sub-sampled for silicon isotopic measurements into 100-ml acid cleaned high-density polyethylene (HDPE) bottles, after filtration on polycarbonate 0.45  $\mu$ m filters and kept in the fridge until precipitation and analyses in the laboratory. Silicon content analyses on the filtrate were completed in Kigoma and Mpulungu laboratories by spectrophotometry (see limnology section) just after sampling or kept cold on board and processed back to the laboratory. Diatoms were collected with phytoplankton net (10  $\mu$ m mesh) along the dissolved fraction at both sites and transferred on polycarbonate 0.45  $\mu$ m filters. These filtered diatoms were leached with a NaOH (0.2 M) solution at 100°C during 45 min in order to reduce residual contamination from clay material. The solution was then neutralized with suprapur HCl and the supernatant was precipitated following the same procedure as for silicic acid.

Samples from tributaries of Lake Tanganyika (Rusizi, Malagarasi, Luiche, Gombe and Lufubu) were transferred in HDPE 100 ml bottles after filtration and analyzed in order to establish the Si source signatures on a regional scale.

Silicon isotopes were measured after quantitative coprecipitation using the Triethylamine Molybdate. Analyses were carried on under dry plasma conditions using a Nu Plasma MC-ICP-MS with a desolvator (to minimize polyatomic interferences), allowing the acquisition of natural silicon isotope abundances with high sensitivity and accuracy (Cardinal *et.al*, 2003).  $\delta^{29}\text{Si}$  values express the differences of  $^{28}\text{Si}/^{29}\text{Si}$  ratios, representing deviations in ‰ from the same ratio of the NBS28 standard reference material.

$$\delta^{29}\text{Si} = \left[ \frac{\left( \frac{^{29}\text{Si}}{^{28}\text{Si}} \right)_{\text{sample}}}{\left( \frac{^{29}\text{Si}}{^{28}\text{Si}} \right)_{\text{NBS28}}} - 1 \right] \times 1000$$

We have measured and used exclusively the  $\delta^{29}\text{Si}$  notation as the  $^{30}\text{Si}$  signal is disturbed by isobaric interference at low resolution. The  $\delta^{30}\text{Si}$  notation, often used in previous silicon isotopic works, can be attained assuming a mass dependent fractionation between  $^{30}\text{Si}$ ,  $^{29}\text{Si}$  and  $^{28}\text{Si}$  ( $\delta^{30}\text{Si} = 1.934 \times \delta^{29}\text{Si}$ ). A reproducibility test that included molybdate coprecipitation and isotopic analyses of 10 individual aliquots from a single sea water sample gave a standard deviation on the  $\delta^{29}\text{Si}$  of 0.035 ‰ (1  $\sigma$ ) (Cardinal *et.al* 2005). Several replicates performed on particulate and dissolved Lake Tanganyika samples produced a similar reproducibility.

## 2.14 Time series

Several time series were processed to detail some of the main variability linked with seasonality and internal waves. The report is mainly presenting the data of the 0-40 m depth average when several depths have been sampled. In some cases, the data were deseasonalized (Droesbeke, 2001) to better identify the effects of internal waves. In this case, because of the method; 6 months of data are not usable at each time series extremities.

### 3. RESULTS

#### 3.1 Environmental monitoring

##### 3.1.1 Meteorology

Average and standard deviation of air temperature, winds speed and rainfall for different periods are indicated below (tables 1 and 2). The meteorological series is presented in figure 1. The seasons are clearly identified. The strong wind and air temperature decrease in 2003 (Mpulungu) is noted.

Periods	From	To	Av. Wind Speed (m/s)				Av. air T° (°C)				Rains (mm)			
			Kigoma		Mpulungu		Kigoma		Mpulungu		Kigoma		Mpulungu	
			Moy	Std	Moy	Std	Moy	Std	Moy	Std	Moy	Std	Moy	Std
2002-04	01-01-02	31-12-04	1.4	0.32	2.8	1.01	24.1	1.26	24.0	1.99	2420	15.6	4101	14.3
2002	01-01-02	31-12-02	1.5	0.33	3.0	0.92	24.1	1.22	24.0	1.84	843	17.9	1368	14.4
2003	01-01-03	31-12-03	1.4	0.28	3.2	1.12	24.2	1.25	24.1	2.10	889	19.0	1101	11.7
2004	01-01-04	31-12-04	1.4	0.34	2.3	0.70	24.1	1.31	24.0	2.01	688	9.4	1632	16.5
RS 2002*	01-01-02	19-04-02	1.3	0.33	2.5	0.38	24.2	1.19	23.7	1.97	559	17.1	918	19.4
DS 2002	20-04-02	29-10-02	1.6	0.31	3.4	1.08	24.3	1.22	24.1	1.52	5	NA	7	0.4
RS 2002-03	30-10-02	24-04-03	1.3	0.26	2.5	0.45	24.0	1.11	24.1	1.94	807	21.5	1200	17.7
DS 2003	25-04-03	27-10-03	1.5	0.25	3.8	1.23	24.1	1.36	23.9	2.24	35	2.3	27	1.3
RS 2003-04	28-10-03	20-04-04	1.3	0.26	2.2	0.60	24.3	1.11	24.3	2.09	616	12.6	1372	18.3
DS 2004	21-04-04	22-10-04	1.6	0.31	2.6	0.73	24.1	1.54	23.9	1.92	95	8.4	20	1.2
RS 2004**	23-10-04	31-12-04	1.2	0.20	1.8	0.28	23.7	0.96	24.1	2.10	304	11.0	557	23.5

Table 1: Average and standard deviation of main meteorological variables.

During the rainy season in 2002, the wind was rather similar as other rainy seasons in Mpulungu and Kigoma. The air temperature was the lowest in Mpulungu for the 3 years. The variability is high however as observed in Fig. 3. The dry season 2002 showed the second highest wind season during the three years period in Mpulungu while air temperature was the highest of the three dry seasons of observations. This dry season was the warmest in Kigoma. During the rainy season of 2002-03, the air temperature was low in Kigoma. This is probably linked to the high rainfalls (a fast drop of temperature during rains is observed). The dry season of 2003 had the highest wind in Mpulungu and temperature was low. The air temperature was low in Kigoma also. The wind was low in Mpulungu during the rainy season of 2003-04 but air temperature the highest of the 3 rain periods. In Kigoma, the air temperature was high also. During the dry season of 2004, the wind was the lowest of the three dry season period in Mpulungu. The air temperature was as cold as in 2003 but the

repartition was different (fig. 1.2) and probably less efficient for water mixing as the cold sub-period was less extended in time. In Kigoma the 2002 air temperature was as low as in 2003. The wind was low during the rainy season 2004 in Mpulungu while air temperature was similar to 2002-03 (on average). The air temperature was the coldest of the rainy seasons in Kigoma.

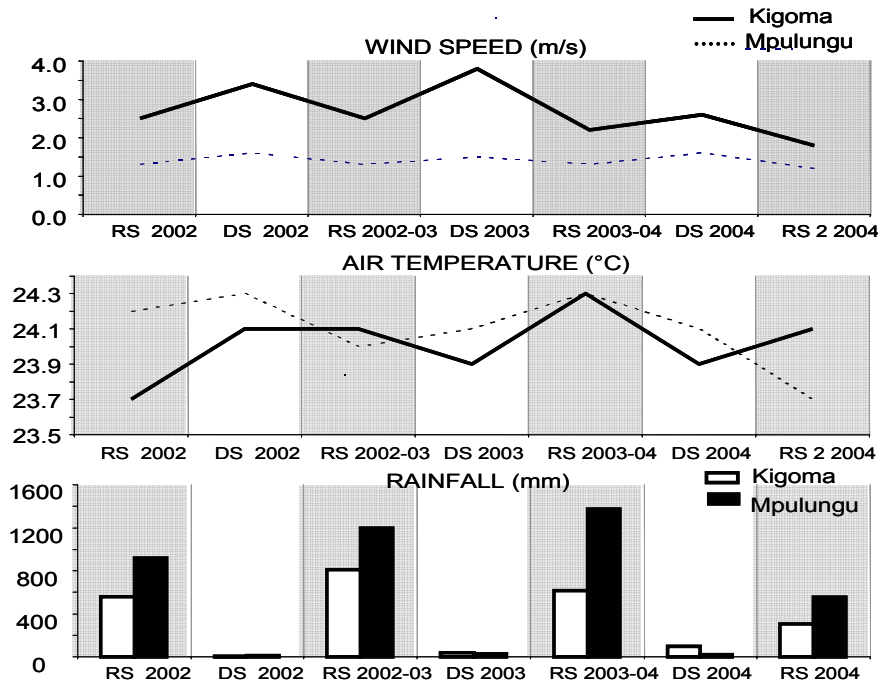


Figure 3: Average wind, air temperature and total rainfall at Kigoma and Mpulungu from January 2002 to December 2004 for the rain and dry seasons.

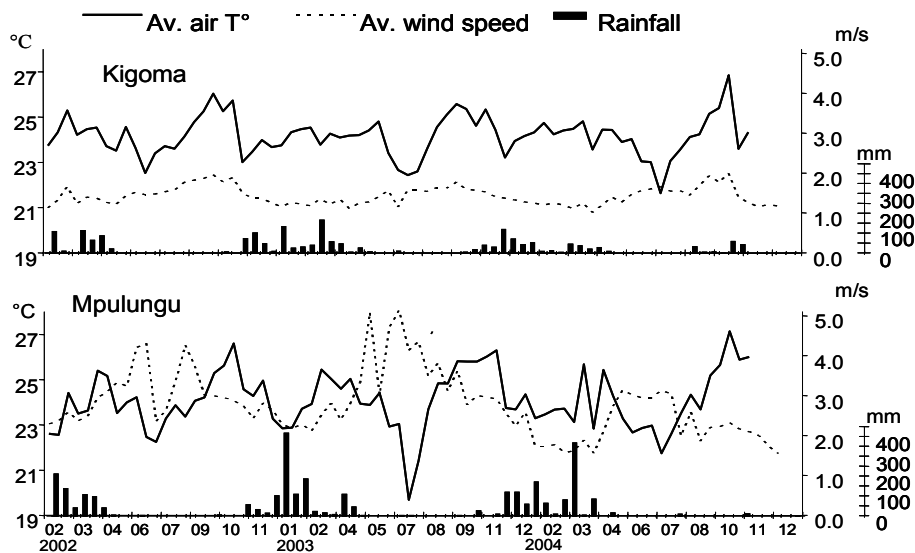


Figure 4: Wind, air temperature and rainfall at Kigoma and Mpulungu from January 2002 to December 2004.

### 3.1.2 Limnology

The range of temperature variability was more important in Mpulungu than in Kigoma (fig. 5). The stronger seasonality in the southern part of the lake there explains this. However, for phosphates and nitrates particularly, a higher variability is observed in Kigoma for all the data collected during the monitoring period. This is well seen particularly in deep water. The yearly tilting of the epilimnion near Kigoma explains this since those depths seasonally belong either to the epilimnion or the upper hypolimnion with corresponding different water composition.

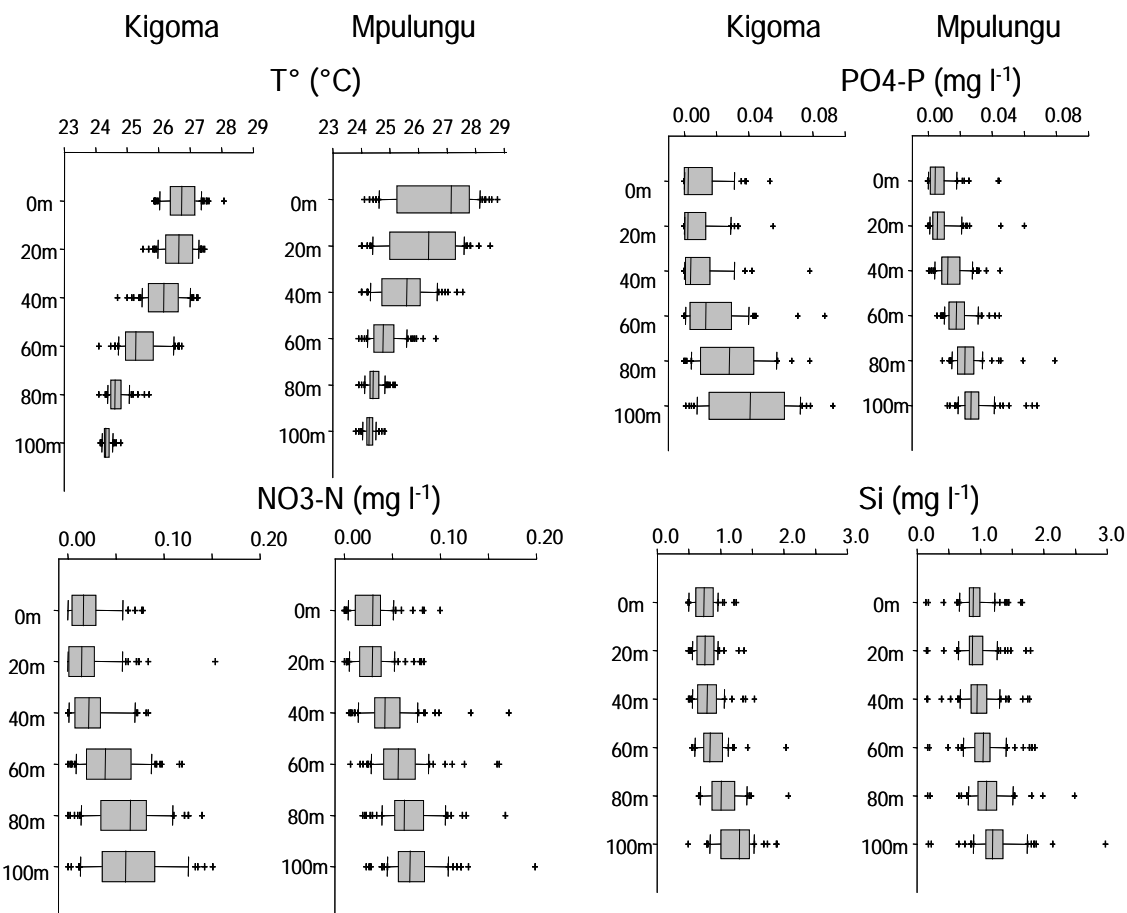


Figure 5. Box plot of temperature, phosphates, nitrates and silica profiles in Kigoma and Mpulungu (median (50%), quartiles (75), whiskers (90%) and outer data).

The box plots of pH and DO values recorded during the cruises are presented in figure 6. For dissolved oxygen, a high variability is observed in deep waters, depending of time and site of measurement in the lake. The pH profile shows decreasing values from surface to bottom.

A high variability of pH in surface waters may be explained by biological activity. Reduced photosynthesis in surface waters is linked to photo-inhibition while the increase of pH at 20 m is linked with the maximum photosynthesis at this depth.

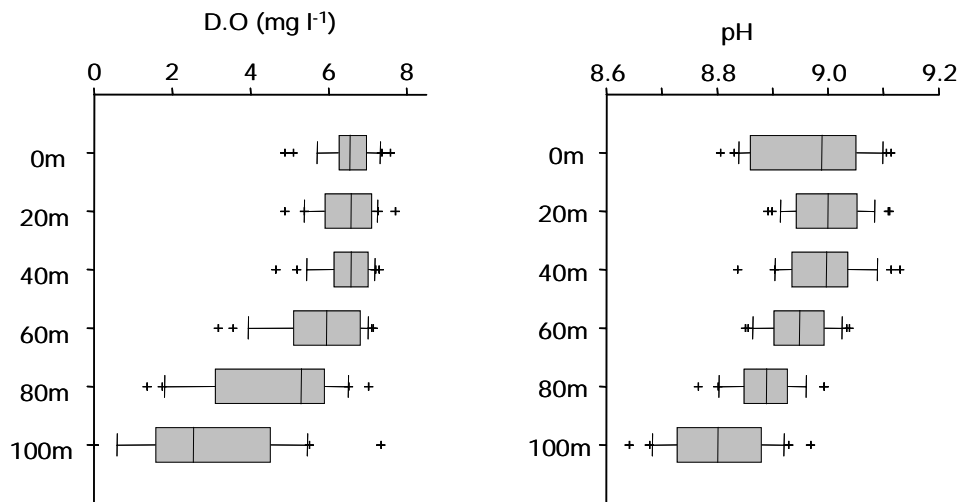


Figure 6. Box plot of dissolved oxygen and pH profiles in Kigoma and Mpulungu during lake cruises (median (50%), quartiles (75), whiskers (90%) and outer data).

The median profile of all observation of Chl<sub>a</sub> (measured by HPLC) by depth in pelagic waters is presented in figure 7. The slightly higher concentrations around 20 m depth are well observed. Concentration of chlorophyll a was generally below 1  $\mu\text{g l}^{-1}$  but reached 2  $\mu\text{g l}^{-1}$  at Kigoma and 4  $\mu\text{g l}^{-1}$  at Mpulungu during some algal blooms. Surface blooms occurred when buoyant cyanobacteria developed and concentrated in the upper waters.

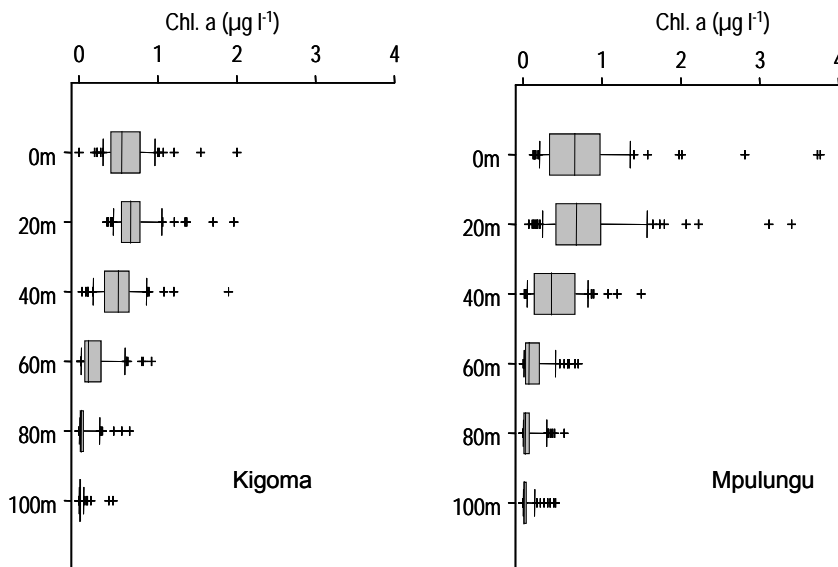


Figure 7. Box plot of chlorophyll a ( $\mu\text{g l}^{-1}$ ) in Kigoma and Mpulungu during 3 lake wide cruises (median (50%), quartiles (75), whiskers (90%) and outer data).



## Water temperature

The seasonality of the thermal structure is well observed from figure 8. A cooling took place in July-November (2002), July-October (2003) and June-August (2004) in Kigoma (dry season variable in intensity and in time period).

Upwelling was well observed every year in Mpulungu. It is important to observe that the upwelling did not occur during the whole dry season (stratification was still present in April to May and September to October). The upwelling of 2003 was clearly more important than in 2002. One should be prudent about the interpretation of the 2004 upwelling at Mpulungu. Although the temperature data in figure 8 show it as apparently strong, other data suggest that it was not so (decreased wind in Mpulungu, stability increase etc.). This can be explained by a change of methodology. In Mpulungu, from May 2004 until the end of December 2004, the CTD was out of use and an oxygen/temperature sensor was used instead every 20 m. Data at 10, 30, 50, 70 and 90 m were interpolated.

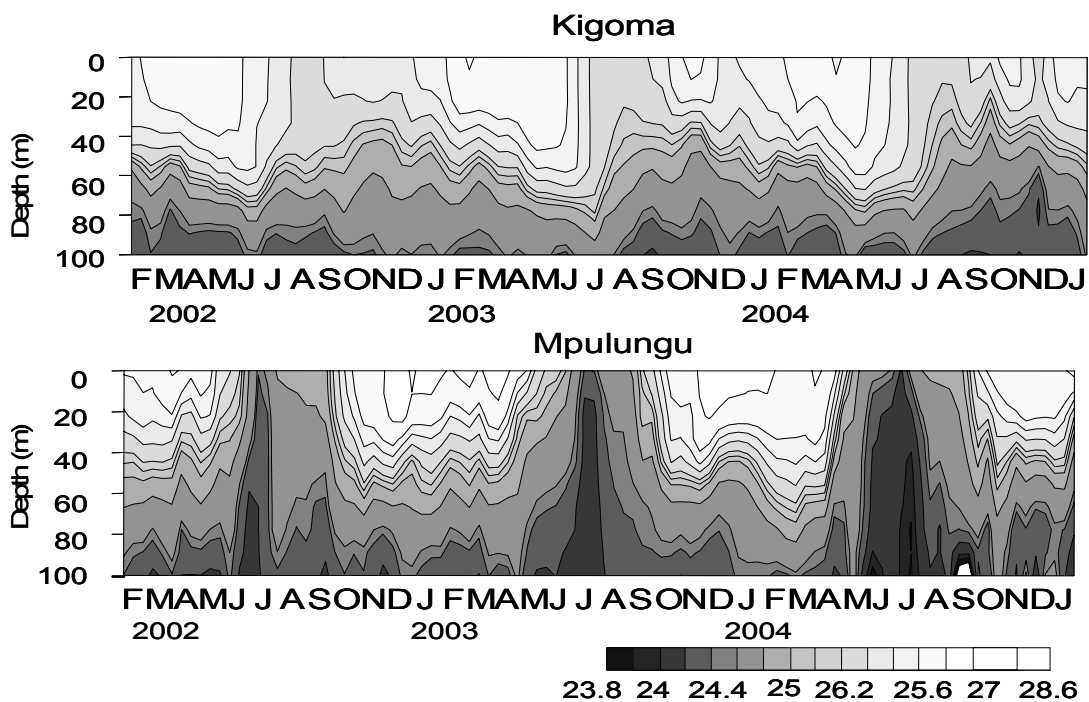


Figure 8: Water temperature from 0 to 100 m at Kigoma and Mpulungu from February 2002 to December 2004.

The period of lower water temperature in the upper 0 to 40 m is compared between stations at fig 9. The seasons can be well identified as well as the stronger seasonality in the southern station (Mpulungu).

The temperature data from 100 m depth have been deseasonalized. The inverse relationship between those temperature profiles is resulting from the internal waves.

The opposed correlation indicates a likely uninodal type of seiche during most of the year (Fig 10).

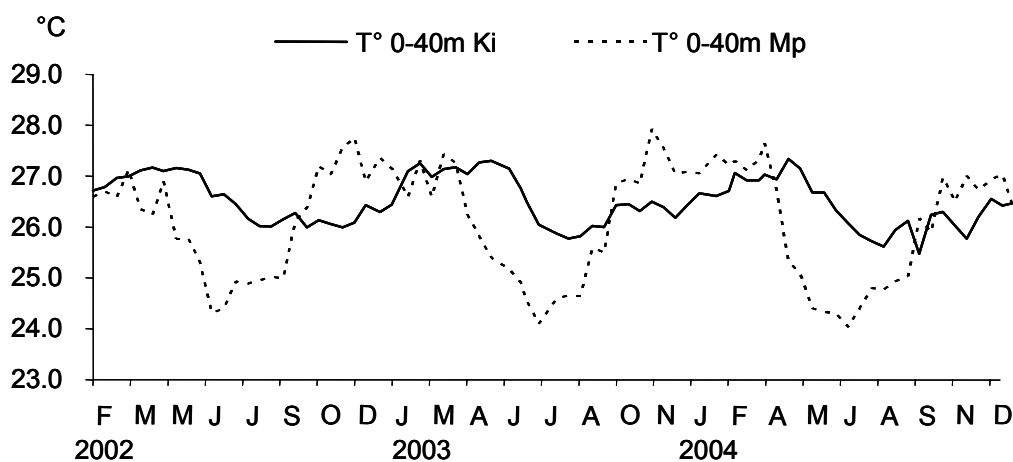


Figure 9: Water temperature (0-40m) at Kigoma and Mpulungu.

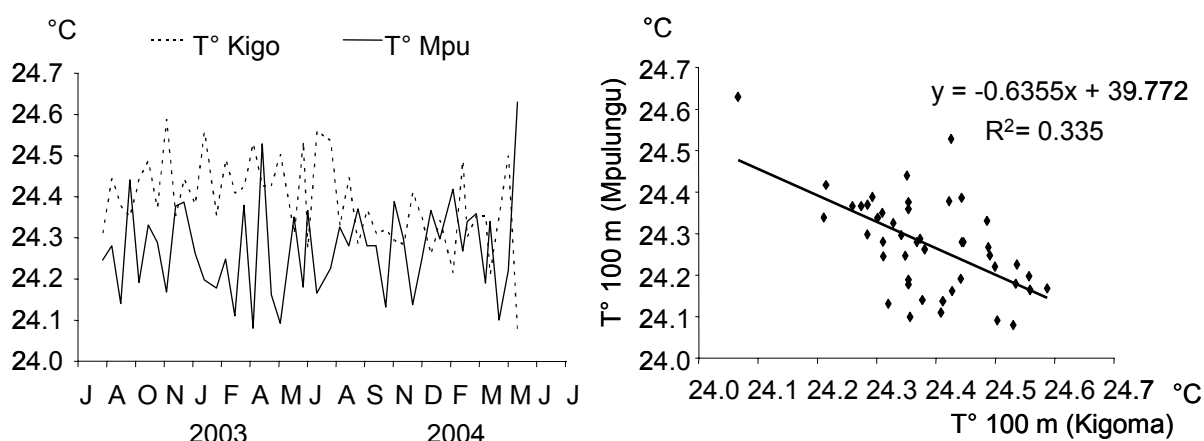


Figure 10: Water temperature (100m) at Kigoma and Mpulungu (deasonalized data).

### Euphotic depth

The euphotic depth (fig 11) is positively correlated to the water temperature (and water stability). The correlation is statistically significant at Mpulungu ( $\alpha=0.01$ ). A warmer temperature and high stability is unfavourable to mixing of water of different density. Since fewer nutrients may reach the surface, less phytoplankton is sustained and water clarity increase.

Average euphotic depth was 38.3 m in Kigoma (range: 25.2m to 55.7m) compared to 35.2 m in Mpulungu (range: 13.8m to 65.1 m). The variability is thus higher in Mpulungu, where the impact of internal waves is stronger due to the geographical position at the end of the lake and occurrence of upwelling during which internal waves have a strong effect on lake surface conditions.

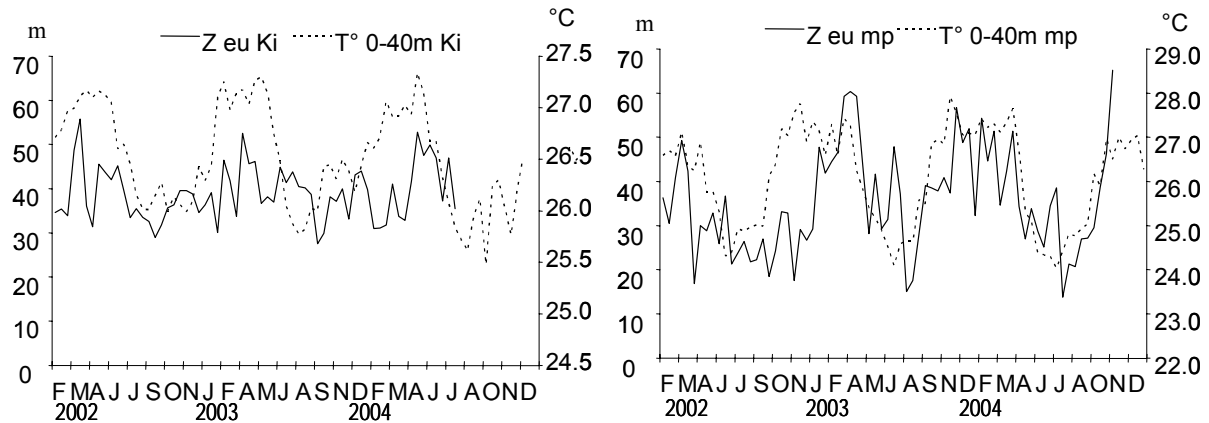


Figure 11: Euphotic depth (m) at Kigoma and Mpulungu.

### Depth of the mixed layer

The depth of the mixed layer (Fig 12) shows important fluctuations mainly linked to the seasonal changes: in Mpulungu, increased wind, lower air T° and lower water temperature is correlated to the depth of mixing. In Kigoma, the same factors influence the vertical mixing, but only air temperature is significantly correlated with depth of the mixed layer.

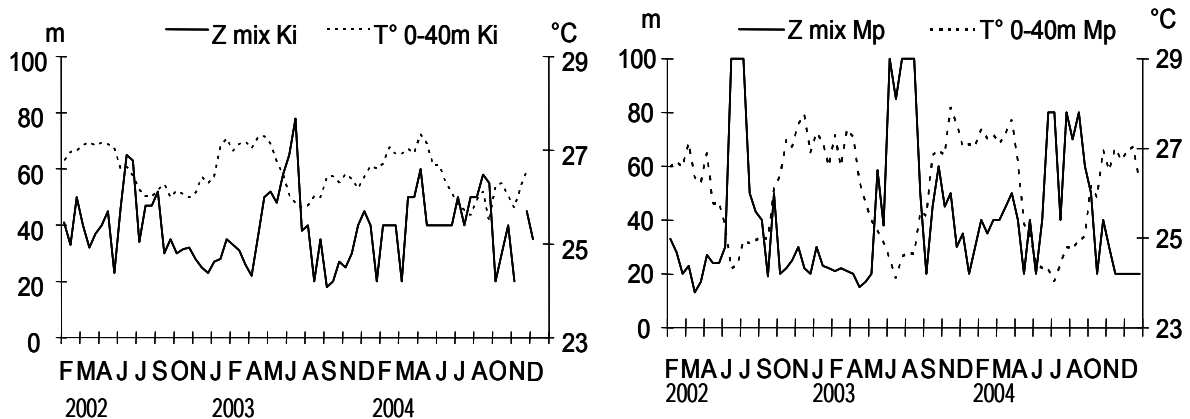


Figure .12: Depth of the mixed layer (m) and water temperature (0-40m) at Kigoma and Mpulungu.

### Water thermal stability

The water thermal stability is related to the work necessary to mix the water column. It depends of the density gradient in the water column. In Lake Tanganyika, most of the density change is temperature dependent. The effect of dissolved salts can be ignored in the upper water. It is thus logic that the stability is highly correlated to the water temperature ( $r=0.98$  in Mpulungu and  $r=0.94$  in Kigoma) (Fig. 13).

The fluctuation was particularly important during the southern upwelling of 2003. The stability variation clearly shows a close relationship with chlorophyll a and euphotic depth change at this moment.

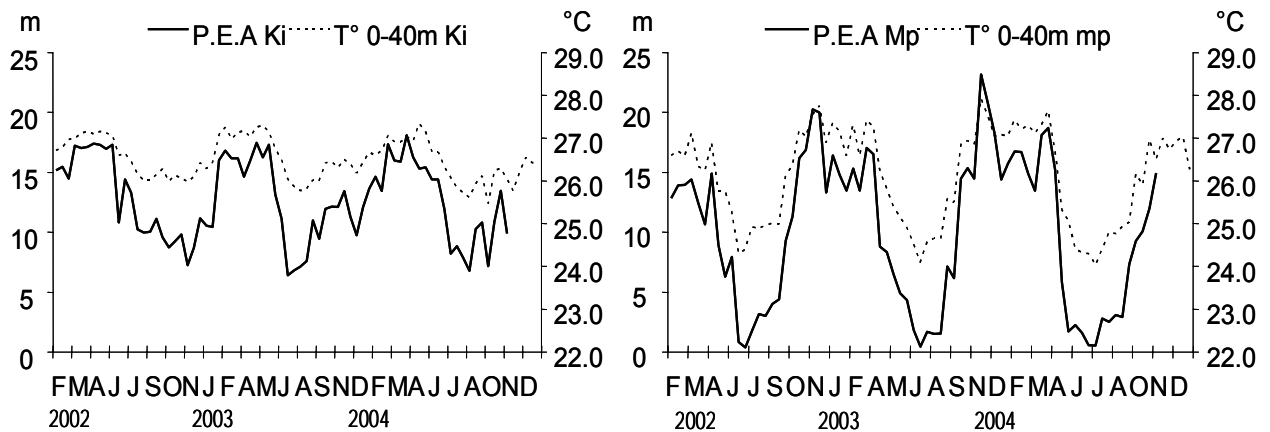


Figure 13: Water stability of the upper 100 m expressed as potential energy anomaly ( $J/m^2$ ) at Kigoma and Mpulungu).

### Dissolved (reactive) phosphorus

During the cold seasons in both stations, phosphorus variations associated to variations in depth of the mixed layer (Fig. 14) are observed in the upper zone of the lake (0-40 m for example). A major increase is observed during upwelling periods at Mpulungu. The correlation ( $r$ ) between dissolved phosphorus and water  $T^\circ$  at Mpulungu (dewaved data) is  $-0.78$ , indicative of a strong seasonality.

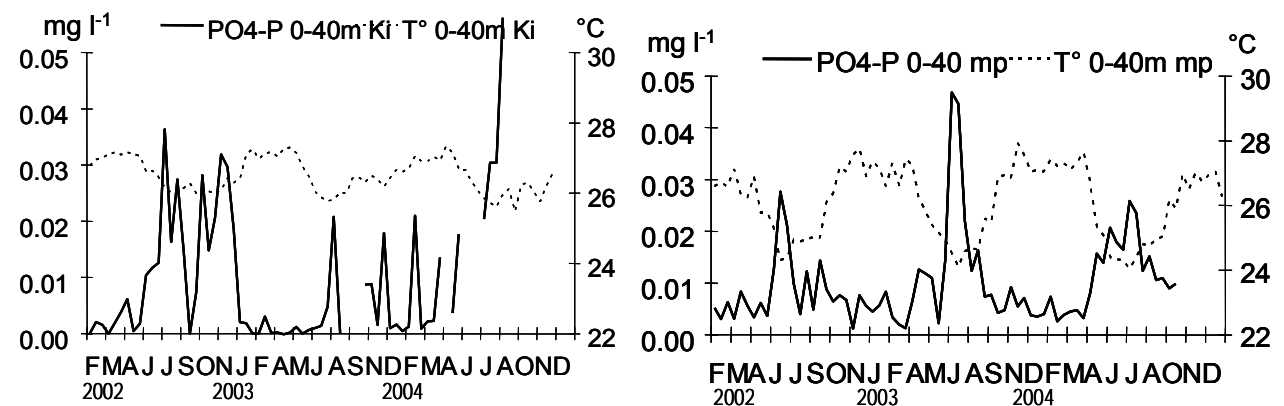


Figure 14: Dissolved phosphorus and water temperature (0-40m) at Kigoma and Mpulungu.

### Nitrate

In Kigoma, the increase of nitrate was well observed at monsoon change periods in 2002 (before and after the dry season). However it was no so afterward. It is not sure if this reflects the environment or other factors such as analytical problems in Kigoma. In Mpulungu nitrate increased generally by pulses, related to internal waves. As those pulses are not blocked by stratification during the upwelling period, the effect can be observed in surface waters (Fig. 15). An increase of nitrate during the stratified period around February 2003 is observed.

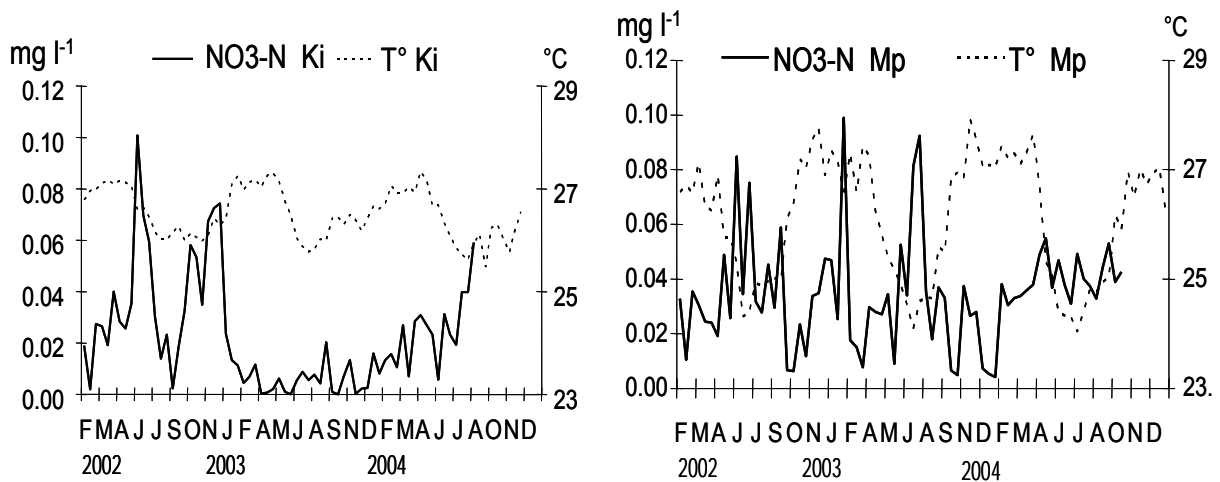


Figure .15: Nitrates and water temperature at Kigoma and Mpulungu (average from 0 to 40m).

### Ammonium

At Mpulungu, ammonium in surface waters (Fig. 16) clearly indicates deep movement of water and mixing linked with monsoonal change (from N to S before the upwelling). Internal waves regularly cause the concentration of ammonium to increase by a factor of 3 or 4). A decreasing trend is noted during the sampling period which might be due to a drift in the measurements.

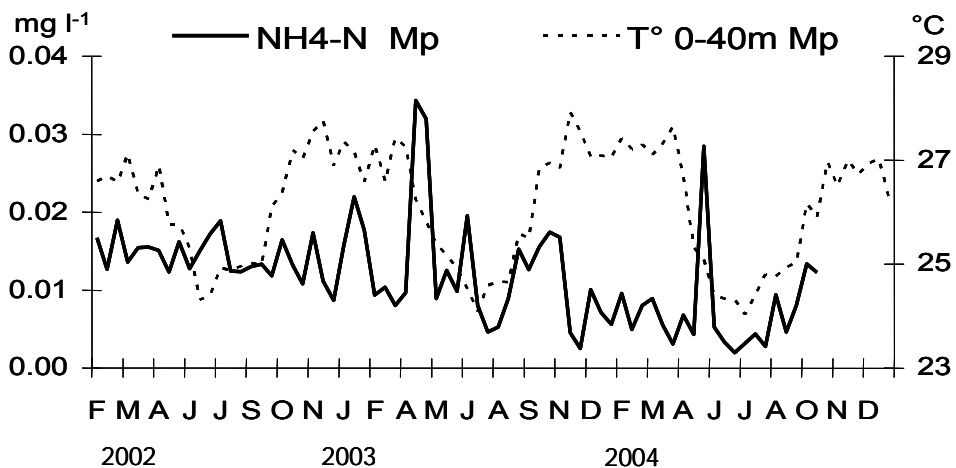


Figure 16: Ammonium concentration and water temperature (average 0 to 40m) at Mpulungu.

### Silica

Silica increased not only during the dry seasons from direct wind-related increase of vertical mixing, but also because of internal waves. Although the average is close from 1 mg l<sup>-1</sup> Si the range of values are between 0.5 and 1.6 mg l<sup>-1</sup> in the upper 40 m (Fig 17).

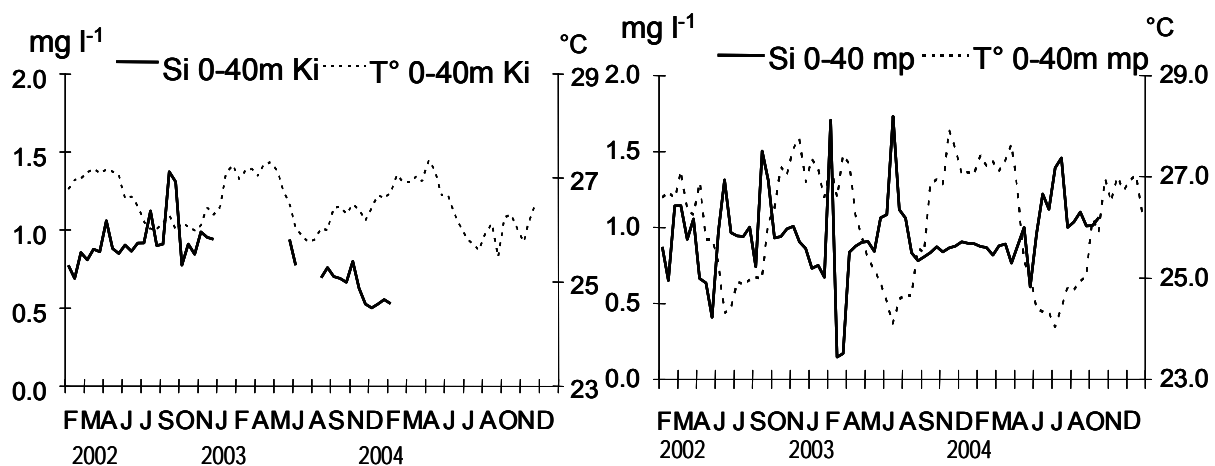


Figure 17: Silica and water temperature (0 to 40m) at Kigoma and Mpulungu.

### Total alkalinity

Total alkalinity increased during cold seasons in both stations but internal waves also strongly affected the variability of alkalinity.

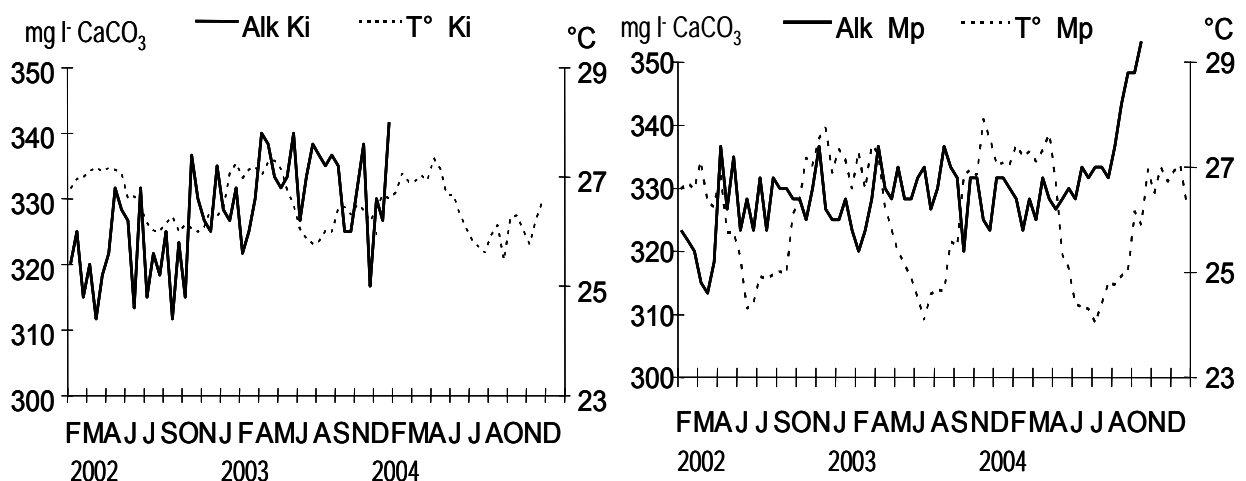


Figure 18: Total alkalinity and water temperature (average from 0 to 40m) at Kigoma and Mpulungu

### Limnological variables and nutrients during cruises

The temperature measured during the two dry seasons show well the decrease in the south of the lake due to the surface water cooling and also the upwelling (Fig. 19). The temperature during the 2003 cruise was lower than in 2002. Warmer and rather homogenous water temperature is observed during the 2004 rainy season cruise. The pH generally showed a decrease from North to South during the dry season. The mixing of deeper, CO<sub>2</sub>-richer water toward the surface was probably the cause of this pH decrease.

A strong increase of nutrients (P, N and Si) is observed in the South (stations TK8 to TK12) during dry season cruise (Fig. 20). In 2003, the upwelling was stronger with clear increase of nutrient concentration at the surface.

Dissolved phosphorus was much lower in all stations sampled during the rainy season cruise of 2004, while nitrate was higher in the North.

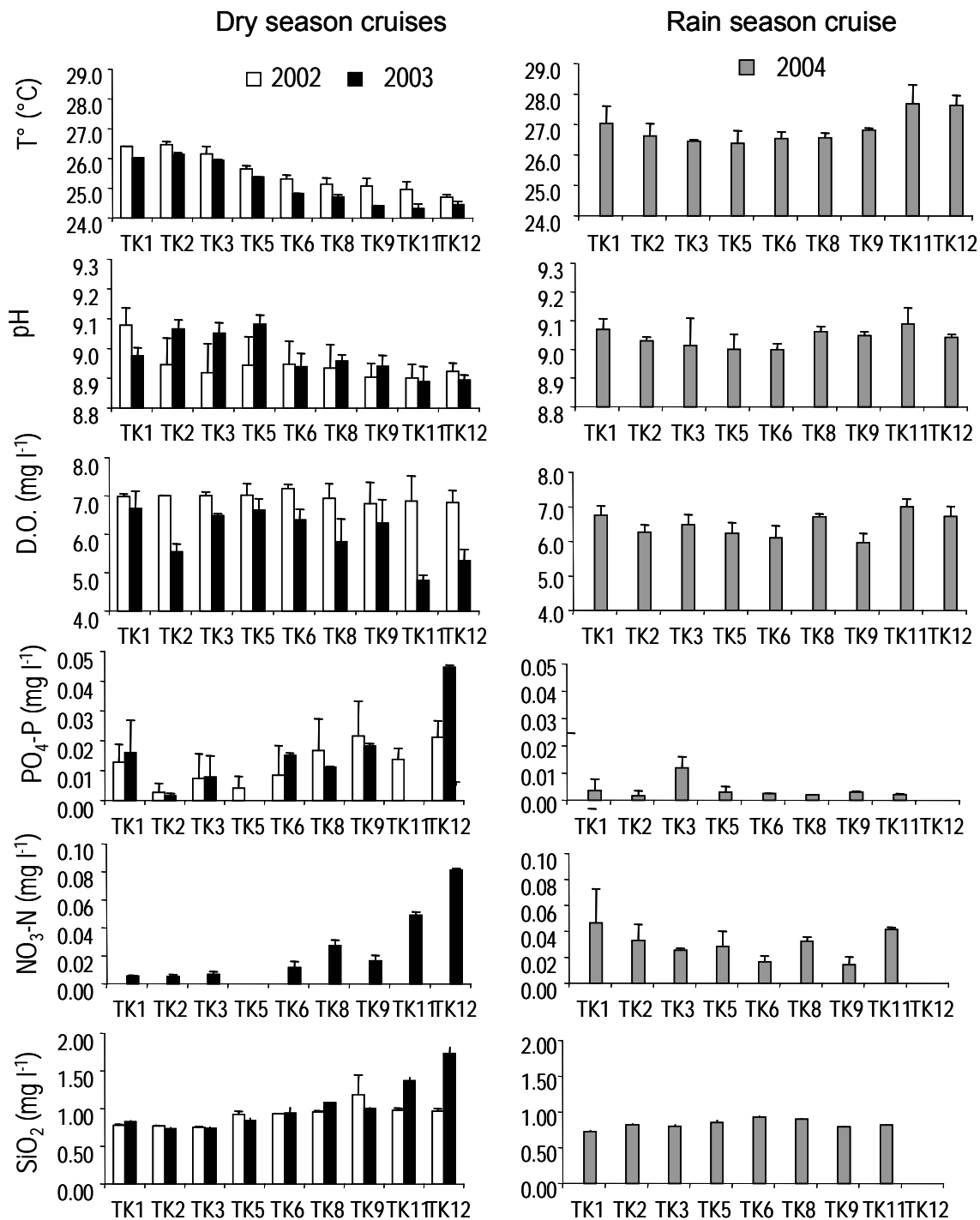


Figure 19: Average (0-40m) temperature, pH, dissolved oxygen, phosphates, nitrates and silica measured during two dry seasons cruises (2002 & 2003) and one rainy season cruise (2004) (standard deviation are shown; TK12=CLIMP-M).

The stability of the 100 upper meters of the water column (Fig. 20) showed strong difference between seasons. The stability during the 2002-2003 dry season cruises of decreased regularly toward the south. This is an effect of the stronger seasonality in the south where air temperature is lower in that season than in the north. Decreased thermal stability allows stronger vertical mixing in the south (not only the upwelling at the extreme end). During the rainy season cruise of 2004, the stability was stronger in all sites sampled.

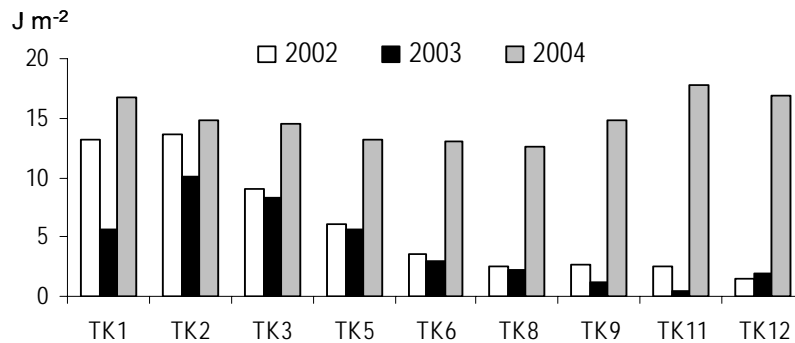


Figure 20: Stability (Potential energy anomaly in  $J. m^{-2}$ ) of the upper 100 m during two dry season cruises (2002 and 2003) and one rainy season cruise (2004).

### Coastal sampling

The water temperature in coastal waters (Fig. 21) displays well the amplitude higher in the south of the lake (Mpulungu) than in the north (Kigoma), very much as in the pelagic waters.

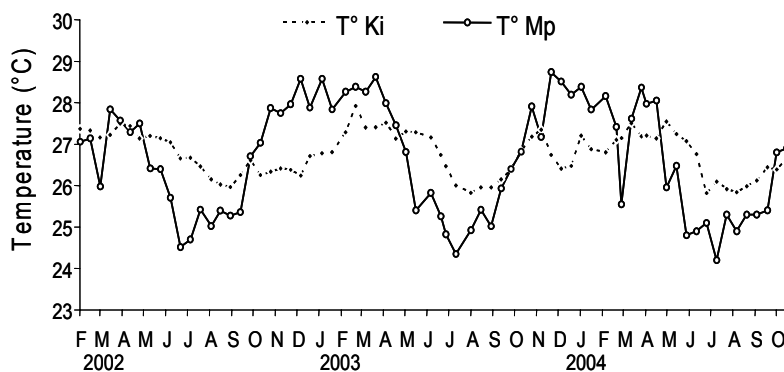


Figure 21: Water temperature of surface coastal water near Kigoma (CLIMC-K) and Mpulungu (CLIMC-M).

A nutrient increase in coastal waters was observed mainly during the dry seasons. The effect of internal waves on nutrient increase is also observed, even in these littoral waters (Fig. 22).



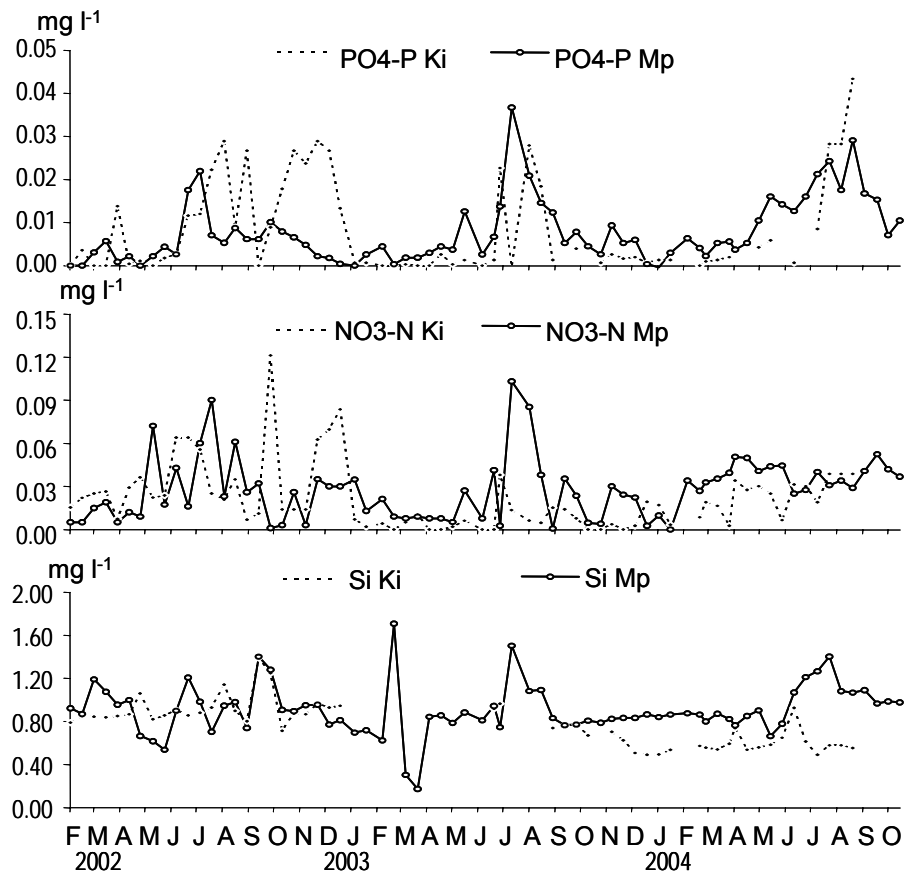


Figure 22: Dissolved phosphorus, nitrate and silica concentration in surface coastal waters from February 2002 to October 2004 at Kigoma and Mpulungu.

### 3.1.3 Remote sensing

The lake surface temperature is a key factor, which gives indications on the physical structure of the water column and is a witness of global and regional climatic variables. For instance, upwelling of deep, nutrient-rich cold waters, which are a strong potential driver of primary production, is easily seen by remote sensing. Satellite images allow to see areas of low and high temperature and to determine their spatial distribution at the scale of the whole lake. Other hydrodynamic processes, occurring at a lower scale than major upwellings, are also detectable by the study of surface water temperature.

This information can be acquired at a very low spatial resolution level (~ 1 km) but high temporal frequency (~ 1 time per day) from the AVHRR (Advanced Very High Resolution Radiometer) instrument onboard NOAA Polar Orbiting Satellites active since October 1978. AVHRR data are usually exploited to compute sea surface temperature (SST). Two kinds of algorithms are generally used. The first one is applied for open-sea surface temperature determination and the other one for coastal water temperature computation. Both algorithms types are based on the Planck's law

inversion principles. An application to Lake Tanganyika has been run successfully in 2002 in the framework of the CLIMLAKE project.

A total of about 200 images of the lake surface temperature were obtained from the processing of the AVHRR images. Figure 23 shows a selection of four images which allow to visualise contrasted seasonal situations: warm surface water indicating the stratification conditions at the end of the rainy season (April 27); a relative cooling in the South basin while the North remained warm (mid-May); overall decrease of surface temperature in June, more important in the south, with the blue spot at the southern tip indicating the upwelling (July 5); return to a stratified situation in late September with the warming of the lake surface. From all images available, temperature data were extracted and arranged in arrays according to their position (geographical coordinates).

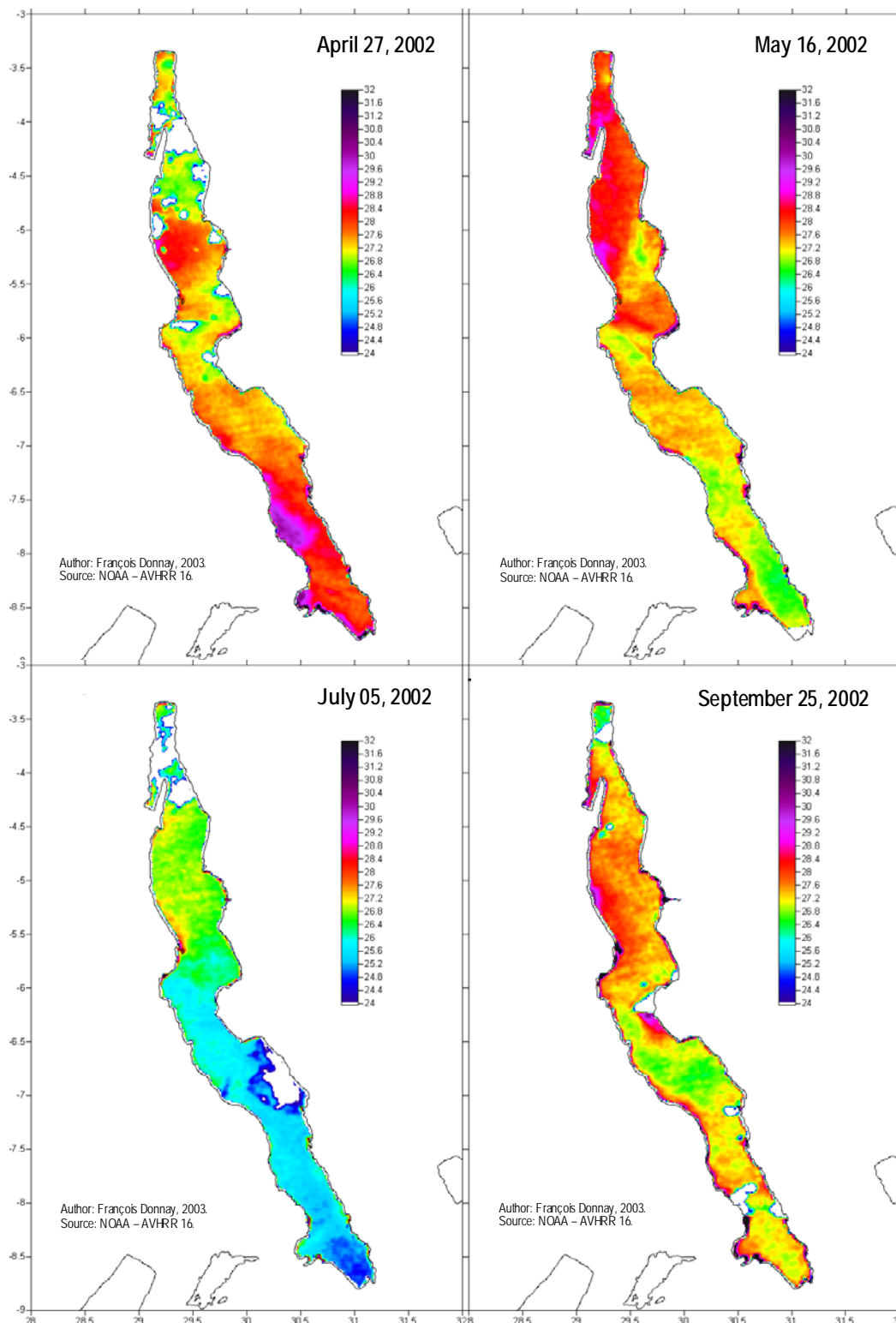


Figure 23: Temperature of the water surface of Lake Tanganyika, as recorded from remote sensing (NOAA – AVHRR 16) for different contrasted situations in 2002.

### 3.1.4 Present plankton in the pelagic waters

#### Chlorophyll a, particulate organic carbon and seston stoichiometry

Here we present the main results for the three years of observations and discuss the main temporal and spatial variations. A detailed account on variations of algal biomass and algal classes in Lake Tanganyika has been published in Descy *et al.* (2005). This publication also addresses vertical profiles of chlorophyll a and of phytoplankton categories, which are not presented here.

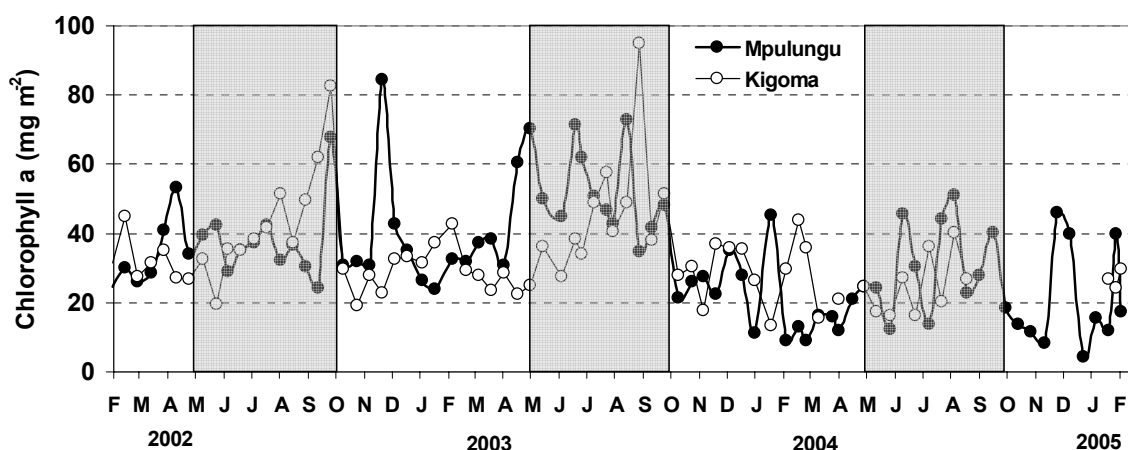


Fig. 24 Chlorophyll a concentration in the mixed layer in Lake Tanganyika, at the two monitoring sites (2002-2004). The boxes indicate the dry season period.

Average chlorophyll a was 36.4 (2002) and 37.3 (2003)  $\text{mg m}^{-2}$ , and at Mpulungu 38 (2002) vs. 41.3 (2003)  $\text{mg m}^{-2}$ . Chlorophyll a in the mixed layer (Fig. 24) was comprised between 20 (lowest values, in the rainy season) and close to 100  $\text{mg m}^{-2}$  (highest value, in the dry season). In 2002 the highest values were recorded in the beginning of October, immediately after the dry season, at both stations. A significant difference in chlorophyll a content of the water column (Student t test,  $p < 0.05$ ) was found between the means for the dry seasons 2002 and 2003 at Mpulungu, and between rainy and dry seasons 2003 at each station. Chlorophyll a data for 2004 were lower at both stations, particularly in the dry season. By contrast, POC concentrations (see below) of the dry season in Mpulungu were similar to those of the previous years, which indicates that chlorophyll a measurements were possibly less reliable in 2004, for technical reasons.

POC concentration (Fig. 25) can be considered as a measure of autochthonous organic matter (in the 0-40 m layer, grossly the euphotic zone). Indeed, it can be assumed that, in the pelagic zone of the lake, the amount of detritus is low. If so, POC reflects total plankton biomass, including phytoplankton, bacteria, micro- and meso-zooplankton.

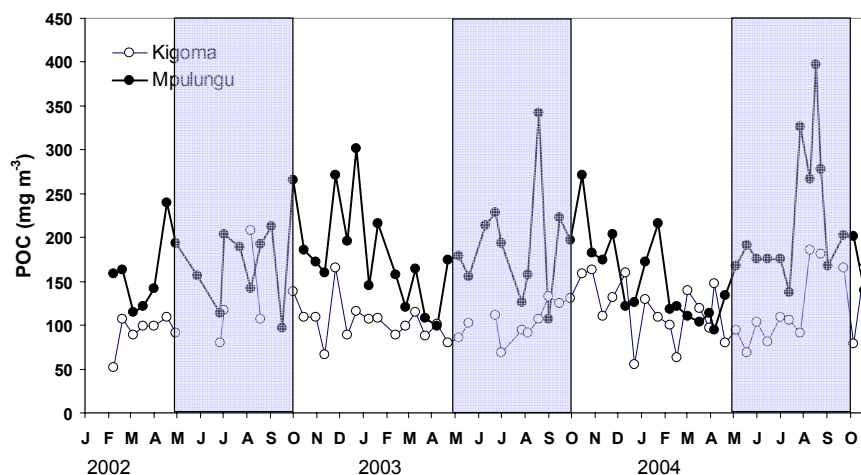


Fig. 25 Particulate organic carbon (POC) in the 0-40 m layer in Lake Tanganyika at the two monitoring sites (2002-2004). Values are averages or single measurement on integrated samples. The boxes indicate the dry season period.

As expected from seasonal variations of nutrient availability, maximal plankton biomass tend to be reached during the dry seasons, except in 2002 when, as for chlorophyll a, maxima were reached after the end of the dry season. POC concentration was higher in Mpulungu than in Kigoma (t-test highly significant), in agreement with the expected higher production at the southern station. This difference is observed for both seasons: the dry seasons averages were  $122 \text{ mg m}^{-3}$  at Kigoma vs.  $199 \text{ mg m}^{-3}$  at Mpulungu, and the rainy seasons averages were, respectively,  $108 \text{ mg m}^{-3}$  vs.  $163 \text{ mg m}^{-3}$ . It is to be noted that POC values at both stations in 2004 were not different from those in 2002-2004, contrary to chlorophyll a (see above). Given that a significant correlation was found between chlorophyll a and POC, based on the more detailed 2002 data (see Descy & Gosselain, 2004), it is likely that chlorophyll a measurements were of lower quality in 2004.

If we retain a value of 100 for the C: chlorophyll a ratio in Lake Tanganyika (see Descy & Gosselain, 2004), estimated by linear regression of POC against chlorophyll a, it appears that autotrophic planktonic biomass, integrated on the 0-100 m layer, is often lower than heterotrophic biomass (Pirlot et al, 2005).

Both C: P and C: N ratios suggest that macronutrient limitation of phytoplankton may occur in Lake Tanganyika, but also that P limitation may have been more frequent than N limitation. The seasonal pattern of C: P (Fig. 26) is striking and in accordance with the seasonal mixing pattern of the water column. Neglecting short-term variations possibly due to internal waves and to variation of phytoplankton nutrient demand, seston C: P tended to be higher in the stratified conditions of the rainy season, and tended to be lower in the dry season, when nutrient availability

increased. However, the threshold for severe P limitation (258, Guilford & Hecky, 2000) was rather rarely reached.

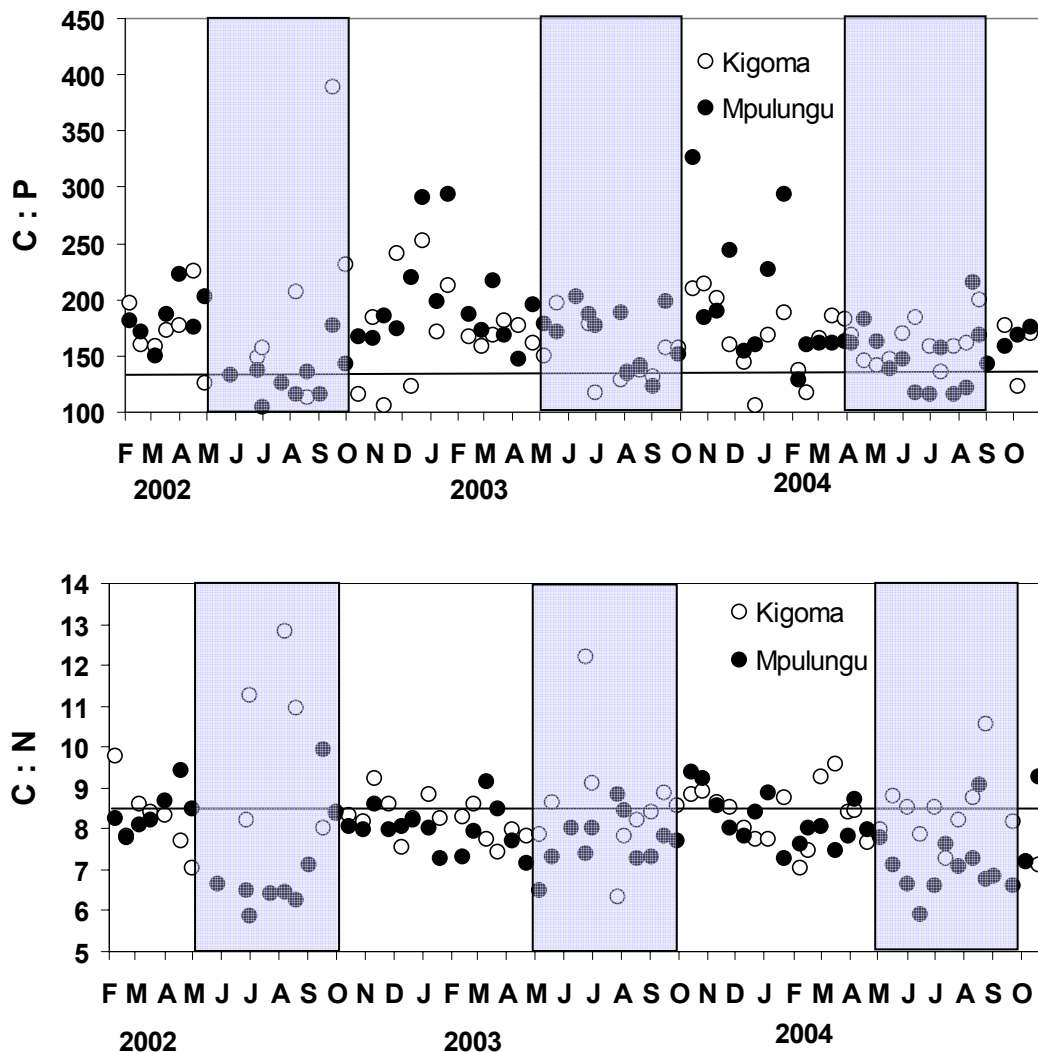


Fig. 26: Seston C:P and C:N in the 0-40 m layer in Lake Tanganyika. Values are averages of single measurement or from integrated samples. The boxes indicate the dry season period. The horizontal line is the theoretical limit upper which P or N limitation occurs.

### Biomass of phytoplankton classes from pigment analysis at the two monitoring sites

Here we focus on the relative contribution of algal categories, which may provide the best descriptor of phytoplankton general composition, for establishing relationships with environmental variables. The study of phytoplankton by microscopy (see below) enabled to identify the taxa present, but, as the examinations were done on samples from a single depth, data from microscopy cannot be directly compared to the algological data from the pigment analysis.

Chlorophytes, cyanobacteria T1 and diatoms were the most important algal groups, as reported in previous studies (Hecky & Kling, 1987). Chrysophytes, not

distinguished from diatoms by the pigment analysis, may have developed at times, but it is likely that the fucoxanthin-containing algae which increased in the dry season were diatoms, given that Chrysophytes were not abundant in the samples examined by microscopy (Cocquyt, 2003; Descy & Gosselain, 2004).

Clear differences in algal composition appeared between the north and the south basin: Chlorophytes dominated in the north (42.7% of chlorophyll *a* biomass vs. 18.3% in the south), whereas cyanobacteria T1 dominated in the south (60.9% at Mpulungu vs. 31.4% at Kigoma), with little variation over time. Despite conspicuous seasonal variations, diatoms (+ chrysophytes) represented on average a similar biomass in both basins, on average 12.0-15.2% of the phytoplankton chlorophyll *a*. Cyanobacteria T2 had a similar average share of chlorophyll *a* in both stations (about 6%), but a more important development during short periods of time. They appeared mostly at the end of the dry season or in the rainy season, and microscope examinations allowed identification of the filamentous cyanobacteria mentioned by Hecky & Kling (1987). Cyanobacteria T1 may correspond mostly to picocyanobacteria, as shown by filter fractionations carried out from February to April 2003 in Mpulungu. These showed that 50% of the total chlorophyll *a* biomass was comprised in the < 2  $\mu\text{m}$  size fraction, and was made of cyanobacteria T1 showing the “*Synechococcus* pigment type” of Jeffrey, Mantoura & Wright (1997). The 2-10  $\mu\text{m}$  fraction also contained cyanobacteria T1, mixed with small chlorophytes. Epifluorescence microscopy and flow cytometry (data not shown) have confirmed that *Synechococcus* was abundant and constituted the bulk of the small size phytoplankton fraction.

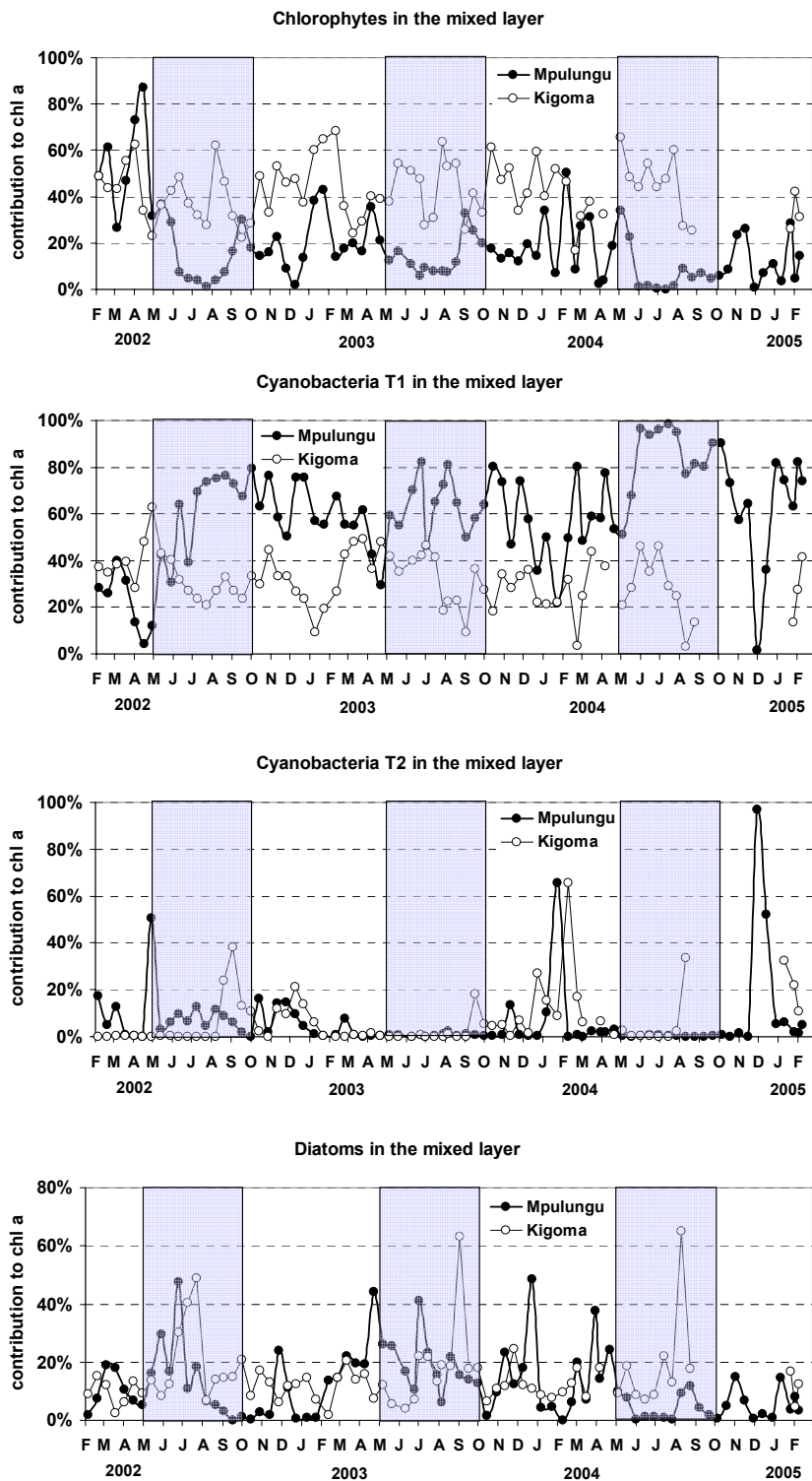


Fig. 27: Relative contribution to chlorophyll a of the main algal groups in the offshore waters of Lake Tanganyika, as calculated from pigment analysis and CHEMTAX processing (Descy *et.al*, 2005). Dinophyceae and Cryptophyceae have been omitted. Chrysophytes are not distinguished from diatoms. The boxes indicate the dry season period



## Phytoplankton biomass and composition from microscopy at the two monitoring sites

The total phytoplankton fresh biomass was low at both stations with yearly averages of 40 and 66 mg m<sup>-3</sup> for 2002 and 2003 in Kigoma and of 81 and 125 mg m<sup>-3</sup> for 2002 and 2003 in Mpulungu. While the maximum observed fresh biomass was highest in 2002 in Kigoma (176 compared to 155 mg m<sup>-3</sup> in 2003), the maximum in Mpulungu was higher in 2003 (794 vs. 158 mg m<sup>-3</sup>). The relative contribution of the phytoplankton groups according to microscope counts is depicted in fig. 28. Phytoplankton groups with a high contribution to the total biomass included cyanobacteria, chlorophytes and diatoms. Dominant species in each of those groups included picocyanobacteria, coccoid (e.g. *Chroococcus*) and filamentous cyanobacteria (e.g. *Anabaena*, *Anabaenopsis*), small non-colonial (e.g. *Chlorella* sp., *Kirchneriella obesa*) and colonial forms of green algae (e.g. *Dictyosphaerium/Lobocystis*) and diatoms (*Nitzschia asterionelloides*). A detailed species list can be found in Appendix 2.

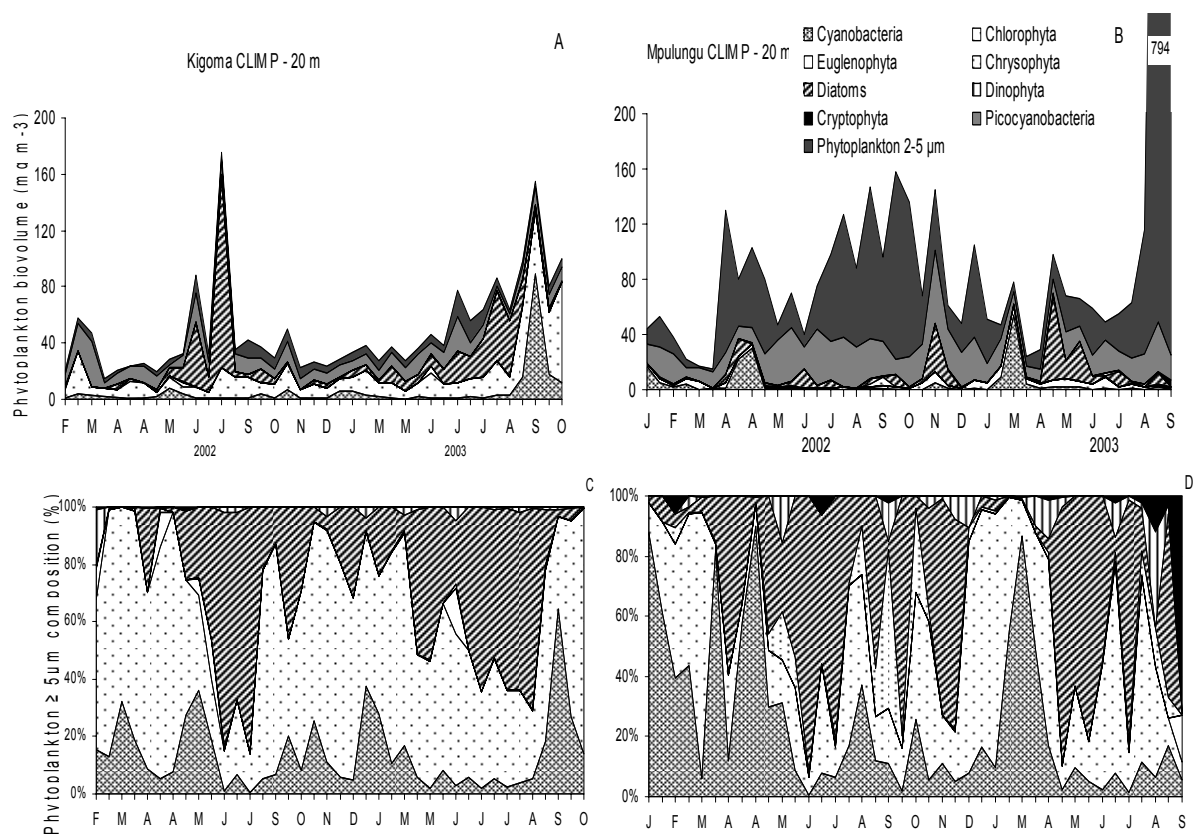


Fig. 28: Seasonal changes in the phytoplankton FW (fresh weight, mg m<sup>-3</sup>). A & B: Total phytoplankton biomass at 20 m depth from February 2002 to January 2004 at Kigoma and to September 2003 at Mpulungu, as determined by inverted ("large" phytoplankton,  $\geq 5 \mu\text{m}$ ) and epifluorescence microscopy ("small" phytoplankton 2-5  $\mu\text{m}$  and picoplankton  $< 2 \mu\text{m}$ ), C & D: Relative abundance of the major phytoplankton groups.

In 2003 we observed at Kigoma a succession from a stable period at the end of the rainy season, with a dominance of chlorophytes (with as dominant species *Kirchneriella obesa*, *Dictyosphaerium/Lobocystis* complex, *Pseudoquadrigula* aff., *Didymocystis bicellularis*, *Oocystis lacustris*) and small phytoplankton, to diatom blooms of *Nitzschia asterionelloides* during the dry season. This was followed by a bloom of filamentous cyanobacteria (*Anabaena flos-aquae*) at the start of the rainy season. In 2002, no filamentous cyanobacteria bloom was observed, while diatom peaks were higher (Descy & Gosselain, 2004). The fact that some of important peaks were short-lived raises the chance to miss these events when the sampling interval is large.

In agreement with the filter fractionations reported above, small phytoplankton (<5 µm) was dominant in Mpulungu throughout the year (on average 79% of the total phytoplankton fresh biomass). Picocyanobacteria were relatively more important during the rainy season. Chroococcales ≥ 5 µm increased at the end of the rainy season and nanophytoplankton (2-5 µm) displayed sharp peaks during the dry season. Diatom peaks were observed during the dry season, continuing during the rainy season up to the end of November. Most major phytoplankton groups had, although sometimes small, seasonal recurring maxima in their abundance. Dinophytes, cryptophytes and euglenophytes have their maximal abundance during the rainy season, as did chlorophytes in Mpulungu. Chlorophytes at Kigoma, along with the remaining phytoplankton groups, had their maximum during the dry season. Variation in the occurrence and dominance of dinophytes, picocyanobacteria and nanophytoplankton 2-5 µm can also be linked to internal waves.

#### *Chlorophytes (20 m) – Fig. 29A*

The fresh biomass of chlorophytes seems to increase during the dry (cold) season at Kigoma while the highest increase is observed during the rainy (warm) season at Mpulungu. This corresponds with the seasonal changes in chlorophytes abundance inferred from HPLC-analysis. Individual dominant chlorophyte species showed marked differences in their occurrence, e.g., the occurrence of species belonging to the *Dictyosphaerium/Lobocystis* complex corresponded with periods of high chlorophytes abundance. This complex illustrates, together with *Kirchneriella obesa*, the contrast in seasonality between both stations. Other examples are *Chlorella* sp. showing high densities near the beginning and the end of the dry season of 2003 and *Elakatothrix viridis* mainly present during the rainy season.

*Diatoms (20m) – Fig. 29 B*

Diatoms clearly exhibited a seasonal pattern in fresh biomass at Kigoma, with high abundances during the dry season. The highest peak was observed in 2002 (78 vs. 61 mg m<sup>-3</sup>). The average biomass of diatoms during the dry season was however higher in 2003 (27 vs. 24 mg m<sup>-3</sup>). At Mpulungu, the highest fresh biomass was observed at the transition of the rainy and dry season (monsoonal shift). The average diatom

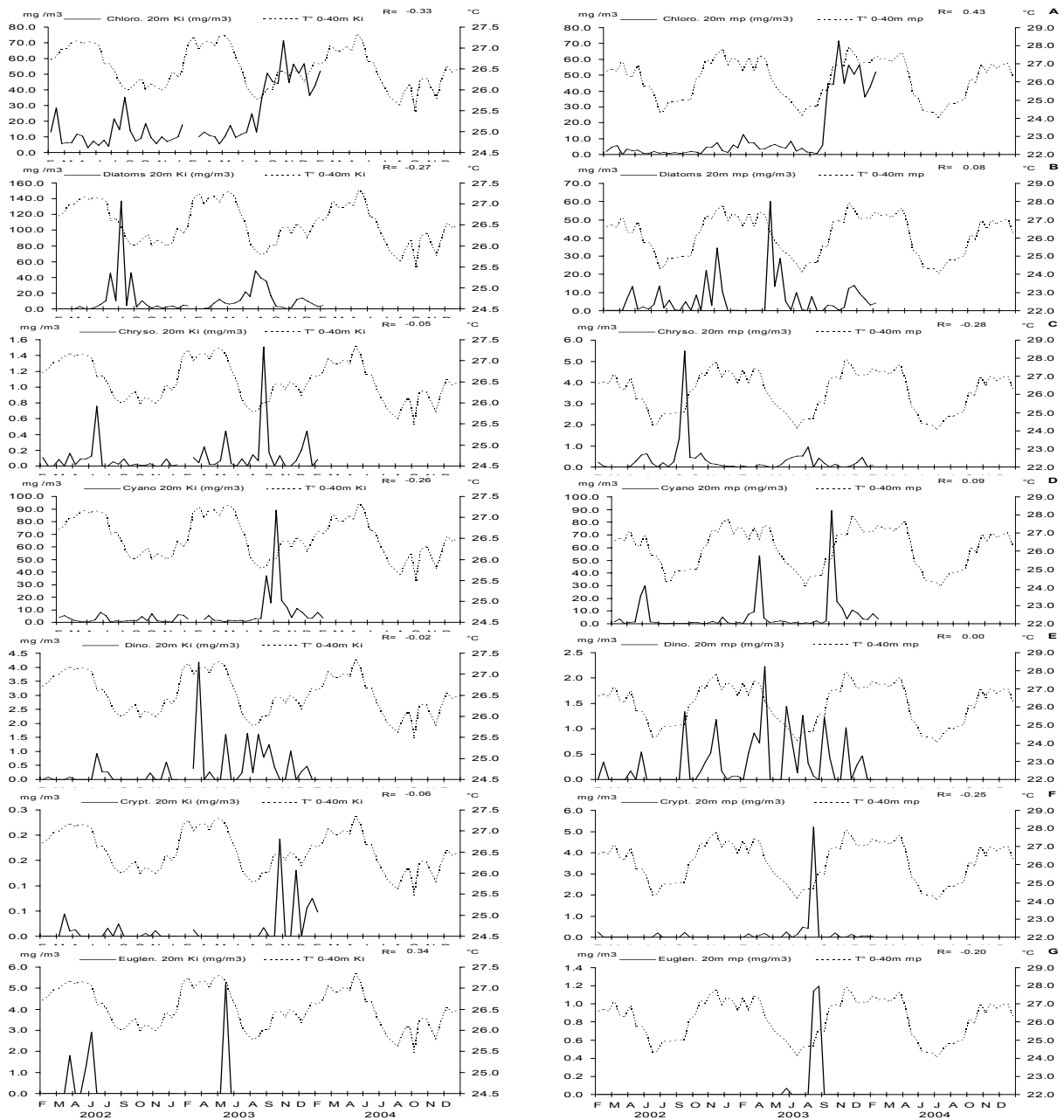


Figure 29: Seasonal changes in the fresh biomass (mg m<sup>-3</sup>) of major phytoplankton groups observed by microscopy from samples taken at 20 m in Kigoma and Mpulungu; (from top to bottom: chlorophytes, diatoms, chrysophytes, cyanobacteria, dinophytes, cryptophytes and euglenophytes).

Biomass at Mpulungu was higher in 2003 (61 vs. 34 mg m<sup>-3</sup>). At the end of the rainy season, a small *Nitzschia* (*N. aff. fonticola*) was dominant. This diatom is known to occur during periods of high stability in the water column (Stager *et.al* 1997). During the dry season the diatom blooms are mainly composed of the long, colony-building *Nitzschia asterionelloides*.

#### *Chrysophytes (20m) – Fig. 29 C*

Chrysophytes were only sporadically observed (only in 3 samples with a contribution higher than 1% of the total fresh biomass) in the inverted microscope counts. Most distinct peaks occurred mostly at Mpulungu. Small peaks were observed at the beginning and near the end of the dry season.

#### *Cyanobacteria (20m) – Fig. 29 D*

Within the cyanobacteria counted with the inverted microscope two groups can be discerned; the filamentous cyanobacteria (*e.g. Anabaena flos-aquae* and *Anabaenopsis tanganyikae*) and chroococcales forming small colonies (*e.g. Chroococcus* sp. and *Chroococcus obliteratus*). The filamentous cyanobacteria formed an important bloom (*Anabaena flos-aquae* accounting for 58% of the total phytoplankton fresh weight) after the dry season in 2003 at Kigoma. A similar bloom was observed by Hecky and Kling (1981). At Mpulungu higher densities of chlorococcales were observed near the end of the rainy season. The highest relative abundance was found during the rainy season of 2003 where it accounted for 69% of the biomass.

#### *Dinophytes (20m) – Fig. 29 E*

Dinophytes were generally low in abundance (maximum contribution to the fresh biomass: 9% at Kigoma, 2% at Mpulungu) and were typically found during the rainy season.

#### *Cryptophytes (20m) – Fig. 29 F*

Cryptophytes were only sporadically observed. A small peak was observed at the end of the dry season in 2003 at both stations.

#### *Euglenophytes (20m) – Fig. 29 G*

Euglenophytes showed a maximum at the end of the rainy season.

## Biomass and phytoplankton composition from research cruises

The cruises show better spatial differences (Fig. 30) than the monitoring at the two distant sites. With the exception of site TK2, possibly influenced by the discharge of the River Malagarazi, chlorophyll *a* integrated over the water column during the 2004 cruise (rainy season) was in the 20–40 mg m<sup>-2</sup> range, with little difference between the north and the south basins of the lake. By contrast, the dry season data showed a near doubling of chlorophyll *a* content of the water column at the south relative to the north.

Results from the two cruises for which detailed data were available largely confirm variations of phytoplankton classes along the lake north-south axis (Fig. 30), as well as the seasonal differences. For instance, the rainy season longitudinal profile show a relatively homogeneous distribution of algal classes, with low diatom biomass, high chlorophyte biomass and greater abundance of cyanobacteria T1 in the south (especially from TK5 to TK11). A particular feature of this rainy season transect was the development of cyanobacteria T2, corresponding mostly to filamentous taxa with heterocysts (*Anabaena* and *Anabaenopsis*) as verified by microscopy. They were more abundant in the north basin, at sites TK2 and TK3. By contrast, those algae were absent in the dry season, which was characterised by higher diatom biomass and by the dominance of cyanobacteria T1, which had greater abundance in the southern basin. Chlorophyte biomass was at similar levels in both seasons.

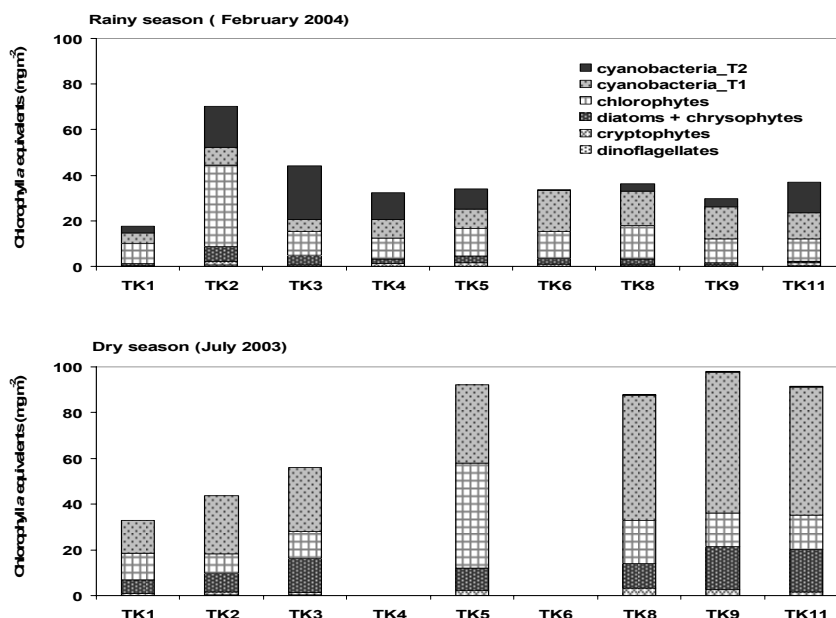


Figure 30: Variation of the biomass of phytoplankton groups (mg chlorophyll *a* m<sup>-2</sup>), inferred from pigment analysis, integrated over the 100 m water column, in Lake Tanganyika during the rainy season cruise (February 2004) and the preceding dry season cruise (July 2003). See site location in Fig. 1

Phytoplankton samples from three north - south transects were also analysed by microscopy. The contribution of different phytoplankton size classes (Fig. 31) clearly differed between the north and the south of the lake. Especially at the three southernmost stations (TK8, TK9 and TK11) phytoplankton smaller than 5  $\mu\text{m}$  was more important. At the northernmost station diatoms were the most important group during the dry season, while chlorophytes dominated during the rainy season. The importance of nanophytoplankton 2-5  $\mu\text{m}$  decreased during the rainy season.

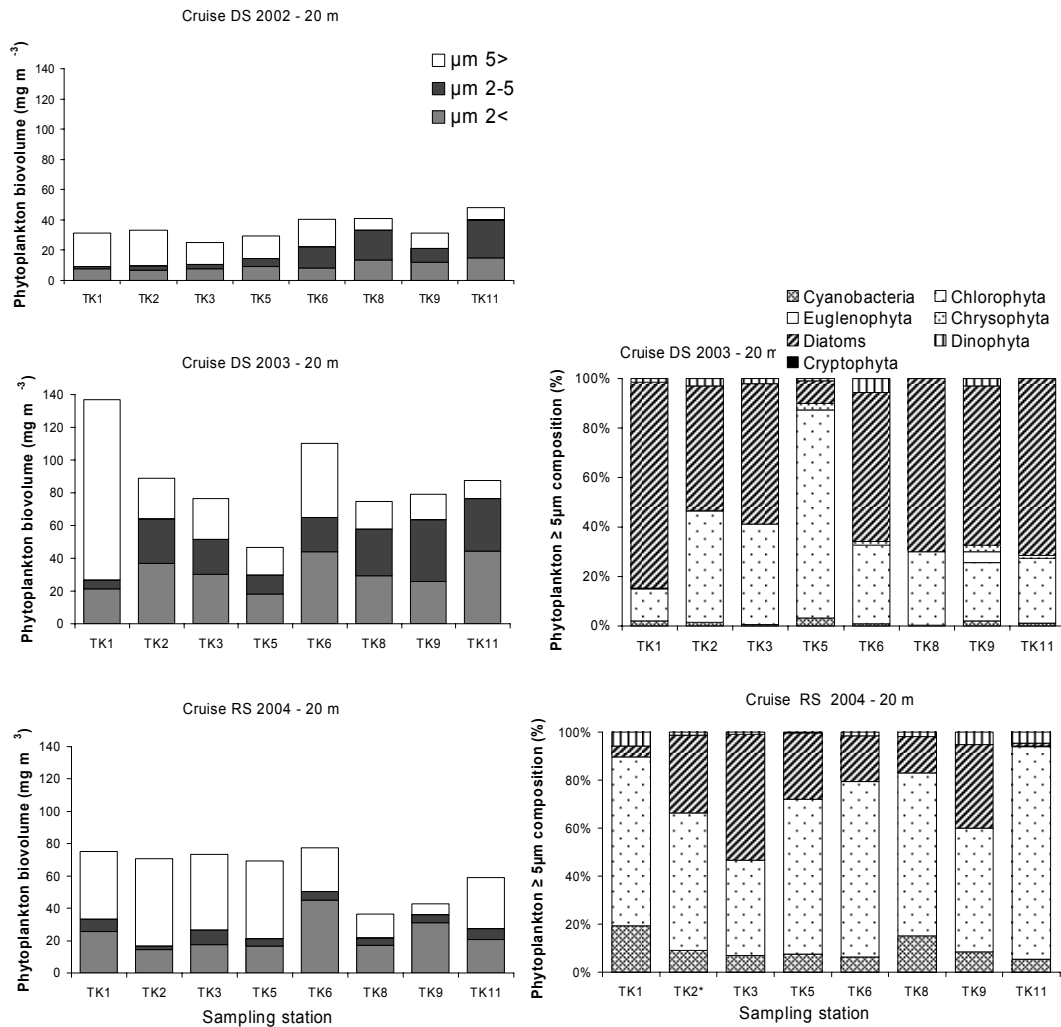


Fig. 31: A-C: Phytoplankton biomass (fresh weight,  $\text{mg m}^{-3}$ ) at 20 m depth at the sampling locations during the research cruises throughout the dry season of 2002, the dry season of 2003 and the rainy season 2004. D-E: Percentage of different phytoplankton groups during the dry season of 2003 and the rainy season 2004.

### Biomass and phytoplankton composition from littoral zone sampling

Samples for phytoplankton analysis using pigments were collected at one depth in the littoral zone during all the monitoring period (Feb. 2002 – Oct. 2004). Here we

present some results for comparison with phytoplankton biomass and composition in the pelagic zone.

The chlorophyll a concentration in the water column of the littoral zone at Kigoma (Fig. 32) was close to that observed in the offshore waters, with similar temporal variations; seasonality was well visible, with maxima in the dry season. At Mpulungu, chlorophyll a concentration were much higher than in the pelagic zone (maximum 6.3 mg m<sup>-3</sup>), but the variation was broadly similar to that in the offshore surface waters, with again maxima in the dry season.

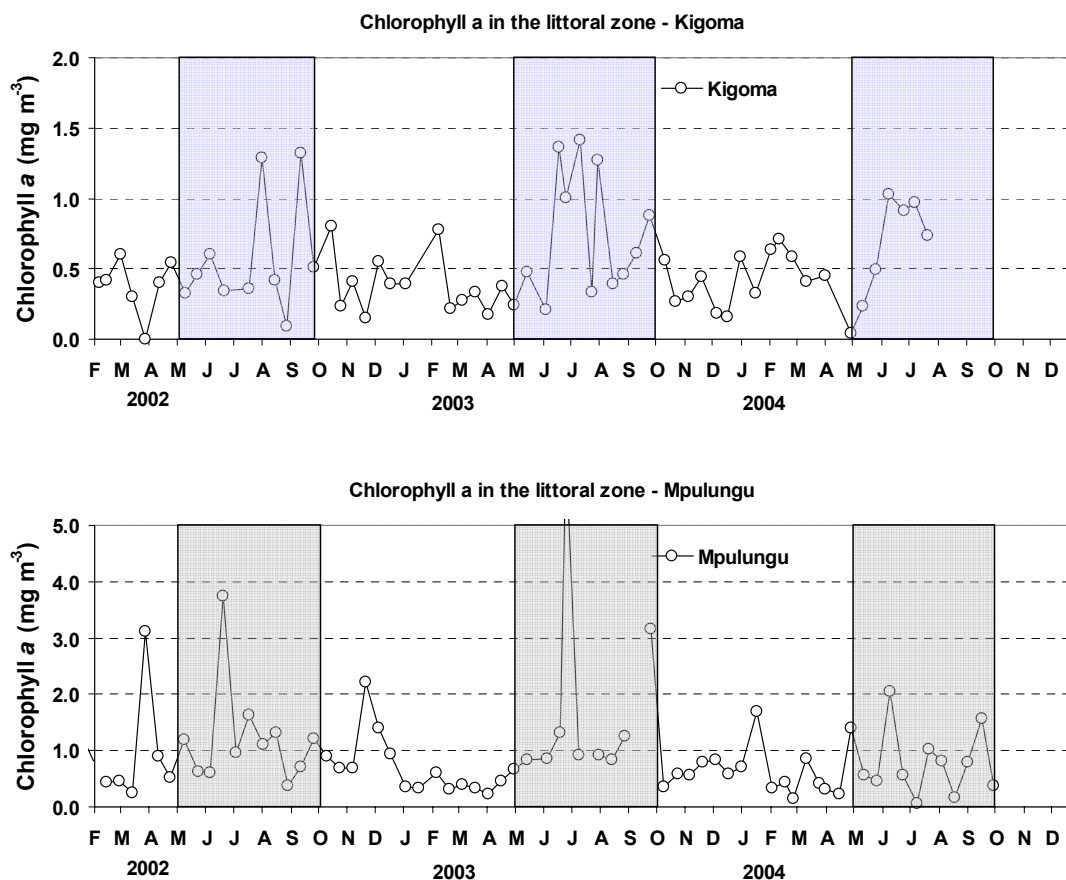


Figure 32: Variation of phytoplankton biomass (mg chlorophyll a m<sup>-3</sup>), inferred from pigment analysis, in the littoral zone of Lake Tanganyika at the two monitoring sites (2002-2004). The boxes indicate the dry season period.

Phytoplankton composition was also similar to that in the pelagic zone, with a large dominance of cyanobacteria T1 (mean contribution to Chl a 56.2%) at Mpulungu, followed by chlorophytes (19.2%) and diatoms (19.1%). At Kigoma, the mean contributions to Chla were: cyanobacteria T1 38.8%, chlorophytes 38.5% and diatoms 14.3%. Other algal groups represented on average less than 5% each, even though they showed maxima linked with characteristic environmental situations. This was the case, for instance, for cyanobacteria T2, which exhibited remarkable peaks

at the same periods as in the pelagic zone (Fig. 33). It is also noteworthy that diatoms showed similar dynamics as in the offshore waters (Fig. 33), even though there was a small contribution of benthic taxa detached and suspended by water movements in those shallow sites. Actually, the diatoms exhibiting peaks of biomass, particularly in the dry season, were the same planktonic taxa as those which developed in the offshore waters.

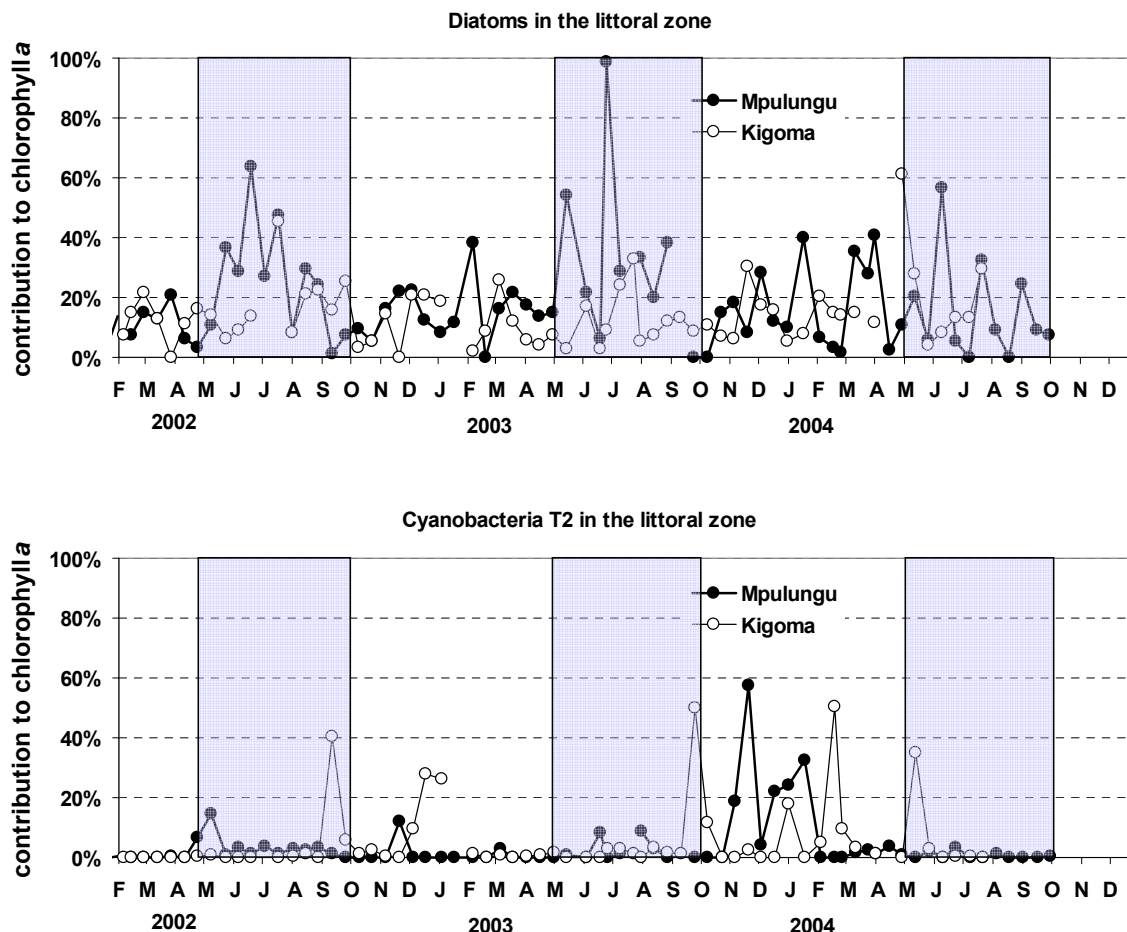


Figure 33: Variation of contribution to chlorophyll a of diatoms and cyanobacteria T2, inferred from pigment analysis, in the littoral zone of Lake Tanganyika at the two monitoring sites (2002-2004). The boxes indicate the dry season period.

### Mesozooplankton abundance and biomass in the pelagic waters

In both stations, copepod biomass was low in the beginning of each year, and increased in the dry season or in the following months. Large fluctuations occurred (Fig. 34), particularly in the dry season, possibly due to variations in sampling efficiency related to generally more difficult conditions in this season. Overall, mesozooplankton biomass follows closely, or with some delay, phytoplankton biomass and production. Annual averages were comprised between 0.56 and 1.0 g C m<sup>2</sup>, which is in the same range as in the years 1994-1995 (0.83 – 1.14 g C m<sup>2</sup>; Kurki *et.al*, 1999). Calanoids copepods were, overall, more abundant in Mpulungu,



whereas cyclopoids usually dominated at Kigoma: this north-south difference was also noted by Kurki *et.al*, 1999).

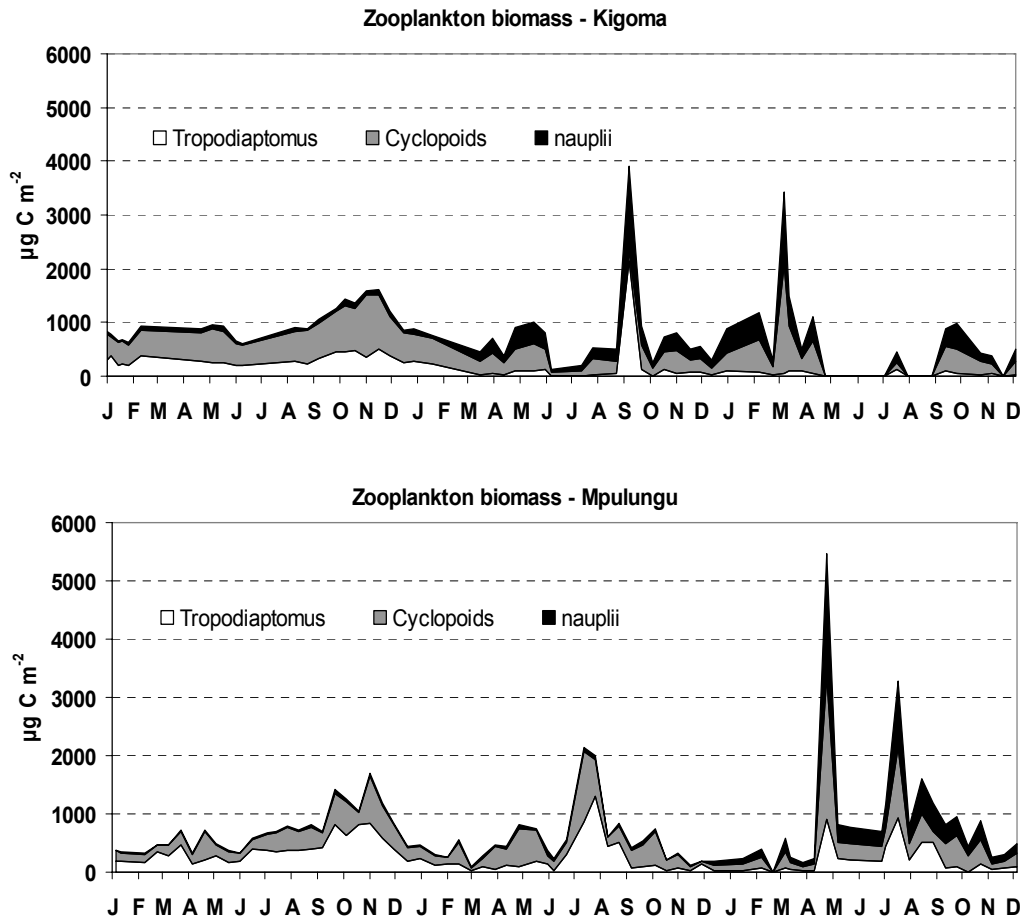


Fig. 34: Variations of mesozooplankton biomass in the offshore waters of Lake Tanganyika, at the two monitoring sites (2002-2004). See text for details on calculations.

### Components of the microbial food web: picocyanobacteria, bacterioplankton and microzooplankton

As reported above, picocyanobacteria were present throughout the sampling period. At Kigoma peaks in their abundance were observed at the start of the dry season when maxima in the mixing depth are observed (cfr Fig. 35). At Mpulungu a high biomass was observed throughout the dry season. In 2002 there was an important peak after the dry season which was also observed in the chlorophyll a measurements. Some peaks in picoplankton density seem to correspond well with the internal waves.

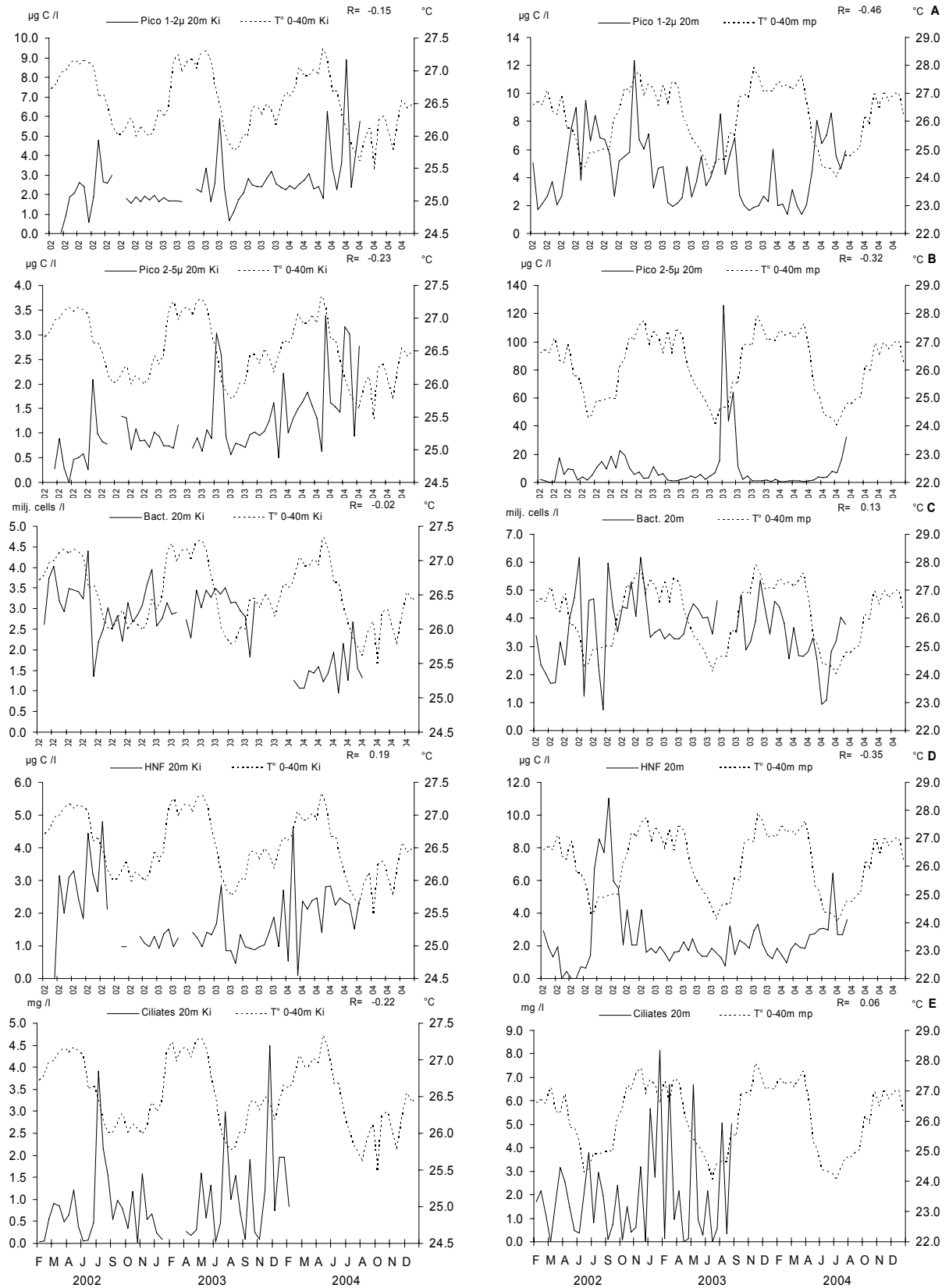


Figure 35: Seasonal changes in the biomass of different components of the microbial food web from samples taken at 20 m in Kigoma and Mpulungu; from top to bottom: Picocyanobacteria 0.8-2 µm, nanophytoplankton 2-5 µm, bacteria, nanoflagellates (HNF) and ciliates.

At Kigoma, nanophytoplankton (Fig. 35 B) exhibited a similar pattern, with high abundance during periods of deep mixing. At Mpulungu, peaks corresponded with the dry season. The maximal biomass was a lot higher in 2003 compared to 2002. The contribution of phytoplankton  $<5 \mu\text{m}$  to total phytoplankton biomass was generally high. At Kigoma the contribution was higher during the rainy season (average in 2002 53% compared to 28% in the dry season; in 2003, 43% in the wet season vs. 26% in the dry season). At Mpulungu small phytoplankton was even more important, representing on average between 65 and 92% of total phytoplankton biomass throughout the year.

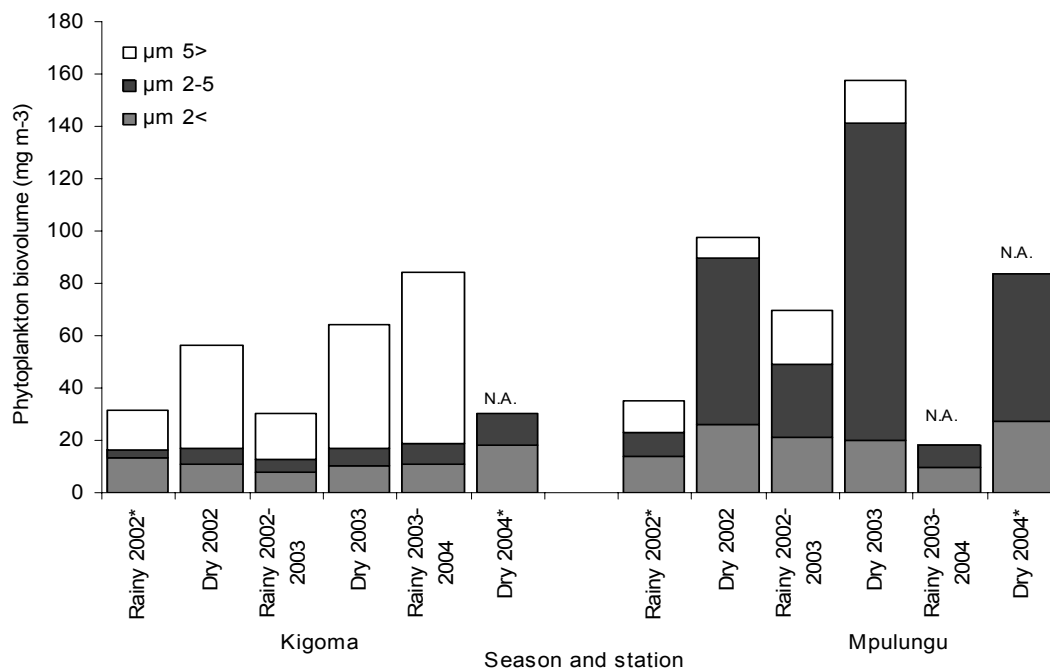


Fig 36: Average contribution of different size classes among phytoplankton during different seasons in Kigoma and Mpulungu. \* data for this season are incomplete. N.A.: no data are available for phytoplankton  $\geq 5 \mu\text{m}$ .

Bacterial densities (Fig. 35 C) were in the range of  $1-6 \times 10^6$  cells  $\text{ml}^{-1}$  throughout the monitoring period. Bacterial numbers are high compared to other oligotrophic freshwater environments, but not exceptional (Wetzel 2001). No clear seasonal changes in the bacterial densities were observed. Densities were higher at Mpulungu (on average  $3.5$  compared to  $2.7 \times 10^6$  cells  $\text{ml}^{-1}$  at Kigoma), but higher variability was observed at this station. During the research cruise of 2002 samples for genetic analysis were taken. Denaturing Gradient Gel Electrophoresis (DGGE) and sequencing of selected bands revealed clear differences in the latitudinal distribution of certain genotypes (De Wever *et.al*, *in press*).

At Kigoma the maximal HNF density (Fig. 35 D) was 1696 cells ml<sup>-1</sup>. High densities were observed throughout the dry season of 2002; in 2003 a maximum occurred in July and in 2004 in February. Densities around 400 cells ml<sup>-1</sup> were observed during the rest of the year. Maximal densities were a lot higher in Mpulungu (3896 cells ml<sup>-1</sup>) and are observed during the dry season, the average density during the rainy season is 674 cells ml<sup>-1</sup>.

At Kigoma, maximal ciliate densities (Fig. 35 E) were observed during the dry season (6600, 1400 and 7000 cells l<sup>-1</sup> in July 2002, August 2003 and July 2004 respectively). In 2003 a second maximum occurred in November (2500 cells l<sup>-1</sup>). Ciliate densities were higher at Mpulungu than at Kigoma (average of 1160 vs. 980 cells l<sup>-1</sup>) and maxima are observed during the transition period of dry and rainy seasons (5400 and 6600 cells l<sup>-1</sup> at the end of September and in April 2004, respectively). The ciliate community was dominated by the peritrich species *Pseudohaplocaulus* sp. and *Vorticella aquadulcis*, and by the oligotrich species *Strombidium* and *Pelagostrombidium* sp.

Most components of the microbial loop display a similar seasonal pattern, with maximal biomass during the dry season and minimal biomass during the wet season. The timing of population maxima however differs somewhat between functional groups. In contrast, bacterial biomass remains rather constant throughout the year. This suggests a strong top-down control during all seasons or a fine balance between a seasonally varying grazing pressure and bacterial productivity, which are both higher during the dry season.

### 3.1.5 Ecological processes

#### ***Primary production***

The phytoplankton photosynthetic parameters often varied significantly between season and stations, so that different values were used for P<sub>max</sub> and I<sub>k</sub> for modelling daily photosynthesis. For Mpulungu, P<sub>max</sub> was set to the average value of 4.67 mg C [mg chl<sub>a</sub>]<sup>-1</sup> h<sup>-1</sup>, and for Kigoma, we used different values the dry season (3.80 mg C [mg chl<sub>a</sub>]<sup>-1</sup> h<sup>-1</sup>) and the rainy season (2.77 mg C [mg chl<sub>a</sub>]<sup>-1</sup> h<sup>-1</sup>). I<sub>k</sub> did not differ between stations, but between seasons, so that the mean values of the measurements in the two seasons were used (389 μE m<sup>-2</sup> s<sup>-1</sup> for the dry season and 318 μE m<sup>-2</sup> s<sup>-1</sup> for the wet season).

Daily phytoplankton production in 2002-2003 (Fig. 37) showed a clear contrast between seasons in Kigoma, with higher production in August –September. This contrasted pattern was also visible in Mpulungu in 2003, but not in 2002. Isolated peaks of primary production occurred in the rainy season, particularly in Mpulungu. Measured values were generally in accordance with the calculated values, except on 2 occasions. The discrepancies are due to differences between light penetration

measured with sensors from those estimated from Secchi depth, and/or between chlorophyll a concentration.

On the basis of these calculations of primary production, we estimated daily average annual production. At Kigoma, similar values are obtained for the two years: 130 (2002) and 138  $\text{g C m}^{-2} \text{y}^{-1}$  (2003) or 0.36 and 0.38  $\text{g C m}^{-2} \text{d}^{-1}$ , respectively. At Mpulungu, as expected from the data of fig., primary production amounted to 167  $\text{g C m}^{-2} \text{y}^{-1}$  in 2002 (0.46  $\text{g C m}^{-2} \text{d}^{-1}$ ) and 224  $\text{g C m}^{-2} \text{y}^{-1}$  (0.62  $\text{g C m}^{-2} \text{d}^{-1}$ ) in 2003.

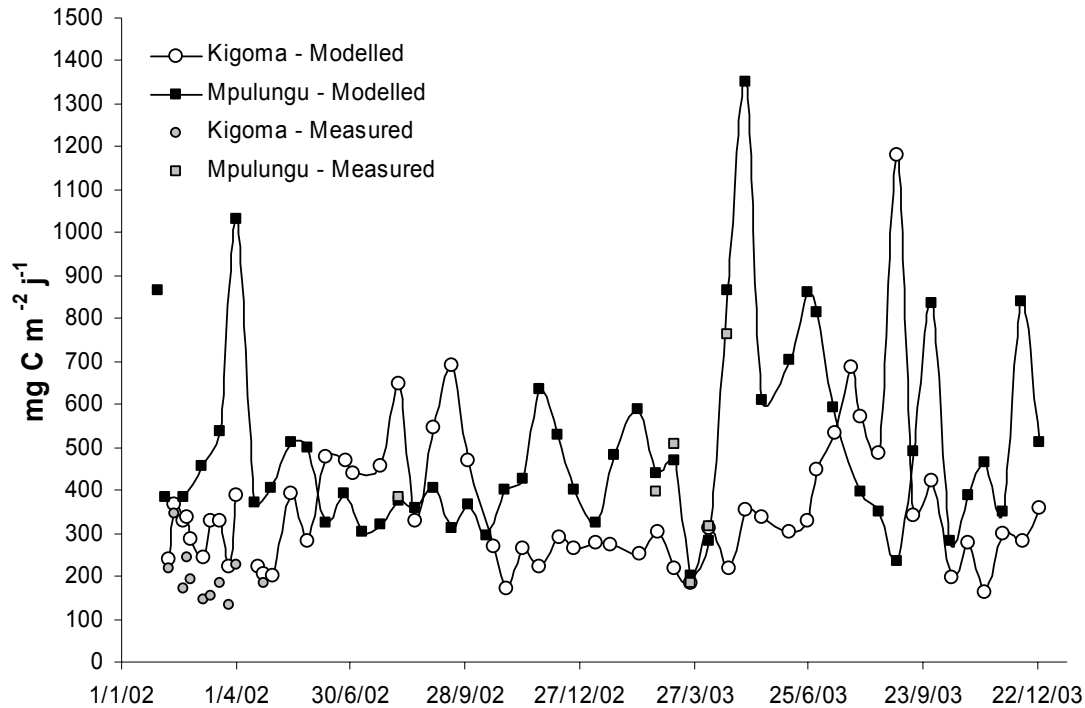


Fig. 37: Daily integrated phytoplankton production in Lake Tanganyika at the two monitoring sites (2002-2003). The squares are measurements obtained in these two years.

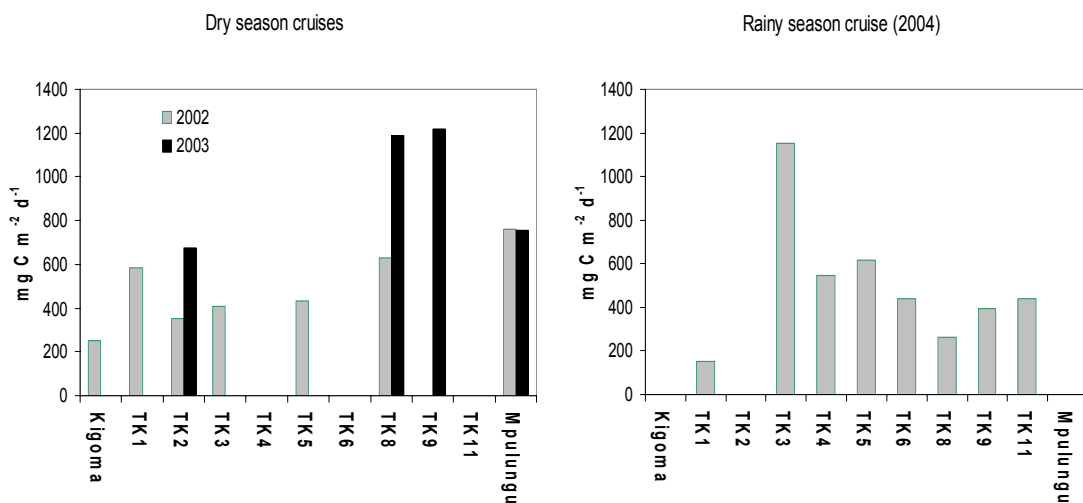


Fig. 38: Daily integrated phytoplankton production in Lake Tanganyika during the cruises (2002-2004).

Data obtained for the two dry season cruises (fig. 38) tend to confirm a difference of primary production between north and south of the lake. Rainy season results were more homogenous over the lake, with the exception of site TK3, which resulted from higher chlorophyll a at this site, possibly influenced by the plume of the Malagarazi river, presumably bringing nutrients into the lake.

**Bacterial production**

During dry season cruises in July 2002 and 2003, bacterial production ranged between 31 and 111 mg C m<sup>-2</sup> d<sup>-1</sup>. Contrasted results were observed between both north and south basins (fig. 39), with highest values usually recorded in the south basin.

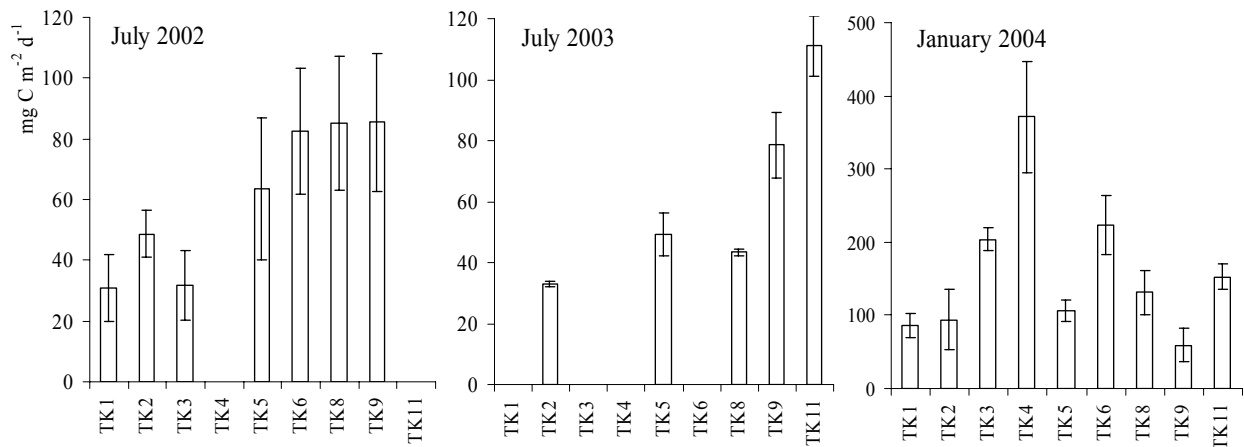


Fig. 39: Bacterial production in the 0-40 m layer at sampling sites (TKn) during research cruises.

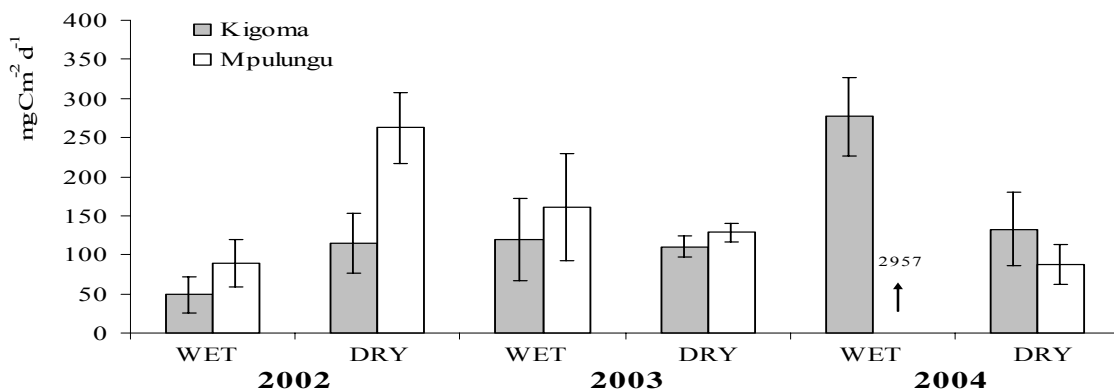


Fig. 40: Bacterial production integrated on the 100 m water column at Kigoma and Mpulungu.

During the only wet season cruise in January 2004, we recorded higher productions than during the previous dry seasons. Bacterial production in the pelagic sites ranged between 59 and 223 mg C m<sup>-2</sup> d<sup>-1</sup>. Results reached highest values in the north basin as in the south basin. The results from station TK4, which was close to the littoral

zone with a production of  $371 \text{ mg C m}^{-2} \text{ d}^{-1}$ , may not totally reflect pelagic conditions in the lake.

We used bacterial production in the mixed layer, at 60 m and at 100 m to integrate results on the whole oxic water column to 100 m depth. If we discard the Mpulungu result of  $2.96 \text{ g C m}^{-2} \text{ d}^{-1}$  during the dry season in 2004, probably due to a contamination, the range of bacterial production was between 49 to  $276 \text{ mg C m}^{-2} \text{ d}^{-1}$ . Highest values were obtained at Mpulungu during the dry season 2002 and at Kigoma during the rainy season 2004: they reached the lower range of phytoplankton production, showing the importance of heterotrophic vs. autotrophic production in Lake Tanganyika.

As for spatial and seasonal variations, significant differences between Kigoma and Mpulungu were observed in the dry season 2002. By contrast, in 2003, no significant differences were found neither between stations nor seasons. In 2004, significant seasonal variations were observed for the Kigoma site.

### **3.1.6 Geochemistry of the water column: Major, minor and trace elements**

Freshwater environments present complex geochemical signatures in relation with intricate interactions between hydrodynamical, biological and physico-chemical processes occurring at various time scale and locations. Monitoring specific tracers of chemical (red-ox processes), biological (with a nutrient-like compartment), detrital or hydrothermal processes, is a key to characterize major limnological features of Lake Tanganyika. In this project, we combined a multi-elemental approach on both the dissolved and particulate fraction in order to assess the Tanganyika Lake peculiar physical properties.

A statistical approach has been undertaken in order to evaluate the relationship between the suite of elements analyzed on the large geochemical data set gathered in this study. Several Principal Component Analysis (PCA) were performed on the two separate sets of data from Kigoma and Mpulungu and for the dissolved and particulate fractions. Most of the variance of the system could be explained with 5 or 6 factors for each data set although only the 3 major factors are highlighted below.

In the particulate fraction, a detrital associated component (Al, Th, Zr, Ge, Fe, La, Ti, Mn, Lu, Rb, K, Co, Sc, Nd, Ho, and Mg) appears in Kigoma and Mpulungu. A second factor is composed of biogenic related elements (Sr, Ca, Ba, U, Mg, and S). The third one is appearing only in Mpulungu data, linked to redox elements (Mn and Co) possibly indicating that redox associated particles induced by upwellings are not as significant in the northern basin. Other minor factors are linked to major elements such as S and P in Kigoma but also to Mg, K and Na in Mpulungu potentially reflecting some riverine influence in the southern station.

In the dissolved fraction, the main factors are first attributed to biogenic elements such as Ca, Sr, Ba, U, Mg and Y in Kigoma while Factor 1 in Mpulungu is linked to Red-ox sensitive elements such as Fe, Co, Mn, Mo, Cu. Such difference may well reflect the strong seasonal upwelling phenomenon in the south of the lake while the geochemical signature of Kigoma waters is more controlled by the biological activity. The second factor is linked to terrigenous elements in Kigoma (Zr, Al, Fe) and to biogenic markers in Mpulungu (Sr, Mg, Ca, Ba but also Mo, Zr). Although less noticeable than in Mpulungu, the variance of the red-ox elements (Co, Mn, Cu) has been noticed by the PCA in Kigoma within the third factor.

Residual variance explained in the last factors seems to be mostly associated to pollutant elements such as (Zn, Pb, and Cd) that could either reflect a similar pollutant source or more realistically some contamination problems during sampling and analyses.

The three cruises presented extremely similar profiles both in the northern and southern basin for most of the elements analyzed. Conservative elements (Na, K, Mg, Al, and Zr, W) showed little variation with depth while biologically reactive elements presented large (P, Si, Ge, U) or small depletion in surface waters (Ca, Ba, Sr, Rb, L-REE). Redox elements controlled by dissolved oxygen content (Fe, Mn, Co) were largely depleted in surface and increased drastically below the oxycline (180-200 m) as shown below (Fig. 41).

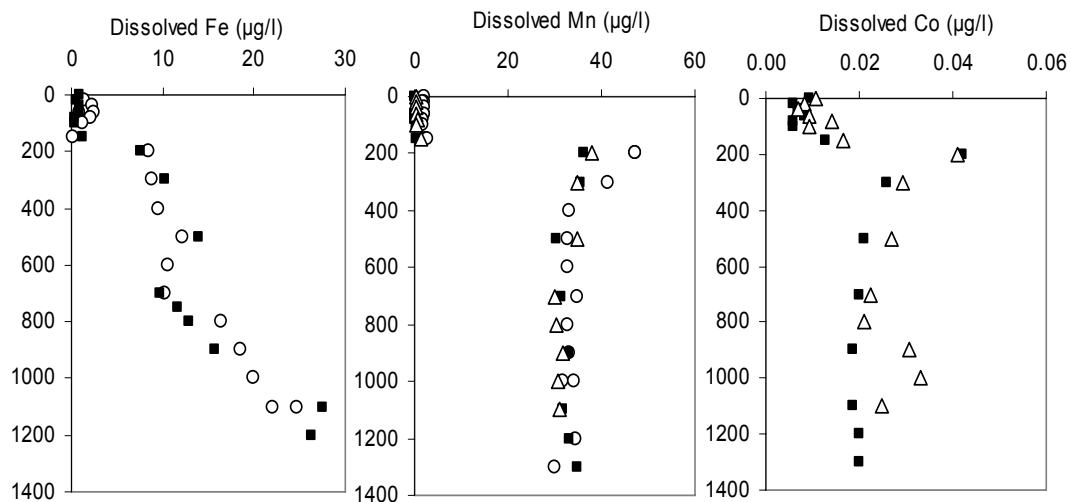


Figure 41: Dissolved Fe (northern basin), and Mn and Co (southern basin) water profiles in 2002 (open circles), 2003 (open triangles) and 2004 (black squares).

Redox and particulate reactive elements such as Mn and Fe presented the most interesting features in the deep north and south profiles (Fig. 42). Within the oxygenated mixed layer (100 to 200 m depth), they both displayed very low dissolved



concentrations as most of their content remained in the particulate phase. A marked enrichment was observed at the oxycline, indicative of the reductive dissolution of the oxy-hydroxides particles. Fe concentration profiles tended to react at slightly greater depth than Mn at the O<sub>2</sub>/H<sub>2</sub>S boundary, which is expected according to its higher oxidation rate.

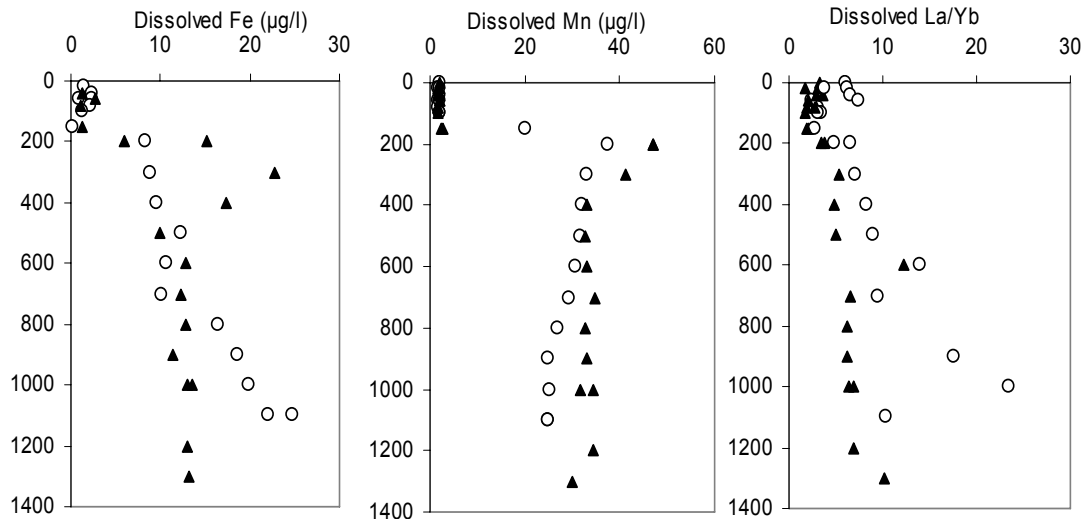


Figure 42: Geochemical water profiles in the north (open circles) and south (closed triangles) basins during the July 2002 transect.

Some specificity for these elements collected in the north and south basin are evidenced on figure 42. While Mn and Fe show a flat profile between 400 and 1400m in the south, they decreased and increased respectively below 750 m depth in the northern basin although under similar anoxic condition in both basins. A comparable behaviour was observed during the 2004 cruise where both northern and southern stations were replicated. La/Yb ratios presented a similar pattern suggesting that some water source variability may explain the discrepancy, as REE were homogenous in the whole lake.

Mn, Fe, Ca, Ba and Mg in the particulate fractions (Fig. 43), only measured in 2002, confirmed this difference between northern and southern profiles below 750 m: such a behaviour could be associated to direct riverine sources (the Rusizi for example) or to interstitial water diffusion.

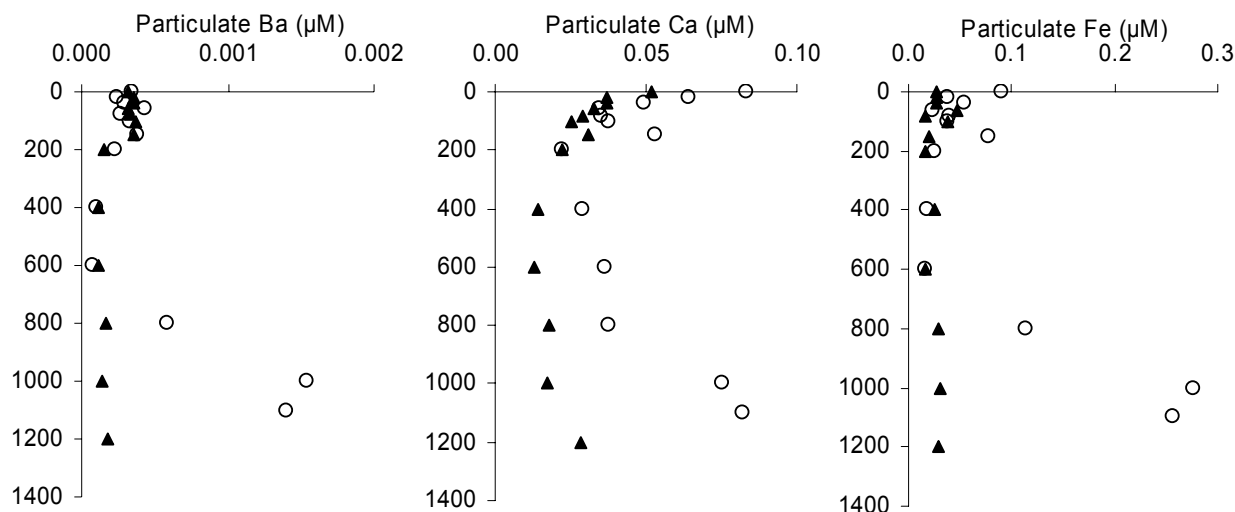


Figure 43: Particulate profiles in the north (open circles) and south (closed triangles) basins

### 3.1.7 The Bivalves Monitoring – Hydrological changes in Lake Tanganyika recorded in bivalve shells

This study explored the potential of the freshwater bivalve *Pleiodon spekii*, endemic to Lake Tanganyika, as a geochemical archive of hydrological changes tuned by monsoon regime.

Recent efforts were done to model effects of thermal and wind changes on the lake hydrology (Naithani et.al 2002, 2003) but lack of environmental data about pre-instrumental periods limits our ability to predict how climate change might affect lake productivity. As they record the chemistry of the solution in which they precipitate, biogenic carbonates constituting the shells have the potential for the reconstruction of seasonal or intra-annual variability, then for high-resolution paleoclimatic records. *P. spekii*, found on the present shore of Lake Tanganyika, but also in both archaeological and geological settings, is a suitable species for this purpose.

Cathodoluminescence microscopy was used to map Mn in shell sections. Periodic pattern of luminescence revealed high concentrations of Mn and a periodic distribution, but no artificial mark resulting from the Mn marking was observed. Then, growth rates were deduced from shell measurements only. The growth rates determined for 11 specimens between July 2002 and February 2003 were similar, *i.e.* an average growth rate of 0.03 mm/day. We assigned a date to each laser pit drilled into the shells, assuming that the growth rate remains constant over the period comprised between July 2002 and the date of collection (Feb 2003; ventral margin).

The Mn and Sr profiles obtained by LA-ICP-MS on specimen MPU-V10 are very similar in shape as well as in amplitudes to these obtained by HR-ICP-MS analysis on an adjacent profile of the same shell, which demonstrates a remarkable intra-individual reproducibility ( $R^2 = 0,75$  and  $R^2 = 0,79$  for Mn and Sr respectively).

Therefore, our laser calibration method is considered to be robust and relevant for quantitative analysis.

The Mn profiles realized on shell MPU-V10 and MPU-V72 are similar and are dominated by a peak in the older part of the shell (Fig. 44a). This peak coincides with the abrupt rise of Mn in the particulate fraction in August 2002 and September 2003 during the upwelling, clearly associated with the supply of Mn from deep layers (data CLIMLAKE). It also matches with the rise of dissolved/colloidal Mn measured in water at the same period in 2003 and 2004 and coming from the same source. The increase in Mn/Ca levels in the shells of *P. spekii* should be a rapid and positive response to the elevation of Mn content in water that is consistent with previous studies on freshwater shells from temperate and tropical areas (Jeffree et.al 1995, Siegele et.al 2001). We postulate that the Mn content in *Pleiodon* shells may be used as a retrospective indicator of upwelling events in Lake Tanganyika.

The Sr concentrations show similar periodic variations, with a minimum that perfectly matches with the Mn maximum (Fig. 44a). A relationship between skeletal  $\delta^{18}\text{O}$  and Sr exists for both shells (Fig. 45) although the correlation coefficient of one shell is low (Fig. 45a). Sr/Ca in *P. spekii* shells does not reflect the Sr/Ca ratio of the surrounding water that remains relatively constant in the lake surface water (data CLIMLAKE). Beside this, the lack of correlation between Sr profiles and temperature suggests a strong biological control as shown in other aragonitic shells (Gillikin et al, 2005) although Sr/Ca is correlated to temperature in many biogenic aragonite including bivalves shells (Stecher et.al 1996). Classically, the oxygen isotopic composition of carbonate ( $\delta^{18}\text{O}_{\text{shell}}$ ) is governed by both the oxygen isotopic composition of the water ( $\delta^{18}\text{O}_{\text{w}}$ ) in which precipitation occurs and the water temperature (Epstein et.al 1953). As the  $\delta^{18}\text{O}_{\text{w}}$  of Lake Tanganyika seems to be constant (Craig 1974),  $\delta^{18}\text{O}_{\text{shell}}$  should mimic the temperature profile if carbonates were in equilibrium with water. Our results give evidence that the  $\delta^{18}\text{O}$  composition of *P. spekii* is not solely controlled by temperature (Fig. 45), although this parameter likely controls the annual amplitude of  $\delta^{18}\text{O}_{\text{shell}}$ .

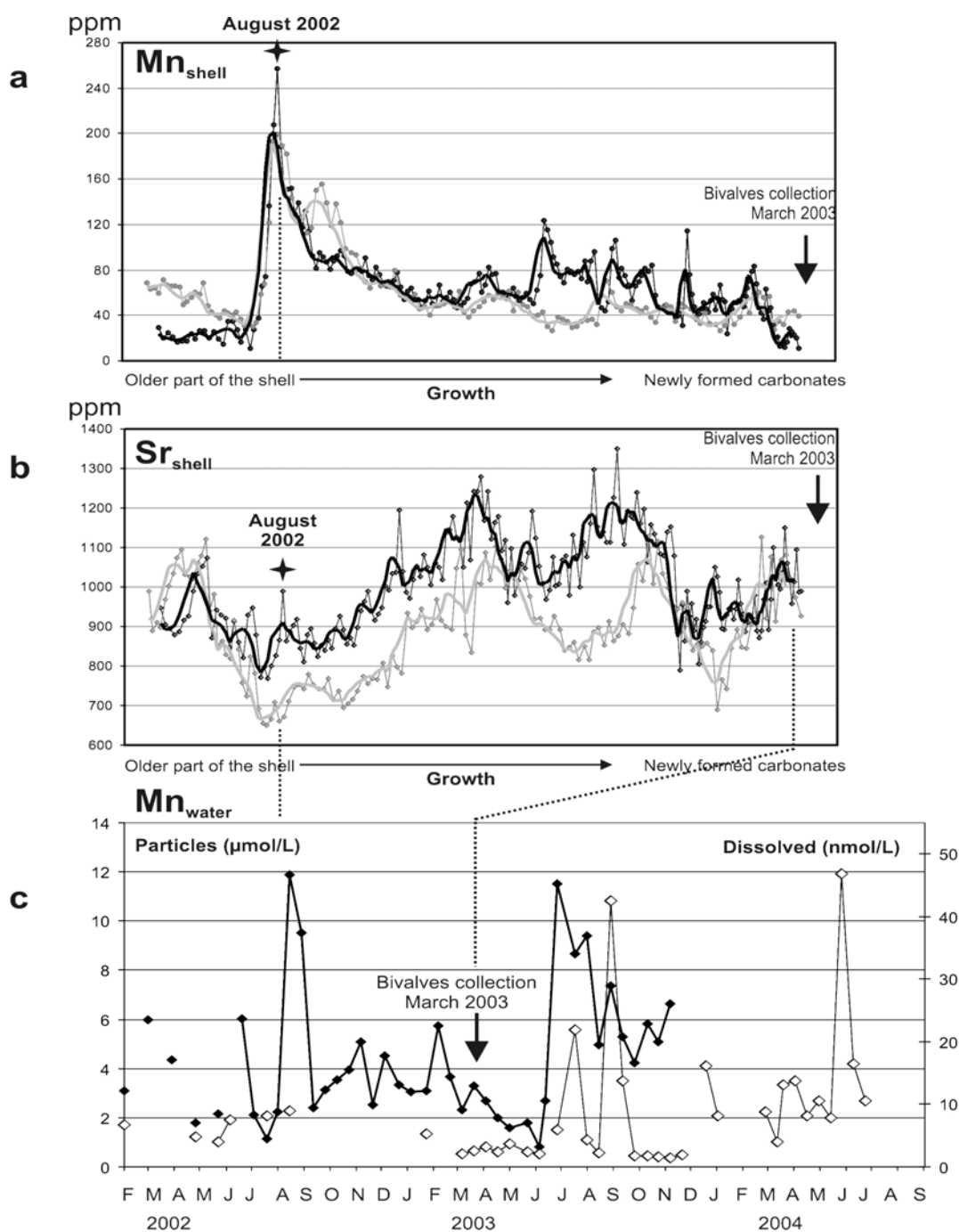


Figure 44: (a) High resolution distribution of manganese (Mn) and (b) strontium (Sr) in two shells of *P. spekii* collected in March 2003. The black and grey lines are moving average curves calculated on 3 periods for specimens MPU-V10 and MPU-V72 respectively. The profiles were matched to each other by assigning a date to each laser analysis. This was done by assuming a mean growth rate between two anchor points: the ventral margin (date of collection) and the peak of Mn, which is dated to June-July 2002 from MPU-V10 shell measurements. (c) Monitoring of Mn in the particulate fraction (black lozenges) in  $\mu\text{mol/L}$  and in the dissolved/colloidal fraction (empty lozenges) in  $\text{nmol/L}$  collected in surface waters. Data were obtained from the fortnightly geochemical monitoring of lake water (CLIMLAKE).

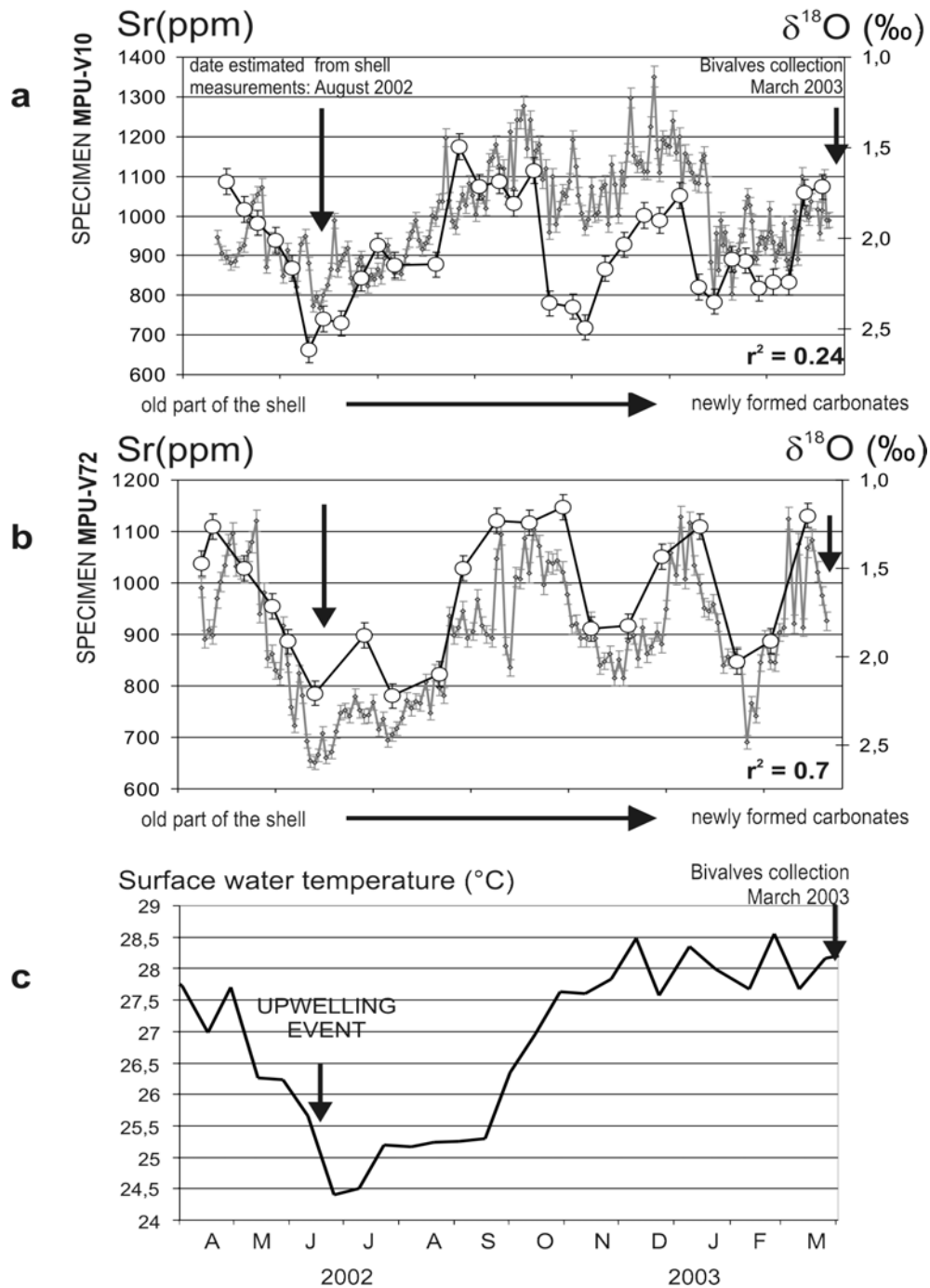


Figure 45: (a, b) Sr variations obtained by LA-ICP-MS *in situ* analyses (small grey lozenges) and the stable isotope composition ( $\delta^{18}\text{O}$ ) obtained by IRMS analyses on acid dissolved micro-drilled samples (large open circles), compared with (c) temporal variations of temperature in lake surface waters (bivalve site) on an annual scale, in relation with the annual variations of wind forces.

### 3.1.8 Silicon isotopic fractionations

In aquatic environments, silicon isotopic compositions are directly related to the relative silicic acid utilization by diatoms to produce opal frustules (Alleman *et.al*, submitted). Measuring this isotopic tracer improves considerably our perception on

how the Si and C cycle are related to each other and which factors are driving the productivity of the siliceous organism in the lake. Si sources variability and diatom fractionation have been evaluated in order to constrain this new proxy with large potential in paleo-productivity studies.

During the one-year monitoring (January 2002 - January 2003) in Mpulungu, dissolved Si concentration displayed substantial variations (15 to 51  $\mu\text{M}$ ) in surface waters collected at 0 m (coastal site) and 20 m (pelagic site). However, mean annual  $[\text{Si}(\text{OH})_4]$  reached  $33 \pm 8 \mu\text{M}$  for both sites/depths, markedly correlated at all times between these two locations ( $r^2 = 0.92$ ). The mean annual Si content at  $32 \pm 8 \mu\text{mol L}^{-1}$  for both stations is confirmed by the monitoring performed over a two-year period in 2002 and 2003 ( $31.5 \mu\text{mol L}^{-1}$ ). Maximum concentrations tended to appear during the upwelling period, represented by the temperature decrease.

$\delta^{29}\text{Si}$  varied significantly from 0.66‰ to 1.03‰ at both southern stations (Fig. 46 B) and presented comparable averaged values ( $0.88 \pm 0.08\text{‰}$  ( $n=19$ ) at 0 m and  $0.86 \pm 0.09\text{‰}$  ( $n=23$ ) at 20m. It must be noted that surface data at TK1, 5 and 8 during the cruise (Table 1) are similar to the ones measured during the same period (July 2002) at the monitoring sites. Small  $\delta^{29}\text{Si}$  differences between the coastal and pelagic sites may suggest some local influences, although presenting generally comparable variations on a seasonal scale (Fig. 46 B).

Five large diatom samples ( $> 10\mu\text{m}$ ) collected along with the dissolved fraction during this survey have been analyzed in duplicate. They display relatively lighter  $\delta^{29}\text{Si}$  ( $0.28 \pm 0.12\text{‰}$ ,  $n=5$ ) compared to the dissolved  $\delta^{29}\text{Si}$  of the surrounding water ( $0.85 \pm 0.05\text{‰}$ ,  $n=5$ ).

Lake Tanganyika Si concentrations profiles at three pelagic stations (TK1, TK5 and TK8) (Fig. 47) presented a characteristic nutrient-like shape with a large depletion in surface water (under-saturated water with respect to biogenic Si:  $44 \pm 10 \mu\text{M}$ ) related to the intense bio-utilisation of Si needed to produce diatom frustules. Below the 100-250 m silicicline (sharp increase of silicic acid content), the dissolved silicon content continuously increases (Si = 60 to 385  $\mu\text{M}$ ), in accordance with previous results (Craig *et.al* 1974, Edmond *et.al* 1993). The largest fractionation effect (enrichment in  $^{29}\text{Si}$  against  $^{28}\text{Si}$  in the dissolved fraction, mean  $\delta^{29}\text{Si} = 0.86 \pm 0.08 \text{‰}$ ) are present in the epilimnion where diatoms are mostly active. The silicicline values, thought to represent the upwelling signature in the south, display a  $\delta^{29}\text{Si}$  of  $0.69 \pm 0.07 \text{‰}$ . The deep waters from both basins exhibit homogeneous equivalent isotopic profiles below 300 m (mean  $\delta^{29}\text{Si} = 0.61 \pm 0.05 \text{‰}$ ). Station TK1 showed a stratified profile, while TK5 and TK8 presented more gradual Si content and  $\delta^{29}\text{Si}$  variations with depth. These Si isotopic profiles present similarities in shape and fractionation

intensity found in various oceanic sites (De La Rocha *et.al*, 2000; Cardinal *et.al*, 2005).

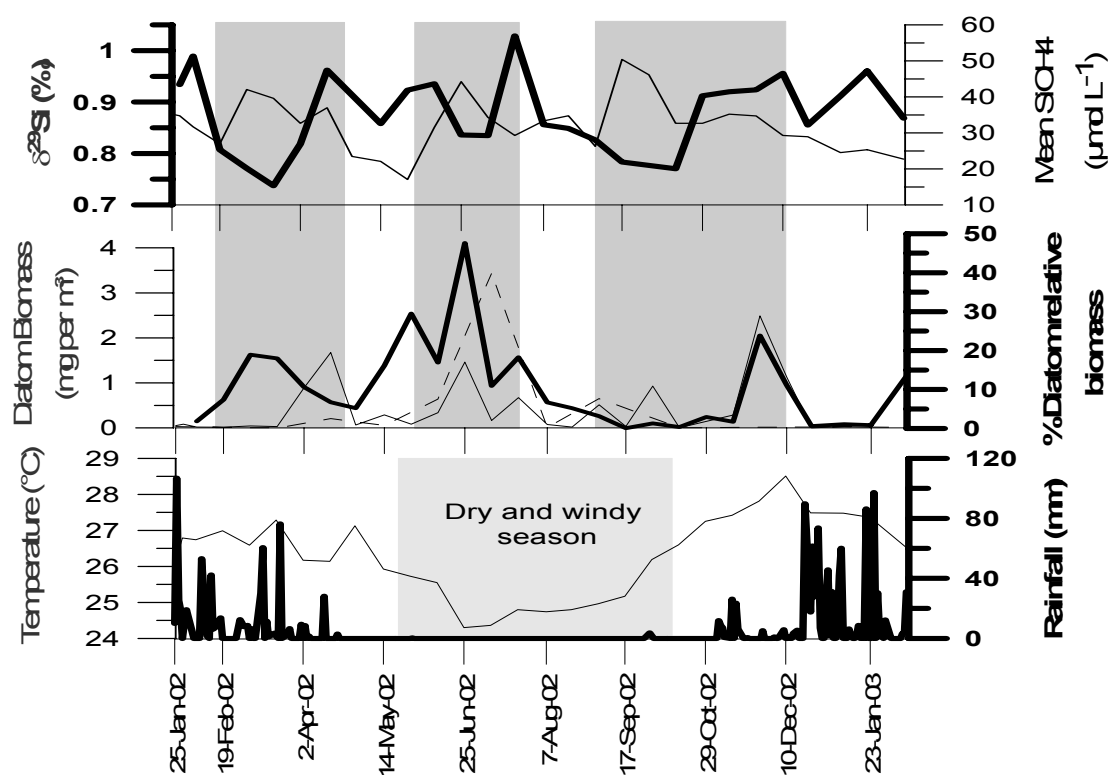


Figure 46: (A) Mean dissolved Si concentrations (solid line) and  $\delta^{29}\text{Si}$  (bold line) from measurements at CLIMC-M (0m) and CLIMP-M (20m) stations from February 2002 to January 2003. (B) Surface water diatom biomass at CLIMC-M (~0m) (dashed line) and CLIMP-M (20m) (solid line) in mg per m<sup>3</sup> and percentage (%) of diatom relative biomass at CLIMP-M, as inferred from marker pigments (Descy *et.al* 2005) (bold line) (C) Surface water temperature monitoring (solid line) and rainfall (bold line) in 2002 in Mpulungu.

In Lake Tanganyika tributaries (Rusizi, Malagarasi, Lufubu, Luiche and Gombe), dissolved silicon concentrations  $[\text{Si}(\text{OH})_4]$  were higher than in Tanganyika surface waters. Although variable over time and between watercourses (mean:  $142 \pm 81 \mu\text{mol L}^{-1}$ ), these concentrations span the range of data obtained by Craig *et.al* (1974) for various rivers collected in spring 1973 and 1974 around the lake (mean:  $145 \pm 63 \mu\text{mol L}^{-1}$ ). The Si isotopic signature of Lake Tanganyika tributaries range from  $\delta^{29}\text{Si} = +0.36 \text{‰}$  for the Lufubu and up to  $\delta^{29}\text{Si} = +1.30 \text{‰}$  for the Rusizi. They tend to vary seasonally and between rivers along with silicic acid contents. Excluding small rivers such as the Gombe stream and the Luiche River, we calculate a mean isotopic composition of  $0.95 \pm 0.20 \text{‰}$  for the riverine input, within the range of published values for large rivers of the world ( $\delta^{29}\text{Si}$  between  $+0.21$  and  $1.7 \text{‰}$ ; De La Rocha *et.al*, 2000; Ding *et.al*, 2004).

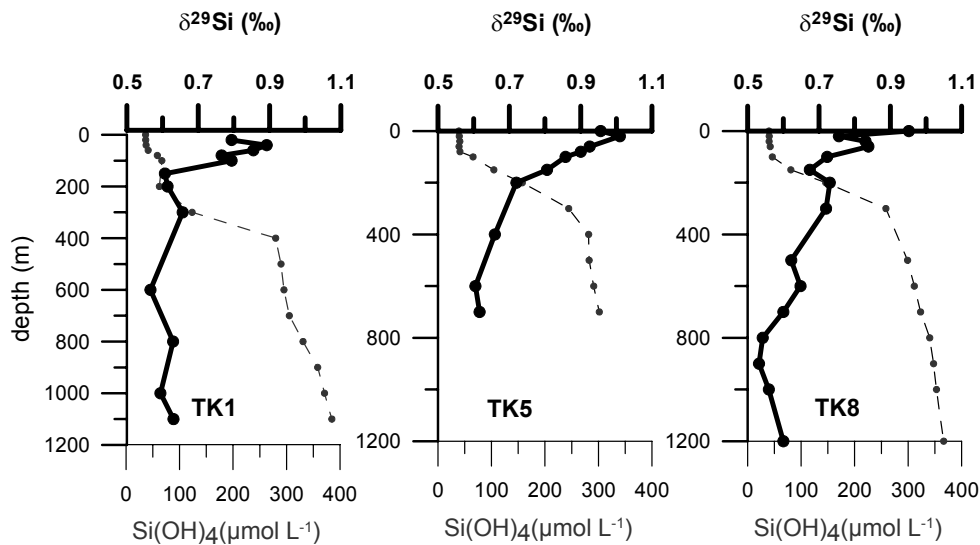


Figure 47: Si isotopic composition and concentrations profiles at stations TK1, TK5 and TK8 in the cruise transect of July 2002

The positive correlation between  $\delta^{29}\text{Si}$  and dissolved Si concentrations in Lake Tanganyika tributaries is very similar to the one published for other world rivers (De La Rocha *et.al* 2000).

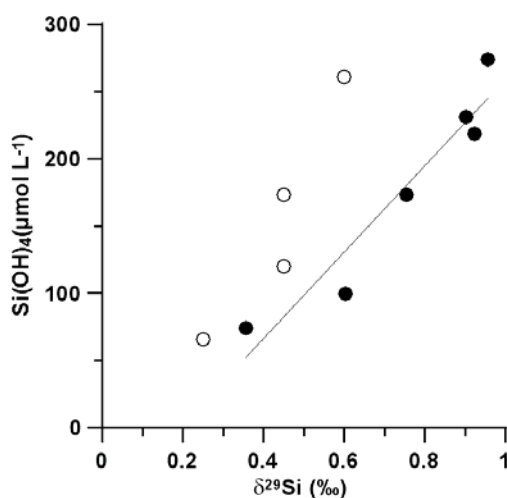


Figure 48: Tanganyika tributaries  $\delta^{29}\text{Si}$  values versus dissolved Si (black circles). (Rusizi values have not been plotted as they are influenced by diatom activity and hydrothermalism from Lake Kivu). World river data are also reported for comparison (white circles) (De La Rocha *et.al* 2000).

It may reflect some mixing processes between two extreme components. The low Si,  $^{29}\text{Si}$ -depleted end member might reflect the crustal rocks or crustal-derived clays, as weathering of insoluble quartz-rich felsic rocks and clays would liberate a solution with low Si contents and  $\delta^{29}\text{Si}$  either undifferentiated (for a pure crustal component:  $-0.05$ ‰) or relatively depleted (for Kaolinite:  $-0.80 \pm 0.25$ ‰, De La Rocha *et.al* 2000). The high Si,  $^{29}\text{Si}$ -enriched end member might correspond to the dissolution of phytoliths, that would produce a solution with high  $[\text{Si(OH)}_4]$  and positive  $\delta^{29}\text{Si}$  ( $+0.6$  to  $+1.2$ ‰), according to the limited database available for phytoliths (Ding 1996). Consequently, dissolved Si in tributaries of Lake Tanganyika should be mostly driven



by changes in the mineralogical components through weathering processes, with little influence from the fresh water diatom activity.

External Si sources (5.84 Gmol/yr; Branchu 2001) represent annually at most 6% of the surface water (0-100m) estimated stock of dissolved Si (95 Gmol Si in 2002). Moreover, neither the high Si content in rivers nor the negative precipitation - evaporation budget could explain the Si depleted surface water of the lake, allowing discarding any significant influence from external Si sources on the lake Si internal reservoir. Consequently, one cannot consider external Si sources as a major driving force of the Tanganyika silicon cycle. Yet, due to a marked rainy season (November to April/May), rivers/run-off and rainfall may locally have some impact during stratified periods, while vertical mixing is most pronounced during the dry and windy season (May-June to October) (Langenberg *et.al* 2003). Internal recycling and mixing are the major sources of fresh dissolved silicic acid to the mixed layer (Hecky *et.al* 1991; Branchu, 2001). Water mass upward advection tends to enrich the epilimnion with a high Si content and low  $\delta^{29}\text{Si}$  signatures. Vertical profiles in both basins present a heavier isotopic signature in surface waters ( $\delta^{29}\text{Si} = 0.86 \pm 0.08 \text{‰}$ ) associated to low Si concentrations and inversely in deep waters ( $\delta^{29}\text{Si} = 0.61 \pm 0.05 \text{‰}$ ) (Fig.1). This is consistent with a preferential  $^{28}\text{Si}$  biological uptake by diatoms in surface waters, which is regenerated by their dissolution in deep waters in a way similar to the one encountered in marine environment. Observations made during the year-long survey contribute to that hypothesis. Three distinct episodes of high Si concentrations (highlighted on Fig.2) echo through a lighter  $\delta^{29}\text{Si}$  signatures, characteristic of nutrient replenishments. They are rapidly followed by a diatom biomass increase, lower dissolved Si and heavier  $\delta^{29}\text{Si}$  values (Fig. 2A, B), a sign of a biological control. To give additional support on such a mechanism, we have determined  $\delta^{29}\text{Si}$  of the biogenic silica from size fraction  $> 10\mu\text{m}$  at various seasons which can be assumed to mainly represent the diatoms signature. Indeed, the choice of this size fraction and the NaOH leaching during the biogenic silicon extraction allow avoiding significant bias from clay minerals. Moreover, perturbations from phytoliths potentially present in riverine particles (Conley 2002) are limited in the Lake Tanganyika samples. The counting of phytoliths and sponge spicules in the five phytoplankton samples represented only 0.5 to 2.5% of the total number of opal particles. The difference between the surrounding dissolved Si and biogenic silica fractions ( $\square^{29}\text{Si} = \delta^{29}\text{Si}_{\text{Si(OH)}_4} - \delta^{29}\text{Si}_{\text{bSiO}_2}$ ) is  $0.56 \pm 0.1\text{‰}$ . This result is similar to the mean value obtained for the  $^{29}\text{Si}$  enrichment factor ( $^{29}\square$ ) on tropical marine diatoms -  $0.57 \pm 0.2\text{‰}$  (recalculated from De La Rocha *et al.* 1997 using  $\delta^{29}\text{Si} = \delta^{30}\text{Si}/1.934$ ). For small levels of Si isotope fractionations,  $\square^{29}\text{Si}$  offers an excellent approximation to  $^{29}\square$  if an isotopic equilibrium has been reached between the dissolved and particulate phases. This brings first evidence that silicon isotopes are a relevant proxy to diatom relative silicon utilization

in freshwater environments and under high temperature conditions (24-28°C). The non-species dependent character of this proxy underlines its general applicability for monitoring past changes in diatom activity in both marine and fresh water palaeoenvironments.

### 3.1.9 Data base

A great amount of data was collected during CLIMLAKE by researchers from Tanzania, Zambia and Belgium. Some data were also downloaded from electronic devices (weather stations, thermistors, radiation logger, CTD). Several time intervals were used depending of the data collected (every 15 min, 30 min, daily, weekly or bimonthly, monthly). The great number of data and the processing needed to homogenise, standardize and organise the data as well as gaps due to unavoidable missing data or frequent electrical breakdowns in the Tanganyika area conditions rendered processing much longer than foreseen. There was thus not enough time available to develop a multi-relational database. The data were organised however in a set Excel data files much easier to handle than original files. Those data can be exported as ASCII files for other type of processing (e.g. Matlab). Data were collected from February 2002 until January 2005 (for the longest time series available) for the variables listed in table 2:

- water temperature	- seston stoichiometry
- zone of mixing	- phytoplankton pigments
- dissolved oxygen	- metazooplankton analysis
- conductivity, pH	- phytoplankton biomass counts
- turbidity	- ciliate analysis
- euphotic depth, transparency	- nanoplankton/bacterioplankton
- SiO <sub>2</sub>	-majors and traces elements: Al, Ba, Ca, Fe, K,
- TP, SRP	Mg, Mn, Na, P, S, Si, Sr, Ti, Sc, Co, Cu, Zn, Ga,
- NH <sub>4</sub> <sup>+</sup> , NO <sub>3</sub> <sup>-</sup> , NO <sub>2</sub> <sup>-</sup>	Ge, Rb, Y, Zr, Nb, Mo, Cs, La, Ce, Pr, Nd, Eu, Sm,
- Alkalinity	Gd, Dy, Ho, Er, Yb, Lu, Hf, Ta, W, Pb, Th, U.
- Chl a	

Table 2: Variables for which results were measured and presented in CLIMLAKE databases for the monitoring from February 2002 to January 2005 and research cruises.

### 3.2 Proxies studies: plankton in the sediments

Two key diatom taxa could be distinguished in the water column of the pelagic stations in Lake Tanganyika. They are related to mixing depth and stability of the water column (Fig. 49). The first key diatom is *Nitzschia asterionelloides*. This large, colony forming species was most abundant during the dry season, the period of upwelling and maximal mixing in the water column. This taxon was described from planktonic samples of Lake Malawi by Müller (1905). The second key species is *Nitzschia fonticola*. This small species reached it greatest densities at the end of the

rainy season, the period when maximal stability is reached in the water column and when mixing depth is minimal. This taxon is known to be more abundant during periods of very stable water column conditions and can grow epiphytic on *Microcystis* (Cyanobacteria) colonies under stratified conditions (Haberyan & Hecky 1987, Stager *et.al* 1997). Own observations of the pelagic samples of Lake Tanganyika, however, let us conclude that this taxon, which was never observed attached, is an euplanktonic species. On the other hand, epiphytic specimens were found in the littoral stations. It is likely that the *Nitzschia fonticola* in Lake Tanganyika consists of at least two different entities, comprising euplanktonic and epiphytic populations. Only detailed morphological and genetic analyses could confirm this hypothesis.

A third key diatom species, belonging to the genus *Cyclostephanos* (in earlier literature referred to as *Stephanodiscus*), a dominant taxon during several past periods in the lake history, was not observed in the monitoring nor in the samples from the north-south transects carried out during the CLIMLAKE project. Very rarely a broken fragment from a valve was observed in the net samples. However, *Cyclostephanos* was previously reported as being sub-dominant in the northernmost part of the lake attaining it maximum densities after the *Nitzschia* spp. peak at the start of the dry season (Hecky and Kling 1981).

The occurrence of planktonic diatom species is determined by several factors, including light, intensity of turbulent mixing and the Si: P ratio (Kilham *et.al*, 1986). *Cyclostephanos* is favoured under low Si: P and *Nitzschia* under high Si: P (Haberyan & Hecky 1987). The fact that *Cyclostephanos* was not observed during our plankton monitoring suggests that the environmental variables that favour this species have changed; notably, the Si: P ratio of the mixed layer should have become higher than in the past. High Si: P ratio in the lake water could be induced by lower consumption of Si due to lower diatom production, as a result to increasing surface water stability due to global warming, as suggested, *e.g.* by Verburg *et.al* (2003) and by this study. Indeed, the present study (Alleman *et.al*, submitted) tends to confirm this evolution with mean surface dissolved Si of  $32 \pm 8 \mu\text{mol L}^{-1}$  in the northern and southern basins, amongst the highest ever reported values. *Cyclostephanos* was never present in great quantities in the upper parts of the sediments cores from the southern basin, corresponding to the period from the Little Ice Age to present. This is evidence that the Si: P ratio was never low enough during the historical time in order to favour *Cyclostephanos* in the southern basin were sediment coring has been done during the ENSO project.

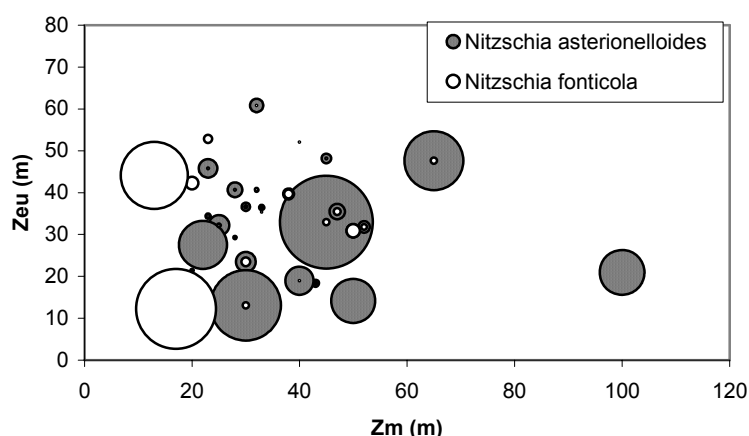


Figure 49: Number of cells per litre of the most important diatoms in the phytoplankton (*Nitzschia asterionelloides* and *Nitzschia fonticola*) at 20 m depth in Kigoma and Mpulungu from February 2002 to January 2003, as a function of mixing depth of the mixed layer ( $Z_m$ ) and thickness of the euphotic zone ( $Z_{eu}$ ).

### 3.3 Eco-hydrodynamic modelling of Lake Tanganyika

#### 3.3.1 Introduction

The objective of the modelling was to understand the relationship between climate, hydrodynamics, nutrients and primary productivity of Lake Tanganyika (Figure 50) and to further study the impact of climate change on lake hydrodynamics and ecology. Hydrodynamic variability in the upper layer of Lake Tanganyika is important for the biological productivity of the lake. Strong wind stress during the dry season pushes surface water away from the southern end, thereby inducing upwelling in this region of cold and nutrient rich bottom water. While the thermocline becomes shallower in the southern part of the lake, it deepens at the opposite end. Superimposed on this movement are thermocline oscillations that are present all year round [Coulter and Spigel, 1991]. The upwelling also reduces the heat storage of the upper layer.

#### 3.3.2 Amplitude and frequency of free oscillations

Free oscillations of Lake Tanganyika were studied using the hydrodynamic model forced with an idealised wind. Model details can be found in Naithani *et al.* [2003]. The model was forced using a constant southeasterly wind stress during the 4 month long dry season and no wind stress during the rest of the year. The spatially uniform wind stress is provided along the whole length of the lake. The model predicted the tilting of the thermocline towards north during the dry season and thermocline oscillations for the whole year (see figure 6a, Naithani *et al.*, 2003). The model simulations predicted well the amplitude (15 to 45 m) and the period (3 to 4 weeks) of

oscillations in the lake (Coulter and Spigel, 1991). Wavelet spectra of downward displacement of the thermocline showed various scales of motion around 6, 12 and 24 days (see Figure 6b Naithani *et.al*, 2003). All these modes of oscillation seem to start from the dry season persist throughout the year and decay towards the beginning of the next dry season. We see that besides the fundamental mode of oscillation, there are several other free modes of the longitudinal oscillations, which are basically the integer divisions of the fundamental mode (Naithani *et.al*, 2003).

### 3.3.3 Origin of thermocline oscillations

The next step was to understand the origin of the thermocline oscillations. First the available measurements from the lake were analysed using the wavelet transform (WT). The WT was performed to study the time evolution of various scales in the time series of near surface wind and temperature at 30 m depth. These measurements were taken near Mpulungu during April 1993 to March 1994 during FAO/FINNIDA project. Since, the oscillations in the lake are induced by wind-stress acting on water surface, the WT spectra of wind-stress is also presented. The WT spectra of wind speed, wind stress and temperature at 30 m depth of the lake showed similar oscillations. In the dry season the dominant scale was found to be of 22 days and in the wet season it was of 33 days period (see Figure 2, Naithani *et.al*, 2002). The presence of similar oscillations at both seasons in the lake temperature spectra and wind stress indicates that the oscillations in the lake are inherited by the intraseasonal variability (ISV) in its forcing mechanism. However, this was still not very clear since in the earlier study, we found similar period of oscillation while providing a continuous wind forcing for the four months dry season. This implies that the ISV in the lake is independent of the ISV in the wind and that these periods can still be there even if the wind had no imbedded oscillations. The question arise, to what extent the free oscillations of the lake (after the strong wind-stress ceases) are influenced by the winds. To know this the model was forced with different wind forcings, including the observed winds at Mpulungu for April 1993 to March 1994. In all model runs the thermocline oscillations matched with the frequency of the forced wind pulses (see Figure 3, Naithani *et.al*, 2002). These tests indicate that the thermocline oscillations in the lake are indeed influenced by the fluctuations in wind forcing. It has been inferred that the response of the lake to the applied wind-stress consists of the directly forced motion and the free oscillations or seiches. The amplitude of oscillations depends upon the lake geometry and wind stress, while the period depends upon the lake-length and the wind forcing period. From earlier studies [Coulter, 1968; Coulter and Spigel, 1991] and this study, it is clear that the geometry, and particularly the length, of the lake is such that the free oscillations in the lake are of the same order as the ISV of winds in this region. Therefore, it is

concluded that the free oscillations in the lake similar to the ISV of wind pulses are being excited (Naithani *et.al*, 2002).

### 3.3.4 Internal Kelvin waves

Another important finding of the hydrodynamic modelling of Lake Tanganyika is the occurrence of internal Kelvin waves. It is generally believed that the Earth's rotation has negligible impact on the water circulation in basins which are very narrow or located near the Equator. Numerical simulations performed above suggest that thermocline displacements are far from being homogeneous in the lateral direction. The simulations exhibited small upwellings at the western shores as a result of thermocline oscillations induced by southeasterly winds of the dry season. These structures tend to propagate cyclonically around the lake similar to internal Kelvin waves. To determine the direction and speed of propagation of structures believed to be Kelvin wave packets, the thermocline displacement at the shore is displayed as a function of time and arc length of the shore increasing in the clockwise direction as shown in Figure 50. In these diagrams, lines with a slope equal to  $\sqrt{\varepsilon gh}$ , the theoretical velocity of Kelvin waves, are also displayed. Kelvin waves should lead to isolines of the thermocline displacement that tend to be parallel to these lines. Figure 50 a suggests that for some periods of time and along some portions of lake shores, there are indeed signals propagating with the phase speed of Kelvin waves. If the width-averaged displacement of the thermocline is displayed in the same type of diagram (Figure 50 b), there is virtually no isoline parallel to the lines with  $\sqrt{\varepsilon gh}$  slope, suggesting that the motions propagating with a phase speed equal to  $\sqrt{\varepsilon gh}$  are, like Kelvin waves, trapped at the coast. As the Rossby radius depends on  $f$ , which is a function of latitude, a sensitivity model run is made in which the lake is assumed to be on the Equator ( $f = 0$ ). The Rossby radius became infinite with  $f = 0$ . In this case, the model results exhibit no features propagating with the appropriate phase speed along the shores of the lake (Figures 50 c, d). By contrast, if the lake is shifted southward so that its centre is at about 20° S (Figures 50 e, f), thereby making the Rossby radius significantly smaller than it is in the actual lake, the structures propagating as Kelvin waves are more pronounced and pervasive. To test the impact of the variation of  $f$  with latitude, *i.e.* the so-called beta effect,  $f$  is kept constant throughout the lake, at the value corresponding to a latitude of 6°S. Then, the model yields results, which are not much different from the ones obtained with the actual Coriolis force (Figures 50 g, h), implying that the beta effect is not crucial for the phenomenon we are looking at. All the results discussed above are consistent with the existence of Kelvin waves in Lake Tanganyika. This study demonstrated the influence of Coriolis force in modifying the dynamics of the internal gravity waves in Lake Tanganyika and that the internal Kelvin waves do exist in this lake (Naithani

and Deleersnijder, 2004). Lake Tanganyika is one of the deepest stratified lakes of the world and is considered to be keeping the record of the past climate in its sediments. Due to the strong upwelling-productivity relationship, the knowledge of Kelvin waves may be important in the shoreline areas where fisheries are concentrated since this region of the lake is the major source of sediment-nutrient recycling during stratification [Horne and Goldman, 1994].

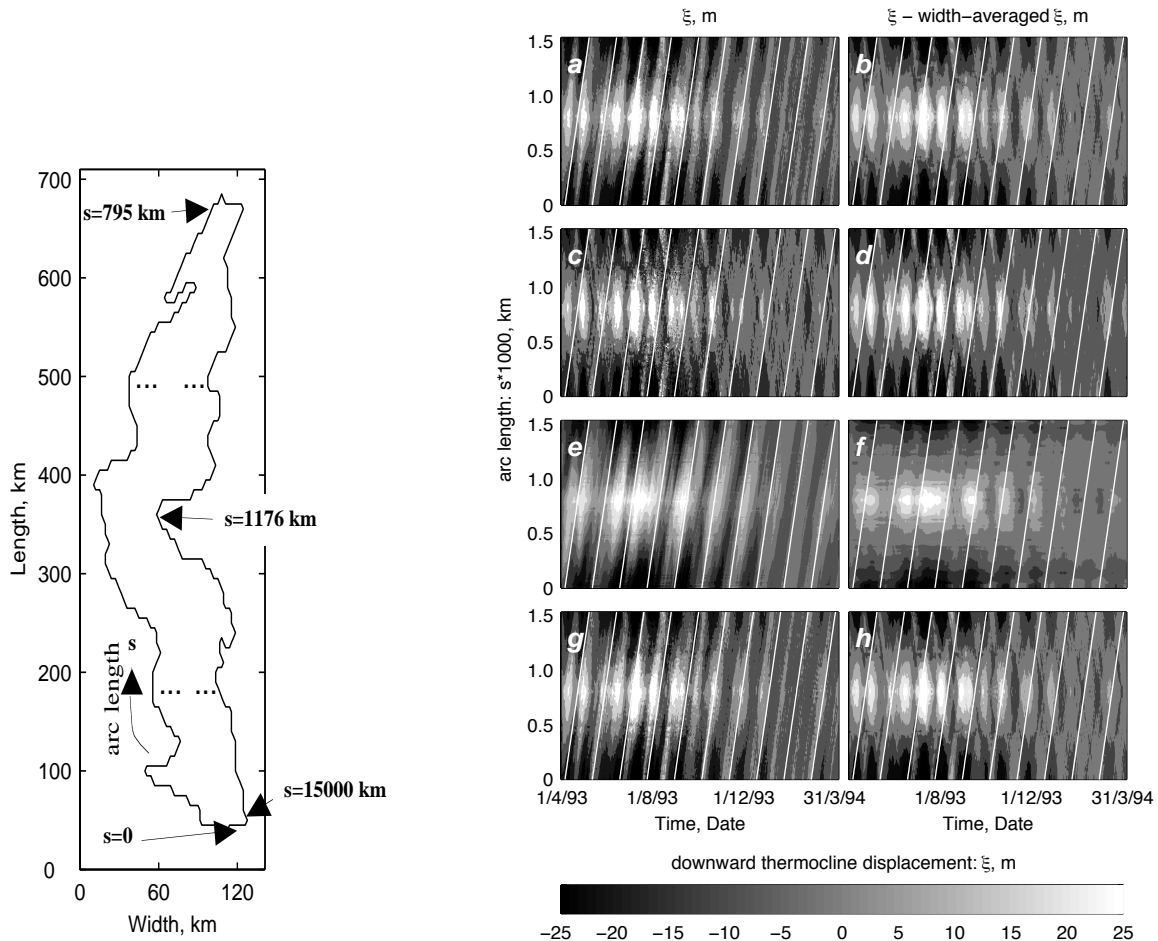


Figure 50: Model domain showing the arc length of the lake and the thermocline displacement at the shore vs time and arc length of the shore. a-b, actual lake position. c-d, Coriolis force = 0. e-f, lake shifted to 20°S. g-h, Coriolis force as 6°S for the whole lake. The white lines represent the slope equal to  $\sqrt{\epsilon gh}$ , the theoretical velocity of Kelvin waves.

### 3.3.5 Eco-Hydro Model

Here the hydrodynamic, thermodynamic and ecological processes are coupled to study the primary productivity of the Lake. The hydrodynamic sub-model in the Eco-Hydro model is the modified version of the non-linear, reduced-gravity model used in the above studies. Here we have included entrainment and detrainment terms. Hypolimnion water is entrained into the upper layer in the upwelling regions during strong winds, and is detrained in the downwelling regions. Model details can be found in Naithani *et.al*, (2005). The thermodynamic sub-model solves an ordinary

first-order differential equation for the temperature of the mixed layer. The ecological sub-model for the epilimnion comprises of three coupled, partial second-order differential equations of the diffusion type for nutrients, phytoplankton biomass and zooplankton biomass. The model takes into account the primary production and nutrient recycling in the mixed layer (Figure 51). It was calibrated using all available relevant measurements: phytoplankton and zooplankton biomass. The model details are given in appendix 1.

**Model Forcing**

The hydrodynamic model was initialized with wind forcing obtained from National Centre for Environmental Protection website (NCEP), given that there was no continuous wind velocity record from the two monitoring sites. The near surface wind data for 30°E, 7.5°S were used to calculate the two-components of the wind stress. The wind-stress was assumed to be uniform over the whole lake. Figure 52 show the time series plots of the horizontal wind, photosynthetically active radiation (PAR) and the surface wind-stress during 2002 and 2003.

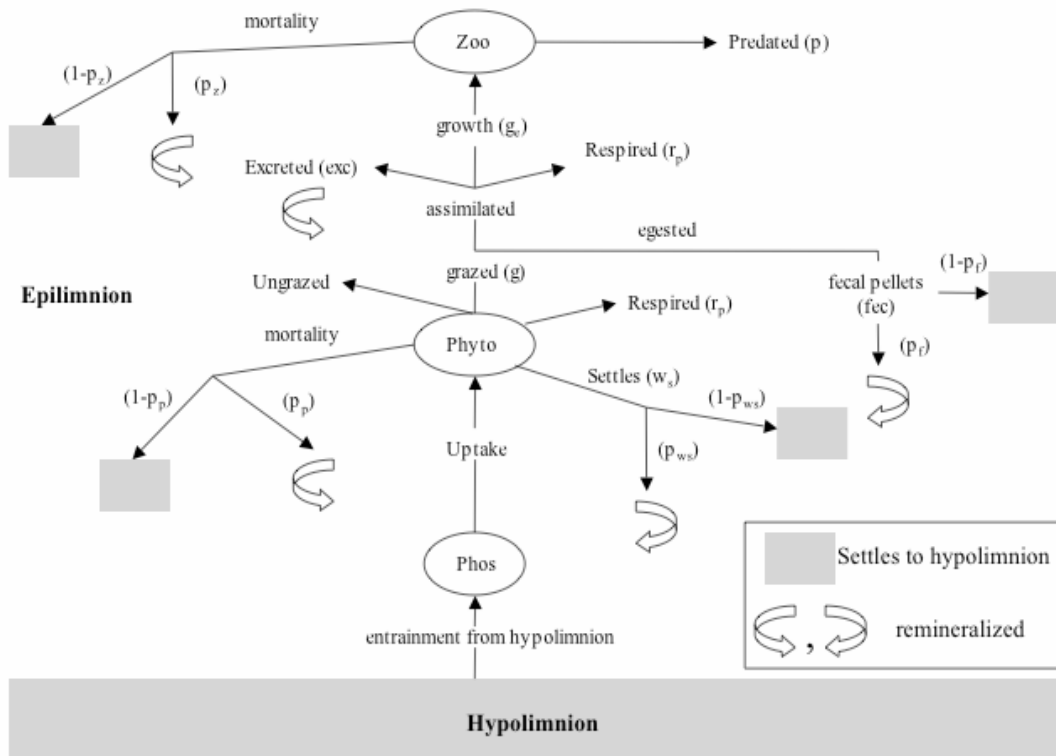


Figure. 51. Flow diagram of the ecological parameters considered in the model



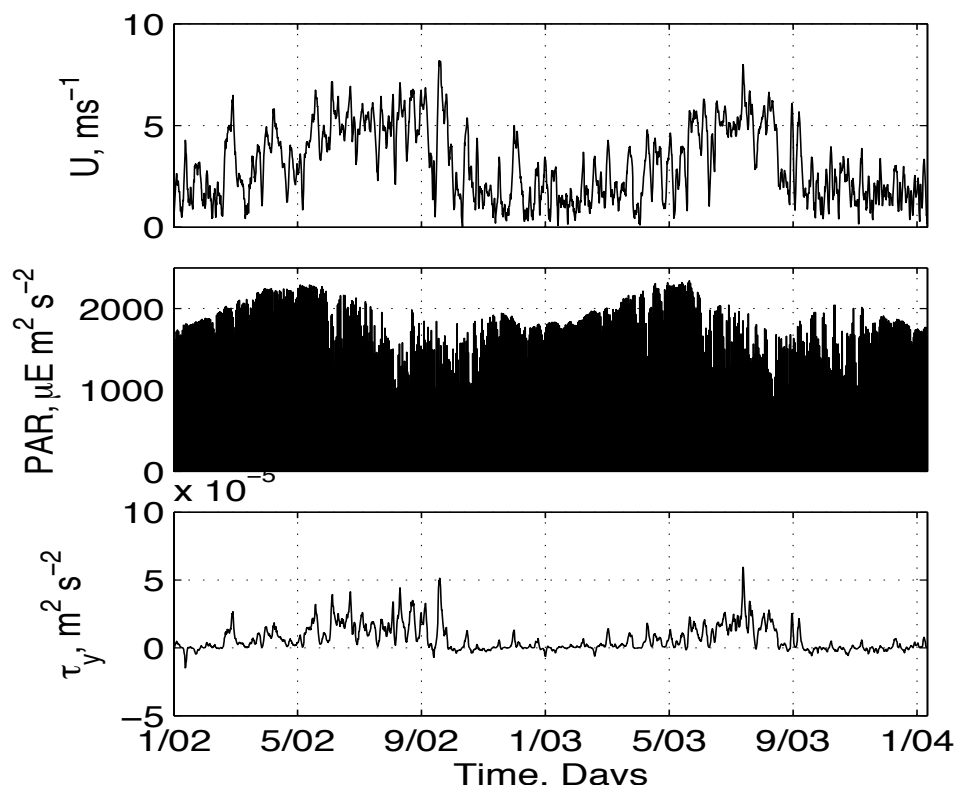


Fig. 52: Forcing variables of the ECO-HYDRO model: NCEP reanalysed horizontal wind speed, PAR and the y component of wind stress.

### **Model Simulations**

Figure 53 (a, b) shows the time series of observed and predicted mixed layer (epilimnion) depth, the depth-averaged concentration in the epilimnion of dissolved inorganic phosphorus, phytoplankton gross production, phytoplankton and zooplankton biomass off Mpulungu and Kigoma, respectively. The physical model simulated well the surface layer depth, its increase during the dry season and decrease at the end of it. The ecological model predicts well the increase of nutrients in the surface layer at the beginning of dry season and their decrease at the end. The model simulates satisfactorily the onset and the magnitude of the phytoplankton increase at the beginning of the dry season, the later resulting zooplankton bloom, as well as the plankton biomass decrease in the middle of the dry season and its second increase at the end of the dry season. The minimum values during the wet season are also well predicted by the model. Furthermore, the model reproduces well the north-south gradient in the magnitude of each variable. Given that the model includes only one nutrient and does not detail phytoplankton components at this stage, simulated variables show a reasonably good relation with the measurements or biomass estimates. The agreement between observations and simulations is better for Mpulungu, likely because measurements were more reliable.

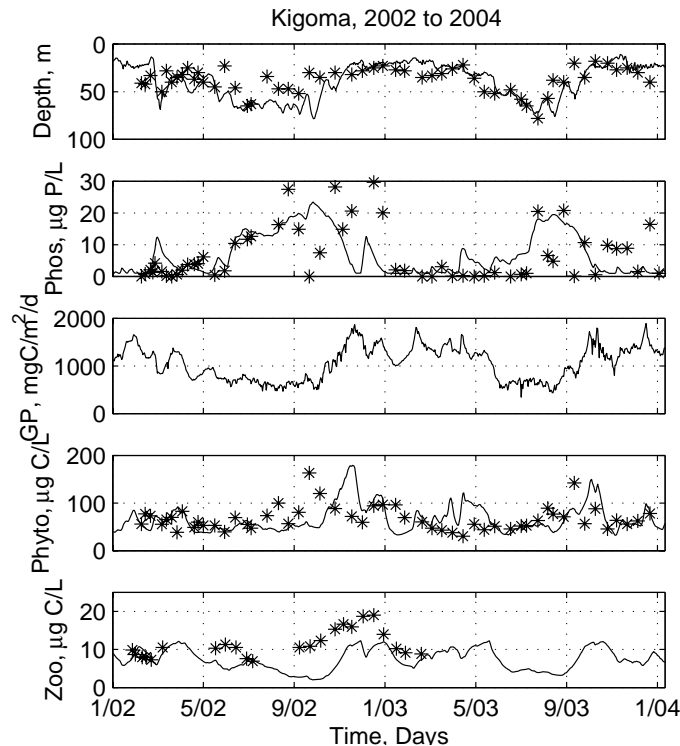


Figure 53a: Ecological model output of the depth of the surface layer and the depth averaged values of phosphorus, gross production, phytoplankton and zooplankton biomass in the surface layer off Kigoma. Measurements and biomass estimates are shown with stars.

The surface layer depth starts increasing at the beginning of the dry season because of the wind driven mixing and remain at greater depth during the whole season. It decreases at the end of the dry season and remain more or less at this depth during the wet season until the beginning of the next dry season. Phosphorus concentration starts increasing with the beginning of strong wind season due to upward entrainment of nutrients from below, remains high for the rest of the dry season because of almost continuous entrainment and decreases at the beginning of the wet season. Increase in the biomass of phytoplankton at the beginning of the dry season is natural because of the input of nutrients in the surface layer. However, the phytoplankton biomass cannot sustain at this high value and decreases in spite of the continuous abundance of nutrients. This is because of the increased depth of the surface layer; the phytoplankton is now subject to light-limitation. Phytoplankton biomass increases a little again at the end of the dry season when there are still enough nutrients and the surface layer depth is shallower. Phytoplankton biomass, though the main algal categories are not represented yet, seems to exhibit a very good compromising dependency on nutrient-limitation and light-limitation.

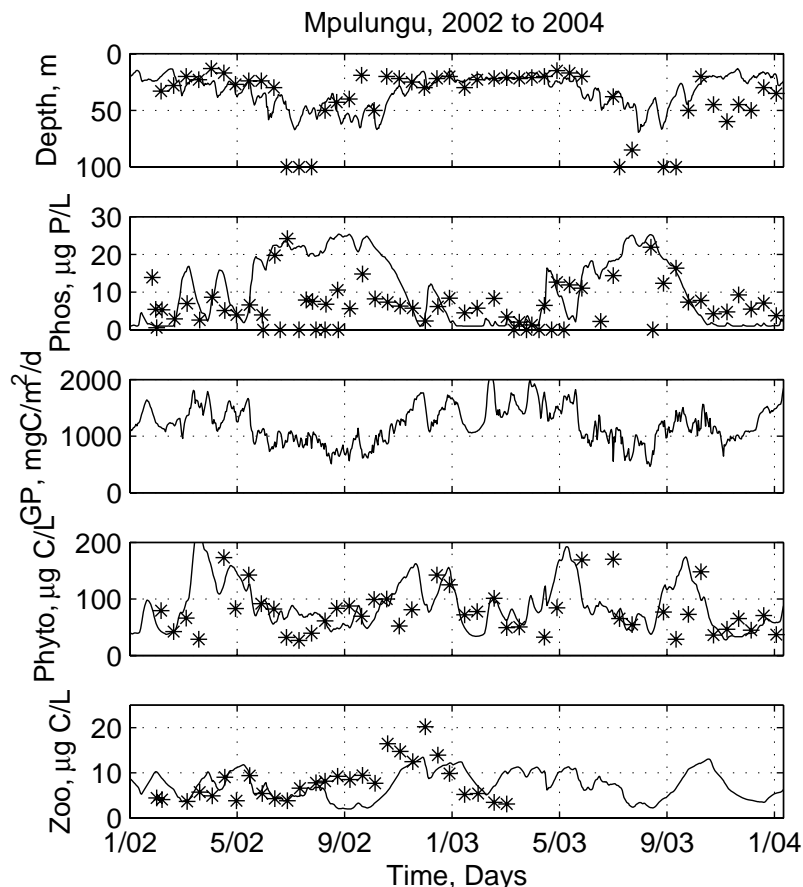


Figure 53b: Ecological model output of the depth of the surface layer and the depth averaged values of phosphorus, gross production, phytoplankton and zooplankton biomass in the surface layer off Mpulungu. Measurements and biomass estimates are shown with stars.

Numerical tests were performed for adjusting the half saturation constant for grazing and for the abundance zooplanktivorous fish. These tests indicate that the half saturation constant for grazing by zooplankton and predator abundance affect the zooplankton biomass measurably more than does phytoplankton biomass.

A simple ecological model coupled to a hydrodynamic model successfully predicted the dynamics of primary productivity in Lake Tanganyika; the agreement between observations and predictions is encouraging. The differences between simulations and observations can be attributed to a number of factors, including the fact that a uniform wind stress was assumed over the whole lake, and that nutrient inputs from rain and rivers were neglected. Despite the shortcomings of the model, the range of predicted plankton biomass is well in the range of observed data and the north-south contrast is correctly represented. Our results are in agreement with earlier studies indicating that Lake Tanganyika phytoplankton is confronted with restricted nutrient supply (Edmond *et.al* 1993; Hecky *et.al* 1993; Järvinen *et.al*, 1999). The estimate of primary productivity is within the range of values given by Hecky and Fee (1981),

Sarvala *et.al* (1999), Langenberg (2003b), and this study. Another interesting result from the sensitivity analyses is that the primary production, which strongly depends upon the light in the water column and entrainment of nutrients, is bottom-up controlled. Moreover, it seems that predator abundance strongly controls zooplankton biomass (top-down control). By contrast, fish predation influence seems quite reduced on the phytoplankton level. Indeed, in our simulations, reduced grazing pressure from top-down control of mesozooplankton did not increase phytoplankton abundance considerably. This should be, however, verified by further field studies on the actual grazing pressure exerted by mesozooplankton, and by surveys of fish populations accurate enough to provide estimates of predation by planktivorous fish.

### **3.3.6 Model Climatological Run**

The Eco-Hydro model run for the last 35 years was performed to study the impact of climate on the hydrodynamics and to some extent on the ecology of the lake. We cannot say for sure if these simulations represent the ecology of the lake since only our representation of phytoplankton is still very simple. Nevertheless, it is worth to study the climatic impact on this single algal component, described as having high light and relatively low phosphorus requirement. Figures 54 and 55 show the monthly and yearly averaged values of model forcings and predictions during 1970-2004. The year 1974 has lowest winds during this study period. Other minimum winds were observed in the years 1996 and 2003. During these years the nutrient supply to the upper layer was lower than during the rest of the years. In the year 1974, however, the productivity off Mpulungu was high and low off Kigoma. The high productivity off Mpulungu might be because the mixed layer depth was shallow during this year, implying more time spend by algal cells in light or euphotic layer. However, in the other two years the ecological productivity was low off Mpulungu. In the year 1986 and 2003 nutrients and the ecological parameters off Kigoma do not show any indication of lower than normal winds, except that phosphorus was low in the year 2003. In the year 1984, zooplankton biomass showed a decrease at both sites. However, phytoplankton biomass does not show any significant change from earlier years. During this year wind was higher and PAR was lower. Another, relatively high wind year was 2002, when phosphorus and phytoplankton biomass were high and zooplankton biomass lower than normal off both sites.

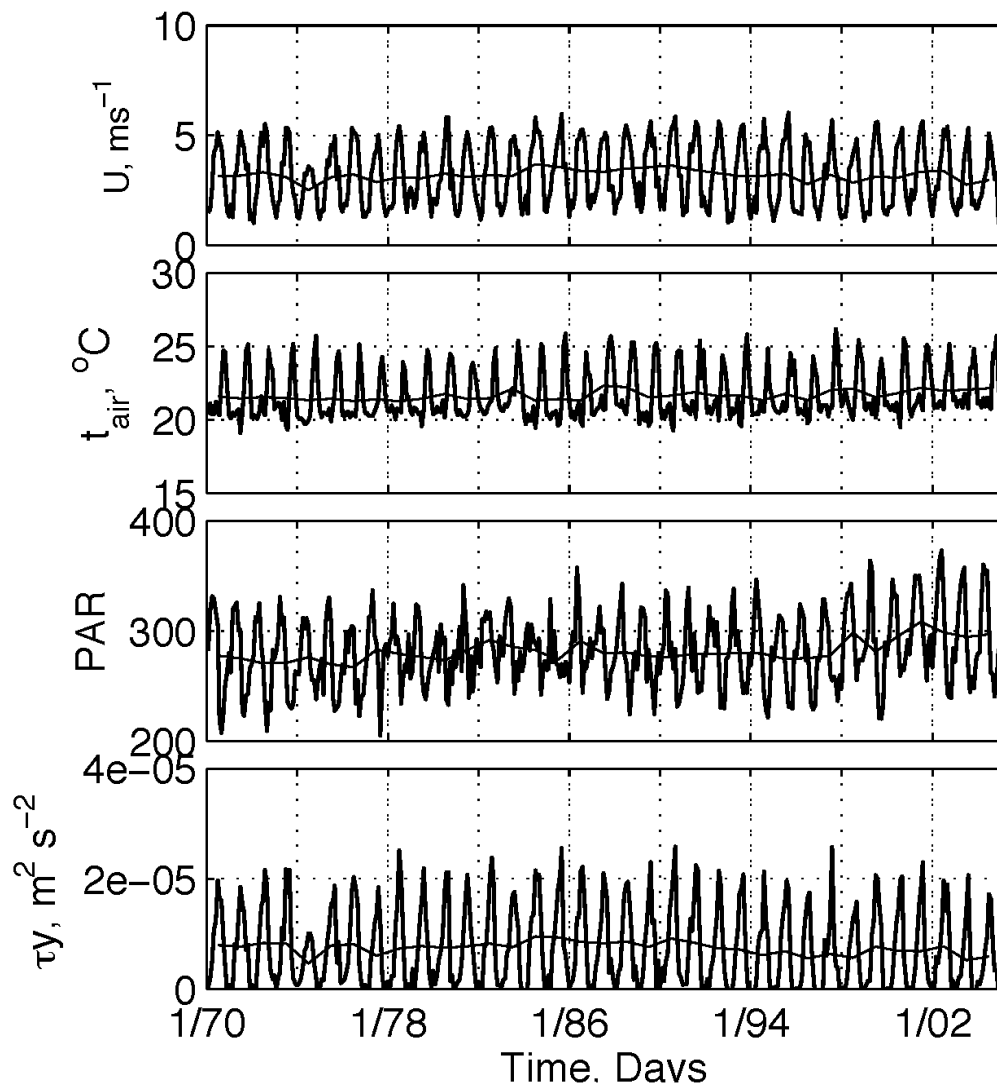


Figure 54: NCEP reanalysed monthly and yearly-averaged horizontal wind speed, air temperature, PAR and the y component of wind stress for the years 1970 to 2004.

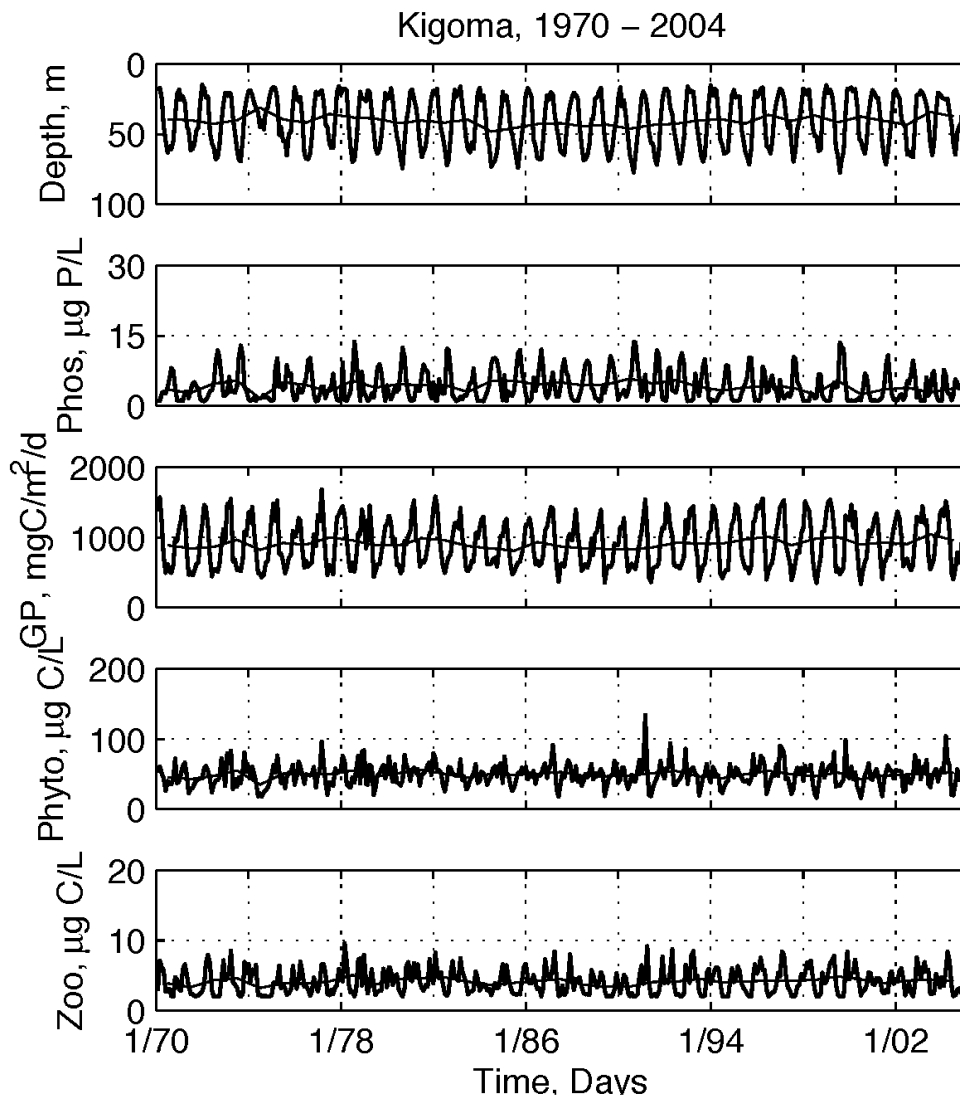


Figure 55a: Ecological model output of the monthly and yearly-averaged values of the depth of the surface layer and the depth averaged phosphorus, gross production, phytoplankton and zooplankton biomass in the surface layer off Kigoma for 1970 to 2004.

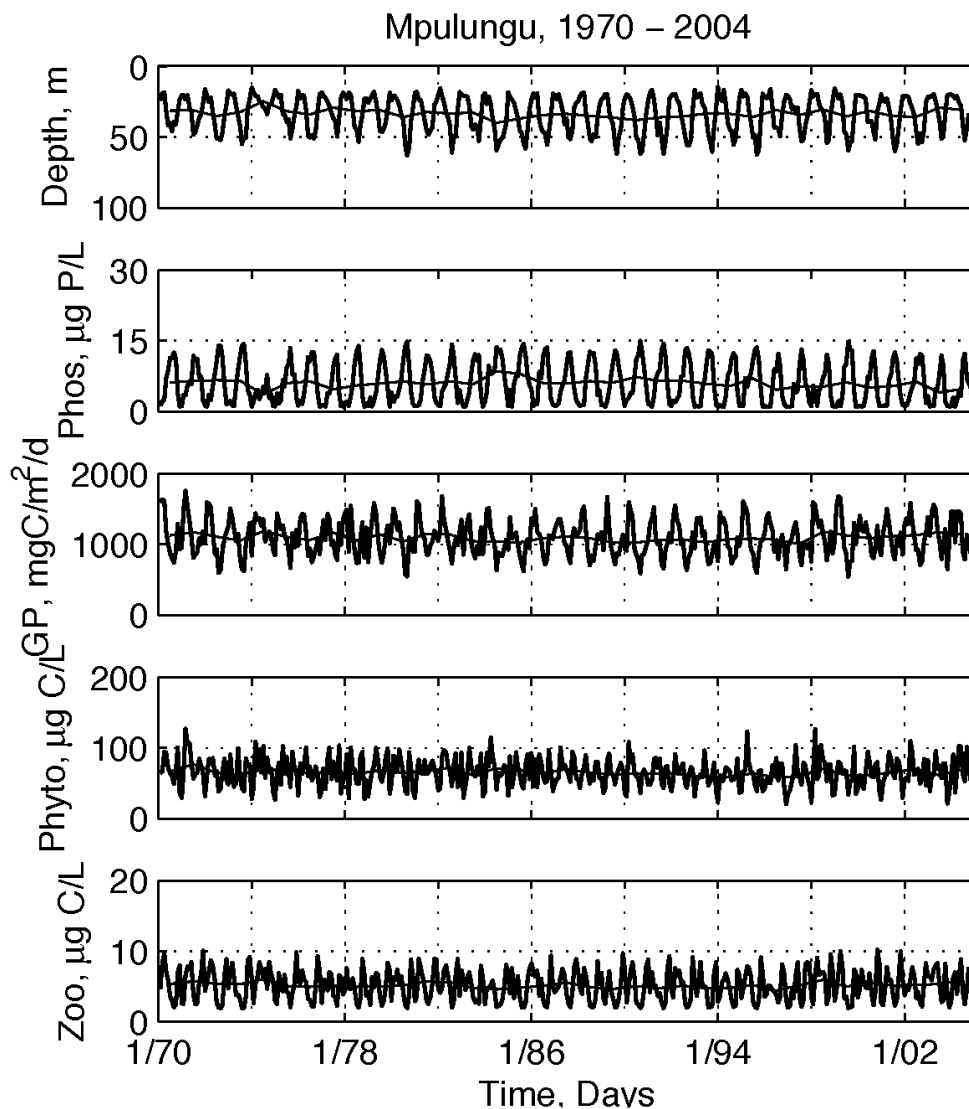


Figure 55b: Ecological model output of the monthly and yearly-averaged values of the depth of the surface layer and the depth averaged phosphorus, gross production, phytoplankton and zooplankton biomass in the surface layer off Mpulungu for 1970 to 2004.

In summary the biological productivity of Lake Tanganyika can be simulated by a simple non-linear, reduced-gravity model, which is forced by the climatological wind. Our present model consists of only one nutrient, one group of average phytoplankton and zooplankton, neglects the microbial loop and lacks a proper estimate of predator abundance. Despite these obvious shortcomings, it reproduces well a number of observations on seasonal and annual variation in the state variables. The model needs improvement by including several species of phytoplankton and zooplankton, as well as the microbial loop and fish dynamics. While this may improve the model robustness, this effort may be constrained by the lack of field data, and this clearly calls for further data acquisition on key ecological processes and communities.





## 4. DISCUSSION AND CONCLUSIONS

CLIMLAKE was primarily organised as a long-term survey of Lake Tanganyika, with the main objective of understanding the relationships between climate, regional weather, limnological variables, plankton and related ecological and (bio)geochemical processes. In addition the analysis of these relationships, the development of an eco-hydrodynamic model enabled to improve the understanding of the wind-driven limnological processes. The ecological modelling allowed putting together some of the results, in order to examine how lake productivity can be determined by weather variations at seasonal and interannual time scales. Here we review sequentially the main conclusions relevant to the different aspects of the study, and finally draw general conclusions and perspectives.

### 4.1 Meteorological and limnological variables

As already put forward in previous publications (*e.g.*, Plisnier & Coenen, 2001), the analysis of results of the three-year survey at two distant stations shows essentially two main types of environmental variability in the meteorological and the limnological variables: the seasonality and the interannual variability. In addition, at a smaller time scale, internal waves affect limnological and ecological variables. All three levels of environmental variability elicit different physical, chemical and biological responses. The seasonal pattern of variation is well documented for all variables at both stations, but variability is greater in the south of the lake, notably with the occurrence of the seasonal upwelling (Coulter, 1990, Plisnier et al, 1999) induced by the south-east winds during the dry season. North-south differences are, however, not limited to this phenomenon: at all times, the gradient of temperature gradient at the northern site was more marked than at the southern site, reflecting greater stability of the water column in the northern station. This resulted in differences in the depth of the mixed layer, a key variable determining nutrient availability and phytoplankton production, which is the sole source of organic carbon for the pelagic food web. Hence, clear differences were observed between the northern and southern parts of the lake with respect to nutrient concentrations and biomass of various plankton compartments (see below). This is largely confirmed by the results from the dry season cruises. Differences in stability of the water column and intensity of vertical mixing also affect the composition of the phytoplankton assemblage in several ways, for instance by promoting diatom development in the typical dry season condition (see below). This has clear implications for the interpretation of seasonality in the sediment record. Although the monitoring period was rather short (3 years), some significant interannual variability was observed. In particular, the dry season of 2003 was the

coldest, and the windiest of the studied period, with visible consequences on nutrient concentrations, chlorophyll *a* standing stock and primary production. This difference between 2002 and 2003 can be seen also from the observations from the dry season cruises. Internal waves are observed during the whole year in both stations, through the fluctuations of several limnological variables. They were particularly strong at two times of the year, when monsoon changes of direction occur: in September-October (monsoon change from SE to NE) and in April-May (from NE to SE). Following these periods the amplitude of internal waves increases, and is followed by a dampening as previous studies have shown (Plisnier & Coenen, 2001). These internal motions affect all the parameters of the water column particularly near the thermocline and sometimes up to the surface (such as during the upwelling). In this study, a detailed analysis and modelling of the FAO/FINNIDA lake temperature data was carried out (Naithani *et al.*, 2003), and allowed for a simulation of the thermocline tilting and oscillations that revealed the relative importance of the seasonal and intra-seasonal variability of the wind forcing (Naithani *et al.*, 2002, 2003, 2004).

## 4.2 Phytoplankton composition and biomass

For our northern station (Kigoma), phytoplankton data confirm observations from previous studies on Lake Tanganyika, but add new information about north-south differences, interannual variability and the overall importance of cyanobacteria. As in 1975 (Hecky & Kling, 1981) and 1998 (Vuorio *et al.*, 2003), phytoplankton in 2002-2004 comprised an assemblage dominated by chlorophytes and cyanobacteria in the rainy season, when stable stratification resulted in high light availability and low nutrients in the mixed layer. A difference with the 1975 survey is, however, the absence of chrysophytes, already noticed by Verburg *et al.* (2003). Diatoms increased in the dry season, presumably favoured by deep vertical mixing driven by south-east trade winds. These conditions resulted in a higher Zm: Zeu ratio which acted as a strong selective factor among planktonic algae (Reynolds, 1984, 1989) and may have led to light limitation of the pelagic primary producers when Zm greatly exceeded Zeu (Tilzer, 1990; Hecky, 1991). Phytoplankton able to cope with lower light may have benefited from improved nutrient availability, resulting from enhanced recycling in the deeper mixed layer and from upward entrainment of nutrients from the layers below the thermocline. Accordingly, total phytoplankton biomass increased in the dry season, mainly as a result of greater abundance of diatoms and green algae. From our results, it can be seen that diatoms are good indicators of the dry season conditions in the north basin, where they grow as well-defined blooms. At the southern station, however, diatoms increases were observed also in the rainy season, probably as a result of stronger thermocline oscillations and lower water

column stability, allowing occasional deeper mixing than in the “normal” rainy season conditions.

We also observed near-surface blooms of echinenone-containing cyanobacteria, which appear to correspond to the *Anabaena* blooms reported in several publications (Symoens, 1959; Hecky & Kling, 1981; Salonen *et.al*, 1999). The conditions which favoured these buoyant and nitrogen-fixing cyanobacteria were presumably greater availability of phosphorus, along with the shallower mixed layer and decreased inorganic nitrogen (Paerl, 1988; Oliver & Ganf, 2000; Reynolds, 1984, 1997). Movements of water linked to the tilting of the thermocline in the northern part of the lake may have favoured pulses of nutrients toward the epilimnion (Plisnier & Coenen, 2001), which were best exploited by phytoplankton with intracellular N and P-storage capacities such as filamentous cyanobacteria (Oliver & Ganf, 2000). However, as noted above, these large cyanobacteria were on average a minor component of the pelagic algal assemblage in terms of chlorophyll a biomass, compared to the cyanobacteria ‘T1’, which represented a consistent 31% mean contribution to total chlorophyll a at the northern station, and were present throughout the year. This changes substantially the picture drawn by Hecky & Kling (1981) who likely did not detect these smallest ‘algae’ (mainly picocyanobacteria), using inverted microscopy, although the *Synechococcus*-like picoplankton in Lake Tanganyika was recently reported by Vuorio *et.al* (2003), with abundances up to  $6 \times 10^5$  cells mL<sup>-1</sup>. Consequently, chlorophyte dominance in the northern basin (43% of chlorophyll a) is actually more pronounced than previously reported (Hecky & Kling, 1981: 40% of the phytoplankton biovolume).

At the southernmost station, Mpulungu, as well as in the whole southern basin (as shown by our cruise data), the phytoplankton assemblage was qualitatively similar but differed in the lower biomass of green algae and in the overall dominance of cyanobacteria T1. The success of small cyanobacteria in the wet season can be explained by higher light availability related to the high water transparency and to the shallower mixed layer characteristic of the rainy season in Lake Tanganyika, resulting in a Zm: Zeu ratio generally < 1. Such conditions, associated with low nutrients, are expected to favour small algal cells with high surface area: volume ratio, capable of fast nutrient uptake (Reynolds, 1997). According to the functional classification of Reynolds *et.al* (2002) and to other sources (*e.g.* Stockner, Callieri & Cronberg, 2000; Agawin *et.al*, 2000) prokaryotic picoplankton should be superior competitors in such conditions, encountered at Kigoma where stratification is permanent. However, the even greater importance of cyanobacteria T1 in the dry season in the south was rather unexpected. Indeed, diatoms developed during this period, but in similar amounts as in the north, while cyanobacteria T1 remained predominant. So, contrary to the expectations that deep mixing would bring about diatom dominance (Reynolds, 1984, 1989), it seems that the small cyanobacteria

were still the best adapted autotrophs to exploit the nutrient input from the upwelling and to develop even under reduced light availability. In culture experiments (Moore *et al.* 1995), *Synechococcus* cells presented remarkable capacities of acclimation to lower light by increasing their chlorophyll *a* and phycobilin content (increase of red and orange fluorescence as growth irradiance decreases). With such a large share of the phytoplankton biomass (and production), it is very likely that picocyanobacteria play a key role in the lake food web.

The analysis of phytoplankton by microscopy allowed identification of the algae at genus or species level, which is necessary for detailed ecological interpretation and for analysing possible changes over the past decades (Cocquyt, 2003; Cocquyt & Vyverman, *in press*). Also, this work helped updating the taxonomic list of algae of Lake Tanganyika, which involved the description of new species (Stoyneva *et al.*, *in print*). New additions to the taxonomic list of the lake are 21 genera and 56 species and infraspecific taxa (see appendix 2). The overall importance of picocyanobacteria and of small nanoplankton, particularly for the south of the lake, was verified by the counts at the epifluorescence microscope. The study of the ecology of planktonic diatoms present in the sediments was a clear focus of this algological study: in particular, the conditions in which two species of *Nitzschia* develop will be helpful for identifying the seasonal variations and possibly interannual variations in the past centuries. The composition of the present diatom assemblage, probably more so than total phytoplankton biomass (Verburg *et al.*, 2003), points to significant changes in environmental conditions in the lake, which are also evidenced by variations of dissolved silica in the lake over the past decades (see below). These changes may have resulted from increased surface temperature of the lake and reduced wind, as a result of the effect of climate change in this region of Africa, as suggested by several recent papers (Plisnier 2000; Livingstone, 2003; O'Reilly *et al.*, 2003, Verschuren, 2003; Verburg *et al.*, 2003).

### 4.3 Chlorophyll *a*

A direct comparison can be made between our chlorophyll *a* data from Kigoma in 2002 and those of Hecky & Kling (1981), who sampled over two transects (in May and October 1975). For the rainy season, our values of chlorophyll *a* are in the range reported by these authors for the offshore waters (mean 0.5 mg m<sup>-3</sup>). By contrast, in October 1975, Hecky & Kling observed higher concentrations (mean 4.6 mg m<sup>-3</sup>) than those we report here for the north basin (< 1 mg m<sup>-3</sup> in October 2002 and 2003). In the south, they measured 0.6 mg m<sup>-3</sup> on average, *i.e.* very close to the chlorophyll *a* concentration we measured at Mpulungu in October-November 2002 and 2003. The data from the LTR (Lake Tanganyika Research) project (Sarvala *et al.*, 1999; Salonen *et al.*, 1999; Langenberg *et al.*, 2002, 2003), from measurements at Kigoma

in the rainy season 1994 and during three cruises (April-May 1995; October-November 1995; November 1996) are in the same range as those of Hecky & Kling (1981), *i.e.* 0.1 – 4.5 mg chlorophyll *a* m<sup>-3</sup>, with the maxima in October-November. Again, there was a good correspondence as far as the minimal concentrations are concerned, but our maximal concentrations were lower (3.40 mg chlorophyll *a* m<sup>-3</sup> at Mpulungu; 1.96 at Kigoma) and were observed in the dry season (respectively in May and September 2003). The lower maximal chlorophyll *a* concentrations we observed may be due to differences in analytical techniques. HPLC measures pure chlorophyll *a*, without interference by other phorbins or degradation products, and several studies reported that HPLC gives lower values than spectrophotometric or fluorometric measurements (*e.g.* Meyns, Illi & Ribic, 1994). Another cause for discrepancies between our chlorophyll *a* data and those from previous studies lies in the distribution of algae in the water column, which is highly variable (see Descy *et al.*, 2005) and in the occurrence of well-defined surface blooms of filamentous cyanobacteria. It seems that the chlorophyll *a* maxima mentioned in the literature were measured when such surface blooms occurred, whereas we did not observe visible blooms in our study. However, by sampling every 10 m at a site of the north basin (TK3, February 2004; Fig. 9A) we detected a development of echinenone-containing cyanobacteria (notably *Anabaena* sp.) over the 0-30 m layer, at concentrations close to 1 mg chlorophyll *a* m<sup>-3</sup> (about 30 mg chlorophyll *a* m<sup>-2</sup>). If those algae had been concentrated in the 0-2.5 m layer, they would have represented about 12 mg m<sup>-3</sup> chlorophyll *a*, which is around the range of the maximum chlorophyll *a* found by Hecky & Kling (1981) and Salonen *et al.* (1999). For these two main reasons, involving differences in techniques and in sampling conditions, we believe that no conclusion should be drawn, from the pigment data available so far, about changes in phytoplankton biomass in Lake Tanganyika between 1975 and the present. In that case, the conclusion of decrease in phytoplankton biomass in the lake by Verburg *et al.* (2003), from comparison of recent phytoplankton counts with those available from the 1975 sampling off Kigoma by Hecky & Kling (1981), must be considered doubtful. Moreover, even though significant climate-induced changes may have occurred in Lake Tanganyika (Plisnier 2000; Livingstone, 2003; O'Reilly *et al.*, 2003, Verschuren, 2003; Verburg *et al.*, 2003), their impact on the lake plankton should be assessed from long time-series data rather than from short-term records. Even if compelling evidence of decreasing productivity over decades can be seen from carbon isotopes in the sediment (O'Reilly *et al.*, 2003), it may be too early to conclude that phytoplankton production changed as a result of warming of the lake from phytoplankton biomass estimates from a few samples (Verburg *et al.*, 2003). Interannual variability in weather pattern and lake hydrodynamics can be high, and only monitoring of phytoplankton composition, biomass and production over long periods of time, and at several sites

to account for spatial variation, allow proper assessment of relative effects of short- and long-term environmental variability on this community.

#### 4.4 Primary production

Daily rates of primary production are usually the lowest in the rainy season, as a result of low phytoplankton biomass and, for Kigoma, of lower light-saturated rate of photosynthesis. Our minimal primary production data ( $< 0.2 \text{ g C m}^{-2} \text{ d}^{-1}$ ) are the lowest ever reported for Lake Tanganyika, but our maximal values, measured in the dry season are in the same range as those measured by Hecky *et al.* (1981) at the same season in 1975. The LTR project (Sarvala *et al.*, 1999), although a slightly different method was used, reported daily photosynthesis in the same range for the same sites as our monitoring sites. By contrast, estimates of annual production from these two previous studies are higher than ours:  $400 \text{ g C m}^{-2} \text{ y}^{-1}$  (Hecky *et al.*, 1981) and  $426 - 662 \text{ g C m}^{-2} \text{ y}^{-1}$  (Sarvala *et al.*, 1999), compared to our range of  $130 - 224 \text{ g C m}^{-2} \text{ y}^{-1}$ . However, the estimates of the two previous studies are whole-lake averages including the more productive Bujumbura basin and, in the case of the 1975 data, a high chlorophyll event, which did not occur at the same scale during our study. In addition, Hecky *et al.* (1981) estimated Lake Tanganyika net production at  $290 \text{ g C m}^{-2} \text{ y}^{-1}$ , which is closer to our annual production in Mpulungu in 2003. For all these reasons, comparisons based on direct measurements are not conclusive, because of probable large interannual variability and of methodological differences. From a dynamic point of view, phytoplankton production responded well to changes in limnological and nutritional conditions, with usually low production in the rainy season and high production in the dry season. This increased algal production is reflected by increased zooplankton production, which tends to occur at the end of the rainy season. However, more variability can be observed at the southernmost station, where increases of primary production may occur even in the rainy season. This pattern is to be related to internal waves, which favour nutrient transport through the thermocline and to windy events that induce deeper mixing, hence greater nutrient availability.

#### 4.5 Importance of heterotrophic plankton

Another important result of the CLIMLAKE study is that, for assessing the productivity of lake, production of heterotrophic plankton has to be taken into account. Indeed, in Lake Tanganyika, the components of the microbial food web are a substantial part of the biomass available to consumers. It has been shown that bacteria and heterotrophic protists, which are able to exploit the organic matter from phytoplankton excretion and lysis over the entire oxic zone, may approach and even exceed phytoplankton biomass (Pirlot *et al.*, 2005). The trophic role of these organisms was

already envisioned by Hecky *et.al* (1981), who estimated bacteria biomass and ciliate abundance, and came up with the hypothesis that heterotrophic production may supplement autotrophic production, thereby explaining mesozooplankton abundance and high fish yield in an oligotrophic system. Being coupled to phytoplankton photosynthetic production, the development of heterotrophs is ultimately dependent on the same environmental factors that drive primary production, and therefore subject to the influence of climate variability.

#### **4.6 Geochemistry of the water column**

Geochemical studies conducted in the past in Lake Tanganyika (Degens *et.al*, 1971; Craig, 1974; Edmond *et.al*, 1993; Branchu, 2001) have observed the compartment of some elements monitored in this work. Yet, the multi-elemental approach on very deep water profiles and long term monitoring performed in the northern and southern basin have improved our knowledge of the chemistry of this lake. The geochemical signature of the lake has been mainly stable, according to the scarce information available. A major finding was to demonstrate a lack of evidence of significant recent inputs of hydrothermally-derived juvenile components in the deep water chemistry in both north and south basins, although some still unexplained geochemical anomalies were detected at depth (below 750m). Redox sensitive elements present strong features due to the well known anoxia of the lake below 200 m. Strong upwelling events occurring in the south tend to influence both the particulate and dissolved geochemical signature compared to the north.

#### **4.7 Mollusk shells as geochemical archives of hydrological changes**

Detailed analysis of the bivalve *Pleiodon spekii* shells have shown that high-resolution profiles of Mn, Sr and  $\delta^{18}\text{O}$  exhibit cyclic variations, similar in all shells analysed. Both environmental and biological factors may have an influence on chemical record contained in the shell.

High-resolution profiles of Mn could provide a detailed record of short-term environmental changes linked with recent or past mixing events in Lake Tanganyika but also in other deep stratified African lakes where an upwelling tuned by monsoon regime occurs. Our results support the idea that paleo-environment researches could benefit from geochemical analysis of recent and well preserved fossils of *P. spekii*.

By contrast, the Sr and  $\delta^{18}\text{O}$  profiles in shells show cyclic variations that are not correlated with the composition or the temperature variations in lake surface waters.  $\delta^{18}\text{O}$  and Sr are mostly controlled by biological activity, which hampers their direct use as temperature proxies. However, they might provide critical data to describe changes in the thermal amplitude.

#### 4.8 Si concentration and Si isotopes

The recently demonstrated warming trend of Tanganyika surface waters (Plisnier, 1997, 2000; O'Reilly *et.al* 2003) has clearly influenced the Si cycle as evidenced by the historical increase in the lake surface water Si concentrations recently published (Verburg *et.al* 2003). The present study confirmed this evolution with mean surface dissolved Si of  $32 \pm 8 \mu\text{mol L}^{-1}$  in both basins, amongst the highest ever reported values. Although historical data may underestimate some regional and seasonal variability, they clearly show a significant (threefold) increase between the 1938-1975 period ( $9.5 \pm 4.6 \mu\text{mol L}^{-1}$ ) and the year 2000 ( $27.3 \pm 2 \mu\text{mol L}^{-1}$ ) (99% confidence level on a t-test). Adding our values collected in 2002-2003 brings the mean 2000-2003 dissolved Si to  $31 \pm 11 \mu\text{mol L}^{-1}$ .

A new methodology for measuring Si isotopes has been developed (Cardinal *et.al*, 2003) to better constrain the recent climate changes in the Si cycle. There has been no evidence of dramatic annual changes in silica loading by tributaries in recent years, although large seasonal changes in both Si river inputs and in the source of dissolved river silica have been clearly demonstrated by our silicon isotopic data (see Alleman *et.al*, 2005). Thus, Verburg *et.al* (2003) considered the Si-cycle evolution to mainly reflect a lower diatom activity due to a decreasing phosphorus and nitrate availability. This lower productivity is linked to a 30-year period of diminishing exchange rate with deep water (higher density gradient and stratification) triggered by a warming trend and less wind (O'Reilly *et.al* 2003).

A declining nutrient-bearing deep water exposure in the mixed layer should translate into an increase of the dissolved silicon and a probable decrease in average  $\delta^{29}\text{Si}$  signatures of both surface waters and falling diatom frustules. The long term evolution should be recorded in the deep water Si isotopic compositions. Indeed, the high Si content of deep waters is generally explained by a gradual dissolution of biogenic opal settling along the water column, favoured by microbial activity, high pH and temperature. This statement is strongly supported by our recent Si isotopic results. The rather heavy silicon isotopic signature of deep water ( $\delta^{29}\text{Si} = 0.61 \pm 0.05\text{‰}$ ) clearly rules out any significant inputs of juvenile magmatic-derived hydrothermal silica which bears a typically light signature ( $\delta^{29}\text{Si} = -0.3\text{‰}$ , André *et.al*, submitted). Therefore, the  $\delta^{29}\text{Si}$  signatures of deep water must record the dissolution-integrated signal of past diatom cells over a time scale corresponding to the residence time of dissolved Si (*i.e.*, a few hundred years, Branchu 2001). The large silicon isotopic differences between the 2002 surface diatoms ( $0.28 \pm 0.12\text{‰}$ ) and both silicicline ( $0.69 \pm 0.07\text{‰}$ ) and deep water ( $0.61 \pm 0.05\text{‰}$ ) may therefore point to a modern lowering of diatom Si utilization compared to the recent past (Alleman *et.al*, 2005). This discrepancy can also be assessed by correlating the dissolved  $\delta^{29}\text{Si}$  with  $\ln[\text{Si}(\text{OH})_4]$  measured in deep waters below 200m ( $y = -0.14x + 1.42$  ( $n = 19$ )),



displaying a fair  $r^2$  value (0.63). The slope (-0.14) estimates the mean offset between the sinking biogenic opal and the dissolved Si in surrounding waters (De La Rocha *et.al* 2000). Subtracting this offset from the upwelled waters signature in the silicicline ( $0.69 \pm 0.07\text{‰}$ ) should be representative of the biogenic opal  $\delta^{29}\text{Si}$  produced in the past ( $0.55 \pm 0.07\text{‰}$ ), which strongly contrasts with the modern ones ( $0.28 \pm 0.12\text{‰}$ ). This difference underlines the non steady state Si cycle of the lake, and is therefore well in accordance with diminishing trend of diatom relative Si consumption in recent years, supporting the Verburg *et.al* (2003) hypothesis. This should be conclusively confirmed by looking at  $\delta^{29}\text{Si}$  signature variations in the upper top sedimentary record. Our Si isotopic data on Lake Tanganyika tributaries are very consistent with the data measured on a worldwide scale. The rather good positive correlation between  $\delta^{29}\text{Si}$  and dissolved Si concentrations is tentatively explained as a mixing curve resulting from contrasted weathering of two major soil components: crustal-derived rocks or clays and phytoliths. Ongoing studies on silicon isotope fractionations by phytoliths and clays (*e.g.* Opfergelt *et al* 2004) should better constrain this hypothesis. These first silicon isotopic determinations in freshwater and biogenic opal of Lake Tanganyika confirm the fractionation process previously evidenced on marine diatoms. It gives further support to the non species-specific, non-temperature dependent character of the silicon isotope fractionation by diatoms. Because of the fast response of  $\delta^{29}\text{Si}$  in siliceous organisms to climate variability, nutrient dynamics and limnological changes, this isotopic tool may help to corroborate the recent decline of diatom Si utilization in Lake Tanganyika. For instance,  $\delta^{29}\text{Si}$  may be used to constrain such a secular trend, by comparing the isotopic signatures of present-day diatoms to their counterparts from the last centuries preserved in the uppermost part of the lake sedimentary column. That should be an objective for future work.

#### 4.9 Modelling

A hydrodynamic model has been developed to study the thermocline oscillations. The model is based on non-linear, reduced-gravity equations in which wind is the dominant forcing variable (Naithani *et.al*, 2003). Internal oscillations are rather well reproduced. In using a reduced-gravity model, one assumes that the density stratification is much more important in determining the internal oscillations than the underlying bottom topography. In Lake Tanganyika, it is appropriate to have recourse to such a model since stratification is present all year round and the depth of the surface layer is generally much smaller than the thickness of the hypolimnion. The model was used to explore the effect of wind forcing on thermocline tilting and oscillations in the lake, and for simulating the physical environment in which ecological processes take place. The presence of internal Kelvin waves was

suggested by the model (Naithani & Deleersnijder, 2004), a finding that is in sharp contrast with previous theoretical predictions.

The ecological model, coupled to the hydrodynamic model, successfully predicted the dynamics of primary productivity in Lake Tanganyika; the agreement between observations and predictions is encouraging. The differences between simulations and observations can be attributed to a number of factors, including the fact that a uniform wind stress was assumed over the whole lake, and that nutrient inputs from rain and rivers were neglected. The range of predicted plankton biomass is well in the range of observed data and the north-south contrast is correctly represented. Our results are in agreement with earlier studies indicating that Lake Tanganyika phytoplankton is confronted with restricted nutrient supply (Edmond *et.al* 1993; Hecky *et.al* 1993; Järvinen *et.al*, 1999). The estimate of primary productivity is within the range of values given by Hecky and Fee (1981), Sarvala *et.al* (1999), Langenberg (2003b), and this study. Another interesting result from the sensitivity analyses is that the primary production, which strongly depends upon the light in the water column and entrainment of nutrients, is bottom-up controlled. Moreover, it seems that predator abundance strongly controls zooplankton biomass (top-down control). By contrast, fish predation influence seems quite reduced on the phytoplankton level. Indeed, in our simulations, reduced grazing pressure from top-down control of mesozooplankton did not increase phytoplankton abundance considerably. This should be, however, verified by further field studies on the actual grazing pressure exerted by mesozooplankton, and by surveys of fish populations accurate enough to provide estimates of predation by planktivorous fish.

In order to explore the sensitivity of primary productivity of Lake Tanganyika to climate variability, we ran a simulation for the past 35 years, using NCEP wind and incident light. The simulations demonstrate the potential of such a model for exploring past variations of the lake productivity in a context of climate change. However, owing to the relative simplicity of the ecological model and the quality of the forcing variables, we consider these results with caution, and suggest different directions for further implementation

#### **4.10 Perspectives**

Some future directions can be indicated from the conclusions of the CLIMLAKE study. First, CLIMLAKE has highlighted the interest of a long-term survey of limnological and planktological variables. Continued monitoring has been partially ensured by the ongoing CLIMFISH project (which runs in the field until beginning of 2006), which also exploits more fully the potential of remote sensing data for whole-lake monitoring of temperature and chlorophyll a. However, there is a clear need for implementing other field and laboratory studies in several areas, in order to

understand further the impacts of recent climate changes on the lake ecosystem functioning

#### **4.11 The microbial food web**

Of particular interest is the study of the relationships within the food web which may highlight the role of the microbial loop in nutrient cycling and in the production of mesozooplankton and pelagic fishes. Data have been acquired allowing estimation of the biomass of the planktonic communities (bacteria, phytoplankton, protozoa, and mesozooplankton) and of algal and bacteria production. Parallel studies have shown the whole-lake importance of bacteria and picocyanobacteria with different counting techniques, and have approached the diversity of these microorganisms using molecular techniques. However, despite some of our studies have addressed the demand of organic carbon by bacteria, and the grazing of bacteria by protozoans, everything remains to be done for assessing the different transfer pathways of primary production to the higher consumers. The fact that the biomass of planktonic heterotrophs may exceed that of autotrophs indicates that autotrophic production is transferred to microorganisms quite efficiently, through different processes providing DOM to heterotrophic bacteria (phytoplankton excretion and mortality, and sloppy feeding), but also by grazing of autotrophic picoplankton by protozoans. So, exploring the microbial food web and microbial diversity should be a major component of further studies designed to understand the processes which govern productivity in Lake Tanganyika.

#### **4.12 Biogeochemical cycles of nutrients**

Some of the results presented here and other studies have shown that classic macro-nutrient limitation of phytoplankton growth may occur in Lake Tanganyika, but bio-assays suggest that Fe limitation should be important. This calls for investigations of Fe speciation in the surface and intermediate waters, and of nutrient (Si, N, and P) cycles (uptake, recycling from organic matter decay and zooplankton excretion) and of their stoichiometry and fate within the planktonic compartment. Such studies may include field and laboratory work on cultures, as well as of the particulate nutrient export to the deep waters, using sediment traps. Here, collaboration with Prof. T.C. Johnson (Large Lakes Observatory, University of Minnesota Duluth, USA) has been already developed with a sediment trap deployment project in the south of the lake. This collaboration would be particularly promising to study the fate of particulate nutrient, including silicon, *i.e.* for assessing the part which is regenerated in the mixed layer vs. that which is exported to the anoxic waters and possibly to the sediment. This of course hold promise for following diatom sedimentation and

dissolution of the siliceous walls, which is needed to understand the transfer of the increased production of the dry season to the sediment record.

#### **4.13 Model development and forcing**

The development of predictive models, which is clearly a challenge for a system as large and complex as Lake Tanganyika, will help to understand the determinism behind the correlation between ENSO, lake ecology and fisheries. Hopefully, once the eco-hydrodynamic model will be coupled with local and regional climate models, it could be used to strengthen fisheries management, taking into account climate change in this part of the world, where aquatic resources are essential. A robust model needs good data as input and for calibration and validation, and prediction of future situation obviously depend on the coupling of the ECO-HYDRO model with a regional atmospheric climate model. In the CLIMLAKE study, in the absence of proper meteorological and astronomical data the use was made of NCEP data, which were easily available through web. However, these data were not available for the lake coordinates. After comparison with the observations available for 2 m level from April 1993 to March 1994 from the FAO/FINNIDA project, NCEP data for 7.5°S; 30°E were chosen. FAO/FINNIDA data was used in the earlier published work to study the lake hydrodynamics.

The present ecological model relies on over 20 parameters. Most of them (like half saturation constants for grazing and predation, mortality rates and the percentages of organic matter to be remineralized) were decided according to literature values and by running model iterations. This greatly delayed the process of model development. In future we plan to include several species of phytoplankton and zooplankton, as well as the microbial loop. While this may improve the model robustness, this effort may be constrained by the lack of field data, and this clearly calls for further data acquisition on key ecological processes and communities.

In the model that is presently used, to allow for entrainment of hypolimnion water and, hence, nutrients into the epilimnion, a rather crude parameterisation is resorted to. The parameterisation of detrainment is even more uncertain. As there is not much hope to improve significantly these parameterisations, it is believed that a model that would not suffer from such drawbacks should be implemented, *i.e.* a fully three-dimensional model including an appropriate turbulence closure scheme that would be able to simulate both the epilimnion and a relevant fraction of hypolimnion — leaving aside the lowest part of the latter for which there is almost no data. If the lower boundary of such a model is sufficiently deep, there is little doubt that the settling flux — toward the lake bottom — could be fairly well simulated.

## 5. ACKNOWLEDGMENTS

The CLIMLAKE project is funded by the Belgian federal Science Policy Office.

CLIMLAKE thanks Dr G. Demarée of the Royal Meteorological Institute of Belgium and Mrs C. Mertens of the Federal Council for Sustainable Development for their appreciated participation to the follow-up committee of the CLIMLAKE project.

The participation of Mrs M. Vanderstraeten of the Belgian federal Science Policy Office as an observer of the follow-up committee of the CLIMLAKE project is greatly acknowledged here also.

Eric Deleersnijder is a Research Associate with the Belgian National Fund for Scientific Research (FNRS).

Samuel Pirlot, Stéphane Sténuite and Aaike de Wever benefited from a research grant, from FRIA and IWT, Belgium.

Prof. Maya Stoyneva, from the Sofia University, Dept. Botany, Bulgaria, benefited from a research fellowship at UGent, financed by the Belgian federal Science Policy Office.

We are grateful to Dr Yves Cornet, University of Liège and François Donnay, for the work on the acquisition of surface water temperature of Lake Tanganyika by remote sensing.

We thank the FAO/FINNIDA project GCP/RAF/271/FIN for the data used in the first phase of the modelling study.

Sincere thanks are due to Eric Wolanski for his constant help and suggestions throughout the course of this project.

We thank the NYANZA-project (Prof. Andy Cohen, Dr Kiram Lezzar, Dr Elinor Michel, Dr Catherine O'Reilly) for its technical cooperation in the Kigoma station and for its help chartering "Maman Benita".

Sincere thanks to Dr Bernhard Wheri and Mr Christian Dinkel (EAWAG) for the excellent collaboration during the sampling cruises.

Our warmest thanks are also addressed to the chief Mazombo, Mr Mupape and the crew of the "Maman Benita", for their very much appreciated collaboration.

We thank Pascal Isumbisho, from ISP/Bukavu (R.D.Congo), for his participation in the 2002 sampling cruise.



## 6. LIST OF PUBLICATIONS RELATED TO THE PROJECT

- Alleman L.Y., D. Cardinal, C. Cocquyt C., P.-D. Plisnier, J.-P. Descy, I. Kimirei, D. Sinyinza & L. André. Silicon isotopic fractionation in Lake Tanganyika and its main tributaries. *Journal of Great Lakes Research*, *in press*.
- Cardinal D., L.Y. Alleman, J. de Jong, K. Ziegler & L. André, 2003. Isotopic composition of silicon measured by multicollector plasma source mass spectrometry in dry plasma mode. *Journal Analytical Atomic Spectrometry*, 18: 213-218.
- CLIMLAKE, 2002. CLIMLAKE (2002-2004). Limnological monitoring. Field and Laboratory Manual. [www.sciences.fundp.ac.be/biologie/urbo/climlake.html](http://www.sciences.fundp.ac.be/biologie/urbo/climlake.html).
- Cocquyt C., 2001. Notes on *Cymatopleura calcarata* Hustedt (Bacillariophyceae), an endemic diatom from Lake Tanganyika. In: Lange-Bertalot-Festschrift Studies on Diatoms, pp. 177-186.
- Cocquyt C., 2002. Het Tanganyika-meer: Paleolimnologische studie van de laatste 1000 jaar. *Diatomededelingen* 26, 14-17.
- Cocquyt C., 2003. *Amphora calumeticoides* spec. nov. (Bacillariophyta), an endemic diatom from Lake Tanganyika. *Journal of Great Lakes Research* 29, 581-587.
- Cocquyt C., 2003. Diatomeeëngemeenschappen uit de pelagische en litorale zone van het Tanganyikameer. *Bull. Séanc. Acad. R. Sci. Outre-Mer*, 49: 457-470.
- Cocquyt C. & Y. Israël, 2004. A microtome for sectioning lake sediment cores on a very high resolution. *J. Paleolimnol.* 32: 301-304.
- Cocquyt C., E. Verleyen, A. De Wever, P.-D. Plisnier & W. Vyverman. Seasonal succession of diatom communities in Lake Tanganyika and its potential to track past short-term climate change. To be submitted.
- Cocquyt C. & W. Vyverman. Phytoplankton in Lake Tanganyika: a comparison of community composition and biomass off Kigoma with previous studies 27 years ago. *Journal of Great Lakes Research*, accepted.
- Deleersnijder E., J.-M. Beckers & E.J.M. Delhez, 2005a, The residence time of settling particles in the surface mixed layer, *Environmental Fluid Mechanics*, submitted.
- Deleersnijder E., J.-P. Descy, J. Naithani, P.-D. Plisnier & E. Wolanski, 2005b. A numerical study of free and forced thermocline oscillations in Lake Tanganyika, *Environmental Fluid Mechanics*, to be submitted.
- Descy, J.-P. & V. Gosselain (eds.), 2004. CLIMLAKE progress report 2002. Presses Universitaires de Namur, 73 p.

- Descy, J.-P., M.-A. Hardy, S. Sténuite, S. Pirlot, B. Leporcq, I. Kimirei, B. Sekadende, S.R. Mwaitega & D. Sinyenza, 2005. Phytoplankton pigments and community composition in Lake Tanganyika. *Freshwater Biology*, 50(4): 668-684.
- Descy, J.-P., B. Leporcq, M.-A. Hardy, S. Pirlot, S. Sténuite, I. Kimirei, B. Sekadende, S.R. Mwaitega & D. Sinyenza. Le phytoplancton du Lac Tanganyika: une vision par l'analyse des pigments algaux. *Bull. Séanc. Acad. R. Sci. Outre-Mer*, submitted.
- Descy, J.-P., P.-D. Plisnier, L. Andre, L. Alleman, D. Chitamwebwa, C. Cocquyt, E. Deleersnijder, I. Kimrei, J. Naithani, H. Phiri, D. Sinyenza & W. Vyverman, 2002. Climate Variability as recorded in Lake Tanganyika (CLIMLAKE). *Bulletin of the International Decade for the East African Lakes*, Summer 2002: 7-8.
- De Wever, A., K. Muylaert, S. Pirlot, K. Van der Gucht, C. Cocquyt, J.-P. Descy, P.-D. Plisnier & W. Vyverman. Vertical and horizontal heterogeneity in bacterial community composition in Lake Tanganyika. *Applied and Environmental Microbiology*, *in press*.
- Naithani J., F. Darchambeau, E. Deleersnijder, J.-P. Descy & E. Wolanski, 2005, Study of the nutrient and plankton dynamics in Lake Tanganyika using a reduced-gravity model. *Ecological Modelling*, to be submitted.
- Naithani J. & E. Deleersnijder, 2004. Are there internal Kelvin waves in Lake Tanganyika? *Geophysical Research Letters*, 31, doi: 10.1029/2003GL019156
- Naithani J., E. Deleersnijder & P.-D. Plisnier, 2002. Origin of intraseasonal variability in Lake Tanganyika. *Geophysical Research Letters*, 29:2093
- Naithani J., E. Deleersnijder & P.-D. Plisnier, 2003. Analysis of wind-induced thermocline oscillations of Lake Tanganyika. *Environmental Fluid Mechanics*, 3: 23-39
- Naithani J., E. Deleersnijder, P.-D. Plisnier & S. Legrand, 2004. Preliminary results of a reduced-gravity model of the wind-induced oscillations of the thermocline in Lake Tanganyika. In: Demarée, G., M. De Dapper & J. Alexandre (eds.), *Proceedings of the Second International Conference on Tropical Climatology, Meteorology and Hydrology*. Royal Meteorological Institute of Belgium and Royal Academy of Overseas Sciences of Belgium, pp. 27-40.
- O'Reilly, C. M., S R. Alin, P. -D. . Plisnier, A.S. Cohen and B.A. Mckee 2003. Climate change decreases aquatic ecosystem productivity of Lake Tanganyika, Africa. *Nature*, 424: 766-768.
- O'Reilly, C. M., P. -D. Plisnier, A. S. Cohen & S. R. Alin, 2004. Ecology: Climate-change effect on Lake Tanganyika? (reply) *Nature* (15 July 2004); doi:10.1038/Nature 02737



- Pirlot S., J. Vanderheyden, J.-P. Descy & P. Servais, 2005. Abundance and biomass of heterotrophic micro-organisms in Lake Tanganyika. *Freshwater Biology*, 50 (6): 1219-1232.
- Plisnier P.D, 2002. Limnological profiles and their variability in Lake Tanganyika. In: Odada, E. & D.O. Olago (eds.), *The East African Great Lakes: Limnology, Palaeoclimatology and Biodiversity*, Kluwer, Dordrecht, pp. 349-366.
- Plisnier P.-D., 2004. Probable impact of global warming and ENSO on Lake Tanganyika. *Bull. Séanc. Acad. r.Sci. Outre-Mer*, 50: 185-196
- Plisnier P.-D. & E.J. Coenen, 2001. Pulsed and dampened annual limnological fluctuations in Lake Tanganyika. In: Munawar, M.H. & R.E. Hecky (eds.), *The Great Lakes of the World (GLOW): food-web, health and integrity*, Backhuys, Leiden, pp. 83-96.
- Stoyneva, M. P., G. Gaertner, C. Cocquyt & W. Vyverman. *Closteriopsis petkovii* n. sp. - a new green alga from Lake Tanganyika. – *Phyton.*, *in press*.
- Stoyneva M., G. Gärtner, C. Cocquyt & W. Vyverman. *Eremosphaera tanganyikae* n.sp. (Trebouxiophyceae) - a new species from Lake Tanganyika. *Belgian Journal of Botany*, *in press*.
- Stoyneva M., C. Cocquyt, G. Gärtner & W. Vyverman. *Oocystis lacustris* Chod. (Chlorophyta, Trebouxiophyceae) and related species from Lake Tanganyika (Africa) with comments on their taxonomy and general morphology. *Cryptogamie Algologie*, submitted.

**Website CLIMLAKE**

**[http://www.fundp.ac.be/recherche/projets/page\\_view/03275101/](http://www.fundp.ac.be/recherche/projets/page_view/03275101/)**



## 7. REFERENCES

- A.P.H.A. 1992. Standard methods for the examination of water and wastewater (eds. A.E. Greenberg, L.S. Clesceri & A.D. Eaton). American Public Health Association, New York, U.S.A.
- Branchu P., 2001. Cycle des éléments majeurs et traces dans les grands lacs de rift tropicaux (lacs Tanganyika et Malawi), processus et enregistrements biogéochimiques. MRAC, Tervuren, Belgique, Annales - Sciences Géologiques, 106.
- Cardinal, D., L.Y. Alleman, F. Dehairs, N. Savoye, T.W. Trull & L. André. 2005. Relevance of silicon isotopes to Si-nutrient utilization and Si source assessment in Antarctic waters. *Global Biogeochem. Cycles*, doi:10.1029/2004GB002364.
- Chitamwebwa D.B.R., 1999. Meromixis, stratification and internal waves in Kigoma waters of Lake Tanganyika. *Hydrobiologia*, 407: 59-64.
- Cocquyt C., 1998. Diatoms from the northern basin of Lake Tanganyika. *Bibliotheca Diatomologica* 39: 276 pp.
- Conley D. J., 2002. Terrestrial ecosystems and the global biogeochemical silica cycle. *Global Biogeochem. Cycles*, 16: 1121.
- Craig H.D.F., V. Craig, J. Edmond & G. Coulter, 1974. Lake Tanganyika geochemical and hydrographic study: 1973 expedition. Publication Scripps Institution of Oceanography Series 75, 5: 1-83.
- Degens E. T., Von Herzen R. P. & H. K. Wong, 1971. Lake Tanganyika: water chemistry, sediments, geologic structure. *Naturwissenschaften*, 58: 229-240.
- De La Rocha, C. L., Brzezinski, M. A., & M. J. Deniro, 1997. Fractionation of silicon isotopes by marine diatoms during biogenic silica formation. *Geochim. Cosmochim. Acta* 61: 5051-5056.
- De La Rocha C. L., M. A. Brzezinski & M. J. Deniro, 2000. A first look at the distribution of the stable isotopes of silicon in natural waters. *Geochimica Cosmochimica Acta*, 64: 2467-2477.
- Descy J.-P., H.W. Higgins, D.J. Mackey, J.P. Hurley & T.M. Frost, 2000. Pigment ratios and phytoplankton assessment in northern Wisconsin lakes. *J. Phycol.*, 36: 274-286.
- Ding T. Jiang S., Wang D., Li Y., Li J., Song H., Liu Z. & X. Lao, 1996. Silicon isotopes. *Geochemistry*, Geological Publishing House, Beijing.

- Ding T., D. Wan, C. Wang, & F. Zhang, 2004. Silicon isotope compositions of dissolved silicon and suspended matter in the Yangtze River. China. *Geochim. Cosmochim. Acta*, 68: 205-216.
- Droesbeke J.-J., 2001. *Eléments de statistiques*. Ed. Univ. Bruxelles, Ellipse, 550 pp.
- Edmond J. M., R.F. Stallard, H. Craig, V. Craig & R. F. Weiss, 1993. Nutrient chemistry of the water column of Lake Tanganyika. *Limnol. Oceanogr.*, 38: 725-738.
- Epstein S., R. Buchsbaum, H.A. Lowenstam & H. Urey, 1953. Revised carbonate-water isotopic temperature scale. *Geol. Soc. Am. Bull.*, 64: 1315-1326.
- Fuhrman J.A. & F. Azam, 1980. Bacterioplankton secondary production estimates for coastal waters of British Columbia Antarctica and California. *Appl. Environ. Microbiol.*, 39: 1085-1095.
- Fuhrman J.A. & F. Azam, 1982. Thymidine incorporation as a measure of heterotrophic bacterioplankton production in marine surface waters: evaluation and field results. *Mar. Biol.*, 66: 109-120.
- Geitler, L. 1932: *Cyanophyceae*. Leipzig.
- Gillikin D.P., A. Lorrain, J. Navez, J.W. Taylor, L. André, E. Keppens, W. Baeyens & F. Dehair, 2005. Strong biological controls on Sr/Ca ratios in aragonitic marine bivalve shells. *Geochem. Geophys. Geosyst.*, 6: Q05009, doi:10.1029/2004GC000874
- Gillikin D.P., H. Ulens, F. De Ridder, E. Keppens, W. Baeyens & F. Dehairs. Assessing the reproductibility and reliability of an estuarine bivalve (*Saxidomus giganteus*) for sea surface temperature reconstruction: implications for palaeoclimate studies. *Palaeogeogr. Palaeoclimatol. Palaeoecol.*, *in press*.
- Guilford S.J. & R.E. Hecky, 2000. Total nitrogen, total phosphorus, and nutrient limitation in lakes and oceans: Is there a common relationship? *Limnol. Oceanogr.*, 45 (6): 1213-1223..
- Healey F.P. & L.L. Hendzel, 1979. Indicators of phosphorus and nitrogen deficiency in five algae in culture. *J. Fish. Res. Board. Can.*, 36: 1364-1369.
- Hecky R.E., R.H. Spigel & G. W. Coulter, 1991. The nutrient regime, p 76-89. In: Coulter G.W. (ed.), *Lake Tanganyika and its life*. British Museum and Oxford University Press.
- Hecky R.E., E.J. Fee, H.J. Kling & J.W. Rudd, 1978. Studies on the planktonic ecology of Lake Tanganyika. Canadian Department of Fish and Environment. Fisheries and Marine Service Technical Report, 816: 1-51.

- Hillebrand H., C.D. Durselen, D. Kirschtel, U. Pollinger & T. Zohary, 1999. Biovolume calculation for pelagic and benthic microalgae. *Journal of Phycology*, 35 (2): 403-424.
- Jeffree R.A., S.J. Markich, F. Lefebvre, M. Thellier & C. Ripoll, 1995. Shell microlaminations of the freshwater bivalve *Hyridella depressa* as an archival monitor of manganese water concentration: experimental investigation by depth profiling using secondary ion mass spectrometry. *Experientia*, 51: 838-848.
- Kilham P., S.S. Kilham & R.E. Hecky, 1986. Hypothesized resource relationships among African planktonic diatoms. *Limnol. Oceanogr.*, 31(6): 1169-1181.
- Komárek J. & B. Fott, 1983. Chlorophyceae (Grünalgen) Ordnung: Chlorococcales. In: *Das Phytoplankton des Süßwassers*, 7 (1): 1-1044.
- Kurki H., I. Vuorinen, E. Bosma & D. Bwebwa, 1999. Spatial and temporal changes in copepod zooplankton communities of Lake Tanganyika. *Hydrobiologia*, 407: 105–114.
- Langenberg, V. T., S. Nyamushahu, R. Roijackers & A. A. Koelmans, 2003. External nutrient sources for Lake Tanganyika. *Journal of the Great Lakes Research*, 29: 169-180.
- Livingstone D.A., 2003. Global climate change strikes a tropical lake. *Science*, 301: 468-469.
- Maclsaac, E. & J. Stockner, 1993. Enumeration of phototrophic picoplankton by autofluorescence microscopy. p.187-197. In: Kemp P.F., B.F. Sherr, E.B. Sherr & J.J. Cole (eds.), *Handbook of methods in aquatic microbial ecology*. Lewis Publ., Boca Raton.
- Mackey M.D., D.J. Mackey, H.W. Higgins & S.W. Wright, 1996. CHEMTAX - a program for estimating class abundances from chemical markers: application to HPLC measurements of phytoplankton. *Mar. Ecol. Progr. Ser.*, 144: 265-283.
- Montagnes, D.J.S. & D.H. Lynn, 1993. A quantitative protargol stain (QPS) for ciliates and other protists. In: Kemp, P.F., B.F. Sherr, E.B. Sherr & J.J. Cole (eds.), *Aquatic Microbial Ecology*. Lewis Publishers, Boca Raton. Ch. 27, pp. 229-240.
- Opfergelt, S., D. Cardinal, C. Henriot, B. Delvaux & L. André, 2004. Silicon Isotope Fractionation by Banana Under Continuous Nutrient and Silica Flux. *Eos Trans. AGU*, 85: 47, Fall Meet. Suppl., Abstract V51A-0520.
- O'Reilly, C. M., S.R. Alin, P.-D. Plisnier, A.S. Cohen & B. A. McKee, 2003. Climate change decreases aquatic ecosystem productivity of Lake Tanganyika, Africa. *Nature*, 424: 766-768.

- Pandolfini E., I. Thys, B. Leporcq & J.-P. Descy, 2000. Grazing experiments with two freshwater zooplankters: fate of chlorophyll and carotenoid pigments. *Journal of Plankton Research*, 22: 305-319.
- Plisnier P.-D., 1997. Climate, limnology and fisheries changes of Lake Tanganyika. *FAO/FINNIDA Research for the Management of the Fisheries on Lake Tanganyika GCP/RAF/271/FIN-TD/73(En)*, 50 p.
- Plisnier P.D. 2000. Recent climate and limnology changes in Lake Tanganyika, *Verh. Internat. Verein. Limnol.*, 27: 2670-2673.
- Plisnier P.-D., D. Chitamwebwa, L. Mwape, K. Tshibangu, V. Langenberg & E. Coenen, 1999. Limnological annual cycle inferred from physical-chemical fluctuations at three stations of Lake Tanganyika. *Hydrobiologia*, 407: 45-58.
- Plisnier P.-D., S. Serneels & E.F. Lambin, 2000. Impact of ENSO on East African ecosystems: a multivariate analysis based on climate and remote sensing data. *Global Ecology & Biogeography*, 9: 481-497.
- Sarvala J., K. Salonen, M. Järvinen, E. Aro, T. Huttula, P. Kotilainen, H. Kurki, V. Langenberg, P. Mannini, A. Peltonen, P.-D. Plisnier, I. Vuorinen, H. Mölsä & O.V. Lindqvist, 1999. Trophic structure of Lake Tanganyika: carbon flows in the pelagic food web. *Hydrobiologia*, 407: 140-173.
- Sherr E.B. & B.F. Sherr, 1993. Preservation and storage of samples for enumeration of heterotrophic protists. p. 207-212, In: Kemp P.F., B.F. Sherr, E.B. Sherr & J.J. Cole (eds.), *Current Methods in Aquatic Microbial Ecology*, Lewis Publ., NY.
- Siegele R., I. Orlic, D.D. Cohen, S.J. Markich & R.A. Jeffree, 2001. Manganese profiles in freshwater mussel shells. *Nuclear Instruments and Methods in Physics research, B* 181:593-597.
- Simpson J. H., P. B. Tett, M. L. Argoteespinosa, A. Edwards, K. J. Jones, & G. Savidge, 1982. Mixing and phytoplankton growth around an island in a stratified sea. *Cont. Shelf Res.*, 1: 15-31.
- Starmach K. 1985. *Chrysophyceae und Haptophyceae*. Gustav Fischer Verlag, Stuttgart-New York.
- Stecher H.A., D.E. Krantz, C.J. Lord III, G.W. Luther III. & K.W. Bock, 1996. Profiles of strontium and barium in *Mercenaria mercenaria* and *Spisula solidissima* shells. *Geochimica et Cosmochimica Acta*, 60: 3445-3456.
- Steemann Nielsen E. 1972. The rate of primary production and the size of the standing stock of zooplankton in the oceans. *Internationale Revue der Gesamte Hydrobiologie*, 57: 513-516.
- Uthermöhl H., 1931. Neue Wege in der quantitativen Erfassung des Planktonts. *Verh. Int. Verein. Theor. Angew. Limnol.*, 5: 567.

- Van Meel L., 1954. Le phytoplancton. Expl hydrobiologique du lac Tanganyika - Institut Royal des Sciences Naturelles de Belgique. Résultats scientifiques, 4 (1): 80 p.
- Verburg P., R.E. Hecky & H. Kling, 2003. Ecological consequences of a century of warming in Lake Tanganyika. *Science*, 301: 505-507.
- Verschuren D., 2003. The heat on Lake Tanganyika. *Nature*, 424: 731-732.
- Vollenweider RA., 1965. Calculation models of photosynthesis-depth curves and some implications regarding day rate estimates in primary production measurements. *Mem. Ist. Ital. Idrobiol.*, 18: 425-457.





## 8. APPENDIX

### Appendix 1: Eco-hydrodynamic model of Lake Tanganyika

The model consists of a hydrodynamic component, thermodynamic component and an ecological module.

#### **Hydrodynamic sub-model:**

The hydrodynamic sub-model is the modified version of the non-linear, two-layer, reduced-gravity model developed for Lake Tanganyika and used in earlier studies (Naithani, *et.al* 2002; 2003; Naithani and Deleersnijder, 2004). Here we have included entrainment and detrainment terms. Hypolimnion water is entrained into the upper layer in the upwelling regions during strong winds, and is detrained in the downwelling regions. The epilimnion water budget equation is:

$$\frac{\partial \xi}{\partial t} + \frac{\partial(Hu)}{\partial x} + \frac{\partial(Hv)}{\partial y} = w_e \quad (1)$$

where  $x$  and  $y$  are horizontal axes,  $u$  and  $v$  are the depth integrated velocity components in the surface layer in the  $x$  and  $y$  directions,  $t$  is the time,  $\xi$  is the downward displacement of the thermocline,  $H = h + \xi$  is the thickness of the epilimnion (the surface, well-mixed layer),  $h$  is the reference depth of the upper layer ( $m$ ) and  $w_e$  is the entrainment velocity ( $ms^{-1}$ ) defined as:

$$w_e = \left(\frac{3}{20}\right)^{1/2} \frac{(\tau_x^2 + \tau_y^2)^{1/2}}{(\varepsilon g H)^{1/2}} - w_d - \frac{\xi}{r_{tt}} \quad (2)$$

where the first term on the right hand side of Eq. 2 is inspired by Price (1979),  $\tau_x$  and  $\tau_y$  are horizontal components of specific wind stress in  $x$  and  $y$  direction ( $m^2s^{-2}$ ),  $\varepsilon = (\rho_b - \rho_s)/\rho_b$ , is the relative density difference between the hypolimnion ( $\rho_b$ ) and the epilimnion ( $\rho_s$ ) respectively,  $w_d$  is the detrainment term ( $ms^{-1}$ ).  $w_d$  is defined such that the annual mean of the epilimnion volume remains approximately constant. There are large uncertainties in the parameterization of entrainment and detrainment terms. As a consequence, to avoid occasional occurrence of spurious values of  $\xi$ , a relaxation term ( $\xi/r_{tt}$ ) is needed which slowly nudges the upper layer depth toward its equilibrium position. The relaxation timescale,  $r_{tt}$ , is sufficiently long so that the relaxation term is generally smaller than the entrainment and detrainment terms.  $w_e$  is positive (negative) in the upwelling (downwelling) regions where water is entrained into (detrained from) the upper layer.

The momentum equations are:

$$\frac{\partial(Hu)}{\partial t} + \frac{\partial(Huu)}{\partial x} + \frac{\partial(Hvu)}{\partial y} - fHv = -gH \frac{\partial \varepsilon \xi}{\partial x} + \frac{\partial}{\partial x} \left( HA_x \frac{\partial u}{\partial x} \right) + \frac{\partial}{\partial y} \left( HA_y \frac{\partial u}{\partial y} \right) + \frac{\tau_x}{\rho_0} + w_e^- u \quad (3)$$

$$\frac{\partial(Hv)}{\partial t} + \frac{\partial(Huv)}{\partial x} + \frac{\partial(Hvv)}{\partial y} + fHu = -gH \frac{\partial \varepsilon \xi}{\partial y} + \frac{\partial}{\partial x} \left( HA_x \frac{\partial v}{\partial x} \right) + \frac{\partial}{\partial y} \left( HA_y \frac{\partial v}{\partial y} \right) + \frac{\tau_y}{\rho_0} + w_e^- v \quad (4)$$

where  $f$  is the Coriolis factor ( $<0$  in the southern hemisphere),  $A_s$  is the horizontal eddy viscosity in the  $s$  ( $=x,y$ ) direction,  $w_e^- = \frac{w_e - |w_e|}{2}$  is the negative part of the entrainment velocity, *i.e.*  $w_e^-$  is equal to  $w_e$  if  $w_e < 0$  and is zero otherwise. Below, use will be made of the positive part of the entrainment velocity, which is defined as  $w_e^+ = \frac{w_e + |w_e|}{2}$ .

### **Thermodynamic sub-model**

The surface layer temperature is predicted using the equation:

$$\frac{\partial(H\theta)}{\partial t} + \frac{\partial(Hu\theta)}{\partial x} + \frac{\partial(Hv\theta)}{\partial y} = \frac{\partial}{\partial x} \left( HK_x \frac{\partial \theta}{\partial x} \right) + \frac{\partial}{\partial y} \left( HK_y \frac{\partial \theta}{\partial y} \right) + w_e^+ \theta_h + w_e^- \theta + H \frac{(\theta_s - \theta)}{r_{ts}}$$

where  $\theta$  is the surface layer temperature,  $\theta_s$  is the reference temperature of the surface layer,  $\theta_h$  is the temperature of the hypolimnion water and  $r_{ts}$  is the relaxation time scale for surface fluxes.

### **Ecological sub-model**

The ecological sub-model (Figure 2) simulates nutrient fluxes between dissolved inorganic pools and a simplified 3-compartment trophic chain (phytoplankton – herbivorous zooplankton – planktivorous fish). Fluxes of carbon (C) and phosphorus (P) are modeled. Each scalar variable  $X$  (nutrients, phytoplankton and zooplankton) is modelled using the conservation equation:

$$\frac{\partial(HX)}{\partial t} + \frac{\partial(HuX)}{\partial x} + \frac{\partial(HvX)}{\partial y} = H(G-D)_X + \frac{\partial}{\partial x} \left( HK_x \frac{\partial X}{\partial x} \right) + \frac{\partial}{\partial y} \left( HK_y \frac{\partial X}{\partial y} \right) + \phi_{he} \quad (5)$$

$$\phi_{he} = w_e^+ X_h + w_e^- X \quad (6)$$

where  $X$  is the concentration of the respective ecological parameter in the epilimnion,  $(G-D)_X$  is the growth/destruction term for the corresponding variable ( $X$ ),  $K_s$  is the horizontal eddy diffusivity in the  $s$  ( $=x,y$ ) direction,  $\phi_{he}$  is the flux of  $X$  from the hypolimnion to the epilimnion,  $X_h$  is the value of  $X$  in the hypolimnion and vice-versa.

*Phytoplankton:* The source/sink term for the phytoplankton carbon biomass evolution is:

$$(G-D)_{Phyto} = (\mu - r_p - m_p - w_s) Phyto - grZoo \quad (7)$$

where *Phyto* is the phytoplankton carbon biomass ( $\mu\text{gC/L}$ ),  $\mu$  is the daily growth rate ( $d^{-1}$ ),  $r_p$  is the loss due to respiration ( $d^{-1}$ ),  $m_p$  is the mortality loss ( $d^{-1}$ ),  $w_s$  is the settling rate ( $md^{-1}$ ),  $gr$  is the loss due to grazing by zooplankton ( $d^{-1}$ ) and *Zoo* is the zooplankton carbon biomass ( $\mu\text{gC/L}$ ). The phytoplankton daily growth rate is:

$$\mu = \mu_{\max} f(P) \quad (8)$$

where  $\mu_{max}=2P_{max}f(I)$  is the maximum photosynthetic production,  $P_{max}$  is the maximum carbon-specific photosynthetic rate,  $f(I)$  is the light limitation factor and  $f(P)$  is the phosphorus limitation factor.  $F(P)$  is defined according to Michaelis and Menten kinetics:

$$f(P) = Phos / (Phos + k_{phos}) \quad (9)$$

where  $Phos$  is the concentration of the dissolved phosphate ( $\mu gP/L$ ) and  $k_{phos}$  is the half saturation constant for growth.

The light limitation is defined as:

$$f(I) = (1/k_e H) [\arctan(I_0/2I_k) - \arctan(I_0 e^{-k_e H/2I_k})] \quad (10)$$

where  $k_e = 0.07 Phyto/100 + 0.077$  is the extinction coefficient based on field data,  $I_k$  is the light saturation constant and  $I_0$  is the solar insolation reaching the surface of the lake or the photosynthetically active radiation (PAR). Gross production, GP is defined as:

$$GP = 2P_{max} f(I) z_{eu} Phyto \quad (11)$$

where  $z_{eu} = 4.6/k_e$  is the euphotic depth.

The grazing rate,  $gr$  is defined as:

$$gr = g_{max} \text{ as } Phyto \rightarrow ILL \quad (12a)$$

$$gr = g_{max} \frac{(Phyto)}{(Phyto + k_{phyto})} \text{ for } Phyto > Phyto_{min} \quad (12b)$$

$$gr = 0 \text{ for } Phyto \leq Phyto_{min} \quad (12c)$$

where  $g_{max}$  is the maximum grazing rate per day,  $ILL$  is the incipient limiting level,  $Phyto_{min}$  is the threshold below which zooplankton do not graze and  $k_{phyto}$  is half-saturation constant for grazing.

**Zooplankton:** The source/sink term for the zooplankton carbon biomass evolution is:

$$(G - D)_{Zoo} = \mu_z \cdot Zoo - m_z - pF \quad (13)$$

where  $Zoo$  is the zooplankton carbon biomass ( $\mu gC/L$ ),  $\mu_z$  is the daily growth rate,  $m_z$  is the loss due to mortality ( $d^{-1}$ ),  $p$  is the predation rate by zooplanktivorous fishes ( $d^{-1}$ ) and  $F$  is the zooplanktivorous fish biomass.

The zooplankton growth rate,  $\mu_z$  depends on zooplankton grazing rate. A fraction,  $g_a$  of the ingested food is assimilated through the gut wall, while the rest is egested as fecal pellets (Elser *et.al* 1995). Metabolic requirements consume a fraction,  $g_m$  of the assimilated carbon. The elements not respired are incorporated into new biomass. The zooplankton growth rate is modelled by:

$$\mu_z = (1 - g_m) g_a g_r \quad (14)$$

where  $(1 - g_m) \cdot g_a (= g_e)$  is the growth efficiency of zooplankton. The zooplanktivorous fish biomass is assumed equal to that of zooplankton biomass (Sarvala *et.al* 1999) and the predation rate is

$$p = pred_{max} \frac{(Zoo)}{(Zoo + k_{zoo})} \text{ for } Zoo > Zoo_{min} \quad (15)$$

$$p=0 \text{ for } Zoo < Zoo_{min}$$

where  $pred_{max}$  is the maximum predation rate ( $d^{-1}$ ),  $Zoo_{min}$  is the zooplankton biomass below which predation ceases and  $k_{zoo}$  is the half-saturation constant for predation. Settling is not included in the model, because zooplankton is mobile and can swim to avoid sinking into the hypolimnion (Jorgensen and Bendricchio 2001).

In the model, recycling of phosphate, P from zooplankton grazing process comes from two sources: the remineralization of fecal matter and the excretion of excess P. The amount,  $F_f$  of P egested from the gut and recycled in the water column is defined as:

$$F_f = p_f(1 - g_a) \frac{gr}{C:P_{phyto}} \quad (16)$$

where  $p_f$  is the recycled fraction of egested P. The amount of P assimilated in excess is directly excreted by zooplankton in a dissolved form. This amount  $E$  is defined by:

$$E = \left( \frac{g_a}{C:P_{phyto}} - \frac{g_e}{C:P_{zoo}} \right) gr \quad (17)$$

**Nutrients:** Time evolution of phosphate in the model is determined by uptake by phytoplankton, remineralization of dead phytoplankton and zooplankton, zooplankton egestion and excretion. A percentage  $p_{ws}$ ,  $p_p$ ,  $p_z$  and  $p_f$ , respectively of settling phytoplankton, dead phytoplankton, dead zooplankton and fecal pellets are directly recycled. Therefore,

$$(G - D)_{Phos} = -\mu \frac{Phyto}{(C:P)_{phyto}} + p_{ws} \frac{Phyto}{(C:P)_{phyto}} + p_p m_p \frac{Phyto}{(C:P)_{phyto}} + p_z m_z \frac{Zoo}{(C:P)_{zoo}} + EZoo + F_f Zoo \quad (18)$$

where  $Phos$  is the dissolved phosphate pool ( $\mu gP/L$ ).

Table 1. Parameters, variables and constants used in the numerical model

Name	Units	Value	Description
$\Delta x$	<i>m</i>	6,000.0	Grid size in x direction
$\Delta y$	<i>m</i>	20,000.0	Grid size in y direction
$\Delta t$	<i>s</i>	1800	Time step
<i>h</i>	<i>m</i>	30	Reference depth of the thermocline
$\theta_b$	$^{\circ}\text{C}$	24.5	Average temperature of the bottom layer
$\theta_s$	$^{\circ}\text{C}$	27.0	Average reference temperature of the surface layer
<i>Phyto</i>	$\mu\text{g C/L}$	Variable	Phytoplankton biomass in the epilimnion
<i>Phyto<sub>h</sub></i>	$\mu\text{g C/L}$	0.0	Phytoplankton biomass in the hypolimnion
<i>Phyto<sub>min</sub></i>	$\mu\text{g C/L}$	15.0	Minimum phytoplankton biomass in the epilimnion
<i>k<sub>phyto</sub></i>	$\mu\text{g C/L}$	30.0	Half saturation constant for grazing by zooplankton
<i>ILL</i>	$\mu\text{g C/L}$	60.0	Incipient limiting level
<i>w<sub>s</sub></i>	$\text{m d}^{-1}$	1.0	Settling velocity of phytoplankton
<i>m<sub>p</sub></i>	$\text{d}^{-1}$	0.11	Mortality rate of phytoplankton
<i>r<sub>p</sub></i>	$\text{d}^{-1}$	0.085*P <sub>max</sub>	Respiration rate of phytoplankton
<i>P<sub>max</sub></i>	$\text{d}^{-1}$	1.4	Maximum carbon specific photosynthetic rate
<i>k<sub>phos</sub></i>	$\mu\text{g C/L}$	1.0	Half saturation constant for growth of phytoplankton
<i>I<sub>k</sub></i>	$\mu\text{mol E m}^{-2}\text{s}^{-1}$	350	Light saturation constant
<i>g<sub>max</sub></i>	$\text{d}^{-1}$	0.5	Maximum grazing rate
<i>C:P<sub>phy</sub></i> to		58.1	Carbon to phosphorus ratio in phytoplankton
<i>Zoo</i>	$\mu\text{g C/L}$	Variable	Zooplankton biomass in the epilimnion
<i>Zoo<sub>h</sub></i>	$\mu\text{g C/L}$	0.0	Zooplankton biomass in the hypolimnion
<i>Zoo<sub>min</sub></i>	$\mu\text{g C/L}$	2.0	Minimum zooplankton biomass in the epilimnion
<i>k<sub>zoo</sub></i>	$\mu\text{g C/L}$	5.5	Half saturation constant for predation by zooplanktivorous fish
<i>p<sub>ws</sub></i>		0.5	Percentage of remineralized settling phytoplankton
<i>p<sub>p</sub></i>		0.5	Percentage of remineralized dead phytoplankton
<i>p<sub>z</sub></i>		0.5	Percentage of remineralized dead zooplankton
<i>p<sub>f</sub></i>		0.3	Percentage of remineralized fecal material
<i>p<sub>max</sub></i>	$\text{d}^{-1}$	0.08	Maximum predation rate
<i>m<sub>z</sub></i>	$\text{d}^{-1}$	0.07	Zooplankton mortality rate
<i>g<sub>e</sub></i>		0.32	Growth efficiency of zooplankton
<i>C:P<sub>zoo</sub></i>		77.42	Carbon to phosphorus ratio in zooplankton
<i>Phos</i>	$\mu\text{g P/L}$	Variable	Phosphorus concentration in the epilimnion
<i>Phos<sub>h</sub></i>	$\mu\text{g P/L}$	30.0	Phosphorus concentration in the hypolimnion
<i>Phos<sub>min</sub></i>	$\mu\text{g P/L}$	1.0	Minimum concentration of phosphorus of zooplankton in the epilimnion

## Appendix 2: Phytoplankton and diatoms taxa list (CLIMLAKE 2002-2004)

### Cyanobacteria

*Anabaena* af. *spiroides*  
*Anabaenopsis tanganyikae* (G. S. West) Mill.  
*Anabaena* sp.  
*Aphanizomenon* af. *flos-aquae* (L.) Ralfs  
*Aphanocapsa delicatissima* West & G. S. West  
*Aphanocapsa* af. *grevillei* (Berk.) Rabenh.  
*Aphanocapsa* sp.  
*Aphanothece microscopica* Naeg.  
*Aphanothece minutissima* (W. West) Kom.-Legn. et Cronb.  
*Aphanothece* cf. *nidulans* Richt. in Wittr. et Nordst.  
*Aphanothece* cf. *clathrata* W. & G.S. West  
*Borzia trilocularis* Cohn  
*Calothrix* af. *braunii* Born. et Flah.  
*Calothrix* cf. *stellaris* Born. et Flah.  
*Calothrix* af. *wembariensis* Hieron et Schmidle  
*Calothrix* af. *stagnalis* Gom.  
*Calothrix* spp.  
*Gloeotrichia* sp.  
*Chroococcus dispersus* (Keissl.) Lemm.  
*Chroococcus* af. *distans* (G. M. Sm.) Kom.-Legn. et Cronb.  
*Chroococcus limneticus* Lemm.  
*Chroococcus* af. *limneticus* Lemm.  
*Chroococcus* af. *minimus* (Keissl.) Lemm.  
*Chroococcus* af. *obliteratus* Richt.  
*Chroococcus* af. *planctonicus* Bethge  
*Chroococcus* af. *rufescens* (Kuetz.) Naeg.  
*Chroococcus* af. *subtilissimus* Skuja  
*Chroococcus turgidus* (Kuetz.) Naeg.  
*Chroococcus* spp.  
*Chroococciopsis* sp.  
*Coelosphaerium kuetzingianum* Näg.  
*Cyanothece* sp.  
*Gloeocapsa decorticans* (A. Br.) Richt. in Wille  
*Gloeothece* sp.  
*Pleurocapsa* sp.  
*Leptochaete* sp.  
*Lyngbya epiphytica* Wille  
*Lyngbya* af. *molischii* Vouk  
*Merismopedia glauca* (Ehrenb.) Kuetz.  
*Merismopedia hyalina* (Ehr.) Kuetz.  
*Merismopedia elegans* A. Br. in Kuetzing  
*Merismopedia minima* Beck  
*Merismopedia punctata* Meyen  
*Merismopedia tenuissima* Lemm.

*Merismopedia warmingiana* Lagerh.  
*Merismopedia* af. *danubiana* Hortob.  
*Microcystis* sp.  
*Oscillatoria agardhii* Gomont  
*Oscillatoria lacustris* (Klebahn) Geitler  
*Oscillatoria mougeotii* f. *clathrata* Skuja  
*Oscillatoria pseudogeminata* G. Schmid  
*Oscillatoria* spp.  
*Phormidium ambiguuum* Gom. s.l.  
*Phormidium ambiguuum* Gom. f. *majus* (Lemm.) Elenk.  
*Phormidium* af. *fragile* (Menegh.) Gom.  
*Phormidium* af. *valderiae* (Delp.) Geitl.  
*Phormidium* spp.  
*Planktolyngbya limnetica* Anagn. et Kom.  
*Planktolyngbya* spp.  
*Planktothrix* af. *mougeotii* (Kuetz.) Anagn. et Kom.  
*Pseudanabaena* sp.  
*cf. Raphidiopsis* sp.  
*Romeria* af. *chlorina* Boecher  
*Romeria* sp.  
*Snowella* sp.  
*Stanieria* sp.  
*Symploca* af. *meneghiniana* Kuetz.  
*Synechococcus nidulans* (Pringsh.) Kom. in Bourr.  
*Synechococcus* sp.  
*Synechocystis aquatilis* Sauvag.  
*Synechocystis endobiotica* (Elenk. et Hollerb.) Elenk. et Hollerb.  
*Synechocystis* af. *minuscula* Voron.  
*Synechocystis* spp.  
*Woronichinia ruzickae* Kom. et Hind.

### Dinophyta

*Amphidinium* sp.  
*Glenodinium* cf. *pulvisculus* (Ehr.) Stein.  
*Glenodinium* sp.  
*Peridinium* cf. *cinctum*  
*Peridinium africanum*  
*Peridinium* spp.

### Cryptophyta

*Cryptomonas erosa* var. *reflexa* Marss.  
*Cryptomonas* sp.  
*Rhodomonas minuta* var. *nannoplanctica* Skuja  
*Rhodomonas* sp.

### Chrysophyta

*Chromulina* sp.

*Kephyrion crassum* (Hill.) Starmach  
*Kephyrion litorale* Lund  
*Ochromonas cf. ovalis* Dofl.  
*Ochromonas cf. perlata* Dofl.  
*Ochromonas cf. verrucosa* Skuja  
*Ochromonas* sp.  
*Pseudokephyrion circumvallatum* Bourr.  
*Pseudokephyrion* af. *poculum* Conr.  
*Synura* sp.  
 spp.

### Chlorophyta

*Actinastrum* af. *aciculare* f. *africanum* Comp.  
*Actinastrum gracillimum* G. M. Sm.  
*Ankistrodesmus fusiformis* Corda  
*Botryococcus braunii* Kütz.  
*Characium* sp.  
*Chlamydomonas* spp.  
*Chlorella* sp.  
*Chloromonas* sp.  
*Closteriopsis petkovii* Stoyneva et al.  
*Coelastrum astroideum* De-Not  
*Coelastrum microporum* Naeg. in A. Br.  
*Coelastrum pseudomicroporum* Korsch.  
*Coelastrum reticulatum* (Dang.) Senn  
*Coelastrum sphaericum* Naeg. st. *cubicum* Naeg.  
*Coelastrum* sp.  
*Coenochloris* af. *astroidea* Hind.  
*Coenochloris polycocca* Hind.  
*Coenocystis subcylindrica* Korsh.  
*Coenococcus* sp.  
*Cosmarium* af. *meneghini* Breb. ex Ralfs  
*Crucigenia quadrata* Morr.  
*Crucigenia tetrapedia* (Kirchn.) W. et G. S. West  
*Desmodesmus communis* (Hegew.) Hegew.  
*Desmodesmus denticulatus* (Lagerh.) An, Friedl et Hegew.  
*Desmodesmus intermedius* (R. Chod.) Hegew.  
*Desmodesmus maximus* var. *peruviense* (Hegew.) Hegew.  
*Desmodesmus pleiomorphus* (Hind.) Hegew.  
*Desmodesmus spinosus* (R. Chod.) Hegew.  
*Dictyochlorella reniformis* (Korsh.) Silva  
*Dictyosphaerium tetrachotomum* Printz  
*Didymocystis bicellularis* (Chod.) Kom.  
*Didymocystis* sp.  
*Elakotothrix viridis* (Snow) Printz  
*Eremosphaera tanganyikae* Stoyneva et al.  
*Franceia tenuispina* Korsh.  
*Gloeocystis* sp.  
*Golenkinia* af. *radiata* Chod.  
*Granulocystis* sp.

*Kirchneriella contorta* var. *elegans* (Komárek) Hindák  
*Kirchneriella contorta* var. *elongata* (Kom.) Hind.  
*Kirchneriella obesa* (W. West) Schmidle  
*Kirchneriella subcapitata* Korsh.  
*Kirchneriella* af. *lunaris* (Kirchn.) Moeb.  
*K. majori* (G. S. West) Kom.-Legn.  
*Lagerheimia ciliata* (Lag.) Chod.  
*Lagerheimia cingula* G. M. Sm.  
*Lagerheimia genevensis* (Chod.) Chod.  
*Lagerheimia quadriseta* (Lemm.) G. M. Smith  
*Lagerheimia subsalsa* Lemm.  
*Lagerheimia wratislaviensis* Schroed.  
*Leptosira* sp.  
*Lobocystis planctonica* Tiff. et Ahlstr.  
*Monoraphidium arcuatum* (Korsch.) Hind.  
*Monoraphidium circinale* (Nyg.) Nyg.  
*Monoraphidium contortum* (Thur.) Kom.-Legn.  
*Monoraphidium griffithii* (Berk.) Kom.-Legn.  
*Monoraphidium irregulare* (G. M. Sm.) Kom.-Legn.  
*Monoraphidium komarkovae* Nyg.  
*Monoraphidium minutum* (Naeg.) Kom.-Legn.  
*Mougeotia* sp.  
*Nephrochlamys* sp.  
*Nephrocytium agardhianum* Naeg.  
*Nephrocytium allantoideum* Bohlin  
*Nephrocytium limneticum* (G. M. Sm.) G. M. Sm.  
*Nephrocytium* af. *lunatum* W. West  
*Oedogonium* sp.  
*Oocystis* af. *crassa* Wittr.  
*Oocystis lacustris* Chod.  
*Oocystis* af. *pelagica* Lemm.  
*Oocystis* af. *socialis* Ostenf.  
*Pediastrum* af. *boryanum* (Turp.) Menegh.  
*Pediastrum integrum* Naeg.  
*Pediastrum integrum* var. *pearsonii* (G. S. West) Fritsch  
*Pediastrum kawraiskyi* Schmidle  
*Pediastrum simplex* Meyen  
*Pediastrum tetras* (Ehrenb.) Ralfs  
*Pediastrum* af. *westii* Wolosz.  
*Pediastrum* spp.  
*Phacotus* sp.  
*Planctococcus* af. *sphaerocystiformis* Korsh.  
*Platymonas* sp.  
*Radiococcus* af. *nimbatus* (De-Wild.) Schmidle  
*Scenedesmus aculeolatus* Reinsch  
*Scenedesmus arcuatus* (Lemm.) Lemm.  
*Scenedesmus arcuatus* var. *platydiscus* G. M. Sm.  
*Scenedesmus* af. *bijugatus* Kuetz.  
*Scenedesmus disciformis* (Chod.) Fott et Kom.  
*Scenedesmus* af. *ecornis* (Ralfs) Chod.  
*Scenedesmus obtusus* Meyen

*Scenedesmus quadricauda* (Turp.) Bréb.  
*Scenedesmus* sp.  
*Schizochlamydeella* sp.  
*Selenastrum capricornutum* Printz  
*Siderocelis kolkwitzii* (Naumm.) Fott  
*Siderocelis irregularis* Hind.  
*Sorastrum* sp.  
*Sphaerocystis planctonica* (Korsch.) Bourr.  
*Sphaerocystis schroeteri* Chod.  
*Spirogyra* sp.  
*Tetrachlorella* sp.  
*Tetraedron triangulare* (Chod.) Kom.  
*Tetraspora* af. *limnetica* W. et G. S. West  
*Tetrastrum glabrum* (Roll) Ahlstr. et Tiff.  
*Tetrastrum komarekii* Hind.  
*Thelesphaera* sp.  
*Treubaria setigera* (Arch.) G. Sm.

### Euglenophyta

*Euglena* spp.  
*Lepocinclis* sp.  
*Phacus* sp.  
*Strombomonas verrucosa* (Daday) Defl.  
*Trachelomonas* af. *volvocina* Ehr.  
*Trachelomonas volvocinopsis* Swir.  
*Trachelomonas* spp.

### Bacillariophyta

*Achnanthes* cf. *linearis* (W. Smith) Grun.  
*Achnanthes lanceolata* (Bréb.) Grun.  
*Achnanthes lanceolata* var. *minor* (Schulz) Lange-Bertalot  
*Achnanthes rupestroides* Hohn  
*Amphora copulata* (Kütz.) Schoeman & Archibald  
*Amphora pediculus* (Kütz.) Grun.  
*Capartogramma amphoroides* Ross  
*Capartogramma karstenii* (Zanon) Ross  
*Cocconeis disculus* (Schumann) Cl.  
*Cocconeis placentula* Ehr.  
*Cocconeis placentula* var. *euglypta* (Ehr.) Cl.  
*Cocconeis* sp.  
*Cyclotella kuetzingiana* Thwaites  
*Cyclotella meneghiniana* Kütz.  
*Cymatopleura calcarata* Hust.  
*Cymatopleura solea* (Bréb.) W. Smith  
*Cymatopleura solea* var. *apiculata* (W. Smith) Ralfs  
*Cymbellonitzschia minima* Hust.  
*Diploneis ovalis* (Hilse) Cl.  
*Encyonema grossestriatum* (O. Müll.) D.G. Mann  
*Encyonema minutum* (Hilse ex Rahb.) D.G. Mann  
*Encyonema muelleri* (Hust.) D.G. Mann  
*Epithemia adnata* (Kütz.) Bréb.

*Epithemia sorex* Kütz.  
*Gomphocymbella beccarii* (Grun.) Forti  
*Gomphocymbella gracilis* Hust.  
*Gomphonema aequatoriale* Hust.  
*Gomphonema clevei* Fricke  
*Gomphonema gracile* Ehr.  
*Gomphonema kilhamii* kociolek & Stoermer  
*Gomphonema paddockii* Kociolek & Stoermer  
*Gomphonema parvulum* (Kütz.) Kütz.  
*Gomphonema* sp.  
*Gomphonitzschia ungeri* Grun.  
*Luticola mutica* (Kütz.) D.G. Mann  
*Navicula arvensis* Hust.  
*Navicula barbarica* Hust.  
*Navicula capitata* Ehr. var. *hungarica* (Grun.) Ross  
*Navicula* cf. *modica* Hust.  
*Navicula costulata* Grun.  
*Navicula cryptotenella* Lange-Bertalot  
*Navicula damasii* Hust.  
*Navicula decussis* Ostrup  
*Navicula erifuga* Lange-Bertalot  
*Navicula exigua* (Greg.) Grun.  
*Navicula hasta* Pant.  
*Navicula perlatoides* (O. Müll) Hust.  
*Navicula seminuloides* Hust.  
*Navicula* sp.  
*Navicula subrotunda* Hust.  
*Navicula trivialis* Lange-Bertalot  
*Navicula zanonii* Hust.  
*Nitzschia acicularis* (Kütz.) W. Smith  
*Nitzschia aequalis* Hust.  
*Nitzschia* af. *fonticola* Grun.  
*Nitzschia* af. *frustulum* (Kütz.) Grun.  
*Nitzschia asterionelloides* O. Müll.  
*Nitzschia* cf. *dissipata* (Kütz.) Grun.  
*Nitzschia inconspicua* Grun.  
*Nitzschia intermedia* Hantzsch  
*Nitzschia lacustris* Hust.  
*Nitzschia lancettula* O. Müll.  
*Nitzschia linearis* W. Smith  
*Nitzschia nyassensis* O. Müll.  
*Nitzschia palea* (Kütz.) W. Smith  
*Nitzschia palea* var. *tenuirostris* Lange-Bertalot  
*Nitzschia paleacea* (Grun.) Grun.  
*Nitzschia reversa* W. Smith  
*Nitzschia sigma* (Kütz.) W. Smith  
*Nitzschia spiculum* Hust.  
*Nitzschia subacicularis* Hust.  
*Nitzschia subrostrata* Hust.  
*Nitzschia tubicola* Grun.  
*Nitzschia vanoyei* Choln.



*Nitzschia vitrea* Norman  
*Placoneis gastrum* (Ehr.) Mereschkowsky  
*Rhoicosphenia abbreviata* (C. Ag.) Lange-Bertalot  
*Rhopalodia gibba* (Ehr.) O. Müll.  
*Rhopalodia gracilis* O. Müll.  
*Rhopalodia hirundiniformis* O. Müll.  
*Rhopalodia hirundiniformis* var. *parva* O.Müll.  
*Rhopalodia rhopala* (Ehr.) Hustr.  
*Sellaphora bacillum* (Ehr.) Mereschkowsky  
*Sellaphora nyassensis* (O. Müll.) D.G. Mann  
*Sellaphora pupula* (Kütz.) Mereschkowsky  
*Staurosira africana* (Hust.) Williams & Round  
*Staurosira construens* (Ehr.) Williams & Round  
*Staurosira pinnata* (Ehr.) Williams & Round  
*Surirella biseriata* Bréb.  
*Surirella obtusiuscula* G.S. West  
*Synedra ulna* (Nitzsch) Ehr.